UNIVERSITÀ DEGLI STUDI DI PADOVA

DIPARTIMENTO DI BIOLOGIA

SCUOLA DI DOTTORATO IN BIOSCIENZE

INDIRIZZO DI GENETICA E BIOLOGIA MOLECOLARE DELLO SVILUPPO

CICLO XXIII

PATHOGENETIC ROLE OF *MFN2* GENE: GENETIC ANALYSIS IN PATIENTS WITH CHARCOT-MARIE-TOOTH NEUROPATHY AND DISEASE MODELING IN ZEBRAFISH

Direttore della Scuola: Ch.mo Prof. Giuseppe Zanotti

Coordinatore d'indirizzo: Ch.mo Prof. Paolo Bonaldo

Supervisore: Ch.ma Prof.ssa Maria Luisa Mostacciuolo

Co-supervisore: Dott. Andrea Vettori

Dottoranda: Dott.ssa Giorgia Bergamin

31 Gennaio 2011

Table of contents

Riassunto

Le Charcot-Marie-Tooth (CMT) sono le più comuni patologie ereditarie del sistema nervoso periferico. Il sottotipo CMT2A, uno dei più frequenti, è causato da mutazioni nel gene *MFN2*, codificante mitofusina 2, una proteina GTPasica, per struttura simile alla dinamina, localizzata a livello della membrana esterna dei mitocondri. MFN2 risulta implicata in diversi processi cellulari, quali la fusione della membrana mitocondriale esterna dei mitocondri, il trasporto di questi lungo gli assoni e il *tethering* tra mitocondri e reticolo endoplasmatico. Ad oggi sono state identificate più di 80 mutazioni associate alla CMT2A e a varianti complicate di CMT2. Tali mutazioni sono nella maggior parte dei casi mutazioni puntiformi a trasmissione autosomica dominante, ma recentemente sono state identificate anche alcune mutazioni a trasmissione semi-dominante o recessiva. Con lo scopo di identificare nuove mutazioni in mitofusina 2 e individuare una possibile correlazione genotipo-fenotipo, nella prima parte di questo progetto si è proceduto a condurre un'analisi genetica del gene in 25 pazienti con diagnosi di CMT assonale. Tale analisi è stata condotta primariamente mediante sequenziamento diretto degli esoni di cui il gene *MFN2* è composto. Successivamente, nei soggetti risultati negativi all'analisi per sequenziamento, si è proceduto ad eseguire un'analisi mediante la tecnica della multiplex ligation-dependent probe amplification (MLPA), la quale consente di identificare eventuali riarrangiamenti genici, non identificabili mediante sequenziamento. L'analisi genetica dei pazienti ha permesso di identificare la mutazione causativa in cinque probandi. In quattro di questi sono state trovate mutazioni in eterozigosi, mentre un paziente affetto da una grave forma di CMT assonale è risultato essere un eterozigote composto per due mutazioni in *MFN2* (p.[K38del]+[T362M]). Delle mutazioni così rilevate, quattro (E329del, A738V, R94P, K38del) non risultavano prima descritte. La frequenza delle mutazioni di *MFN2* nel campione indagato (20%) è in accordo con i dati di letteratura. L'analisi di *MFN2* mediante MLPA non ha invece permesso di rilevare alcun riarrangiamento genico.

Attualmente lo studio dei meccanismi tramite cui mutazioni in *MFN2* inducono neurodegenerazione è limitato dal fatto che solo pochi modelli di CMT2A sono stati sviluppati con successo in topo. Considerando che lo zebrafish si è recentemente distinto come un buon modello per lo studio di molte malattie neurodegenerative, si è deciso di investigare la funzione di mitofusina 2 e il suo ruolo nella patogenesi della CMT2A in tale organismo. Mitofusina 2 è

stata quindi silenziata durante lo sviluppo di zebrafish usando un oligo-morfolino antisenso, il quale viene direttamente iniettato in uova fecondate. L'analisi del fenotipo dei morfanti ha permesso di evidenziare come, in assenza di mfn2, gli embrioni presentino evidenti alterazioni fenotipiche ed in particolare risultino avere gravi problemi di movimento, in accordo col fenotipo osservato nei pazienti. Ulteriori analisi hanno evidenziato che il sistema neuromuscolare delle larve è gravemente compromesso, con motoneuroni morfologicamente alterati e una riduzione del numero di giunzioni neuromuscolari correttamente formate. Inoltre, come nei pazienti, le fibre muscolari risultano ipotrofiche e con diametro ridotto, probabilmente a seguito della denervazione dei muscoli dei somiti. Tali risultati, validati da esperimenti di *rescue* con il trascritto umano di *MFN2*, confermano il ruolo fondamentale di mitofusina 2 nello sviluppo dei motoneuroni e suggeriscono che lo zebrafish può essere uno strumento utile per lo studio *in vivo* degli effetti delle mutazioni trovate nei pazienti con CMT2.

Per tale motivo si è proceduto a mettere a punto un metodo che consentisse di valutare l'effetto delle mutazioni in *MFN2* utilizzando lo zebrafish come modello. Ci si è concentrati in primo luogo sull'analisi della mutazione R94Q, la più frequentemente identificata nei pazienti e per la quale sono disponibili svariate informazioni riguardanti il suo meccanismo molecolare, ottenute sia da indagini *in vitro* che *in vivo*. Mediante esperimenti di iniezione dell'mRNA umano mutato, sia in presenza che in assenza del morfolino contro *mfn2*, si è potuto dimostrare che nei primi stadi dello sviluppo di zebrafish, R94Q è, almeno in parte, *loss of function*. Tale risultato è in accordo con alcuni dati ottenuti da studi *in vitro* che dimostrano che tale allele mutato di *MFN2* non è in grado di ripristinare la forma del *network* mitocondriale in cellule derivate da topi knock-out per *Mfn2*. Inoltre una linea di topi knock-in per R94Q non mostra alcun segno patologico quando la mutazione è in eterozigosi, mentre è letale, ma tardivamente rispetto al knock-out, in omozigosi. Tuttavia un solo meccanismo di *loss of function* non è in grado di spiegare il fatto che una linea transgenica di topi in cui R94Q è sovraespressa nel sistema nervoso mostri un fenotipo compatibile con la CMT2A a partire dai 5 mesi di vita. I dati così ottenuti, confrontati con quelli di letteratura, suggeriscono che R94Q, pur avendo funzionalità ridotta, potrebbe avere anche un effetto di *gain of function*, il quale però è in grado di manifestarsi solo dopo lo sviluppo embrionale. Va segnalato che il metodo messo a punto, permette di evidenziare alterazioni solo nei primi stadi dello sviluppo e per tale motivo sarà necessario sviluppare delle linee transgeniche stabili di zebrafish per confermare il meccanismo d'azione di R94Q. Questo potrà permettere di ampliare l'indagine anche valutando gli effetti delle mutazioni in *MFN2* rilevate con la presente indagine.

Nel complesso i dati ottenuti con questo lavoro hanno contribuito a chiarire la possibile correlazione genotipo-fenotipo in pazienti affetti da CMT2A. Inoltre è stato possibile identificare zebrafish come un nuovo strumento per l'analisi del meccanismo d'azione di mutazioni in *MFN2* associate a CMT2. Dato che zebrafish è un organismo modello che si presta meglio di altri a esperimenti di *drug screening*, la validazione di un sistema modello per la CMT2A in zebrafish potrebbe in futuro contribuire all'identificazione di nuovi farmaci efficaci per il trattamento di tale patologia.

Abstract

Charcot-Marie-Tooth diseases (CMTs) are the most common hereditary pathologies of the peripheral nervous system. The dominant subtype CMT2A, one of the most frequent, is caused by mutations in *MFN2* gene, coding for mitofusin 2, a dynamin-like GTPase located in the outer membrane of mitochondria. MFN2 is involved in several cellular processes, as the fusion of mitochondrial membranes, the transport of mitochondria along axons and the tethering of mitochondria with endoplasmic reticulum. To date more than 80 mutations associated with CMT2A and complicated variants of CMT2 have been described. They are mainly point mutations with dominant transmission, but recently some semi-dominant and recessive mutations have been reported. With the aim to identify new causing mutations and possibly identify a genotype-phenotype correlation, in the first part of this project it was performed a genetic analysis of *MFN2* in 25 patients with diagnosis of axonal CMT. This analysis was conducted primarily by direct sequencing of all exons of *MFN2* gene. Subsequently, in subjects where no mutations were detected, it was carried out a multiplex ligation-dependent probe amplification (MLPA), a relatively new PCR-based technique that enables the identification of complex gene rearrangements. The genetic analysis of patients with CMT2A allowed the identification of the disease causing mutation in five probands. In four patients the mutation was found in heterozygosis, while one patient affected by an uncommonly severe axonal CMT resulted a compound heterozygote for two *MFN2* mutations (p.[K38del]+[T362M]). In all, four mutations (E329del, A738V, R94P, K38del) never reported in literature were found. The analysis of *MFN2* by MLPA did not revealed large gene rearrangements in patients without point mutations in *MFN2*, thus meaning that probably other genes are responsible for the disease in such patients and confirming the genetic heterogeneity of CMT neuropathies.

The understanding of the mechanisms by which the mutated forms of *MFN2* lead to neurodegeneration is limited by the fact that few mouse models for CMT2A were successfully developed. Since zebrafish turned useful to study many neurological and neuromuscular disorders, we decided to use it to investigate the function of MFN2 and its role in CMT2A disease. Using the morpholino technique, mitofusin 2 was knocked-down in developing embryos, which resulted severely motor-impaired in accordance with the loss of limbs motility observed in CMT2A patients. Investigations performed on the neuromuscular system of morphants, demonstrated that larvae exhibit misshapened motorneurons and a reduction of

neuromuscular junctions. As in human pathology, possibly because their incorrect innervation, muscular fibres appear hypotrophic and are reduced in diameter. These results, validated by the rescue of morphants with human *MFN2* mRNA, confirm the essential role of mitofusin 2 in motorneurons development and suggest that the zebrafish could be a very useful tool to study in living embryos the effects of mutations identified in CMT2A patients.

Therefore, with the aim to study the mutations found in our patients, we developed a method to evaluate the effect of human mutations in MFN2 using zebrafish embryos as a model. For this reason we first concentrated on the analysis of R94Q, which is a well studied mutation found frequently in CMT2A patients with severe phenotype. By injecting the mutated human *MFN2* mRNA alone and together with the morpholino against zebrafish *mfn2*, we demonstrated that, in the first stages of zebrafish development, R94Q is, at least in part, loss of function. This agrees with some studies performed in cells that demonstrated that this mutant allele of *MFN2* cannot restore the shape of mitochondria in knock-out cells. Moreover, a previously reported R94Q knock-in mouse displayed no phenotype in heterozygous state, while in homozygosity is lethal, but survives longer than the complete knock-out, thus confirming the hypothesis that R94Q mutated mitofusin 2 has a reduced activity. However a pure loss of function mechanism was recently excluded in mouse by the finding that a transgenic model over-expressing this mutation develops movement defects and alterations in mitochondria distributions resembling CMT2A disease by the age of 5 months. Our data, together with that found in literature, suggest that R94Q, even if it has a reduced functionality, may have also a gain of function activity that is disclosed phenotypically later during development. Since our method allows the analysis of *MFN2* mutations effect only during the first stages of development, we will need a stable transgenic zebrafish model to confirm the mechanism of action of R94Q and analyse the effect of MFN2 mutations found in the patients we investigated.

Altogether the results obtained with this work contributed to clarify the possible genotype-phenotype relations involved in CMT2A disease. Moreover it was proposed zebrafish as a new tool to dissect the molecular mechanism by which mitofusin 2 mutations lead to CMT2. Being easily amenable to drug screening, the zebrafish model could be not only a useful complement to the studies performed in mouse, but it may also contribute to identification of effective pharmacological compounds for the treatment of Charcot-Marie-Tooth disease.

Chapter 1: Introduction

1.1: Charcot-Marie-Tooth diseases

Charcot-Marie-Tooth diseases (CMTs), also known as hereditary motor and sensory neuropathies (HMSN), first described in 1886 (3, 4), are the most common inherited neuromuscular disorders, with an estimated average prevalence of 1:2000 (5, 6). Clinically they are characterized by hyposteny and hypotrophy of distal limb muscles, skeletal deformities (*pes cavus* is a very frequent hallmark of the disease), and decrease or absence of deep tendon reflexes. Sensory alterations (loss of sensation to touch, pain and vibration) are generally also present, but can be subtle and become evident late in the disease course or can be apparent only at electrophysiological examination (7). Muscle atrophy and weakness, particularly of lower limbs, are usually predominant, but severe impairment and loss of autonomy are infrequent in CMT.

To date more than 20 genes associated to several subtypes of CMT disease have been identified (8). The classification is mainly based on electroneurography examination (ENG) and in particular on the evaluation of motor nerve conduction velocity (MNCV), usually measured at the median or peroneal nerves. CMTs can be therefore subdivided into two main groups: demyelinating forms (CMT1 or HMSN I), in which there is a severe reduction of MNCV (<38 m/s), and axonal types (CMT2 or HMSN II), in which MNCV is conserved or slightly reduced (≥38 m/s) but there is a decrease of compound motor action potential amplitudes (CMAP) (9). Further subdivisions within those two types are based on the inheritance pattern and on the genetic data.

Frequently, the different subtypes of CMT are clinically indistinguishable and the precise CMT subtype assignment requires a complex approach, which comprehends necessarily the analysis of genetic and molecular data. Nevertheless age at onset and disease severity are highly variable, also in the case of patients with mutations in the same gene and among people of the same kindred. Some individuals may show minimal signs of the pathology and frequently are unconscious of being affected, while others may be significantly disabled. Marked differences in disease severity were reported in identical twins affected by CMT1A (10), and a very high

frequency of non-penetrant subjects (up to 25%) was described for CMT2A (11). The reasons for such clinical variability are unknown and the search for modifier factors is ongoing.

CMT1 accounts for more than two-thirds of all CMTs, and the subtypes CMT1A, caused by duplication of *PMP-22* gene, and CMT1B, associated to *MPZ* mutations, are recognized as the major causes of the disease in the Western and in the Eastern countries respectively (12). CMT2 represents almost one-third of cases and the most frequent subtype is CMT2A, which comprises the 10-33% of all axonal cases and is caused by mutations in the *MFN2* gene.

1.2: Axonal Charcot-Marie-Tooth diseases

1.2.1: Classification of axonal CMTs

Axonal CMTs are characterised by the constant degeneration and regeneration of distal nerves fibres, which can be evidenced by sural nerve biopsy exam, and are easily distinguished from the demyelinating forms through electroneurography. The majority of CMT2 cases have an autosomal dominant inheritance pattern. Some recessive CMT2 subtypes have been described, but are restricted only to a few families. Table 1.1 shows the current nomenclature used for the classification of axonal CMTs.

Although CMT2A is by far the most frequent axonal form, other less common CMT2 subtypes with unusual properties have been described. Some examples are CMT2B, characterised by ulcerative-mutilating phenomena, CMT2C, showing vocal cord paralysis and atrophy of diaphragm, and CMT2D, in which the involvement of hand muscles is predominant. All these characteristics have to be considered and can be of great help in the diagnosis process.

	Gene/Locus	Phenotype
AD CMT2		
CMT2A	MFN2	axonal, severe, optic atrophy
CMT2B	RAB7	axonal, predominant sensory involvement
CMT2C	TRPV4	axonal, vocal cord and respiratory involvement
CMT2D	GARS	axonal, predominant hand wasting
CMT2E	NEFL	axonal, demielinating, early onset severe
CMT2F	HSPB1	axonal, classic CMT
CMT2G	12q12-q13.3	axonal, classic CMT
CMT2I	MPZ	demielinating, late onset axonal
CMT2J	MPZ	demielinating, axonal with Adie's pupil
CMT2L	HSPB8	axonal, classic CMT
AR CMT2		
AR CMT2A	LMNA	axonal, proximal muscles involvement
AR CMT2B	MED25	axonal, classic CMT
CMT2H	GDAP1	axonal, intermediate, demielinating, vocal cord paralysis
CMT2K	GDAP1	axonal, intermediate, demielinating, vocal cord paralysis

Table 1.1: *classification of CMT diseases. Modified from Patzko and Shy (2011).*

1.2.2: Biological processes leading to axonopathies

The majority of the genes implicated in CMT1 are principally involved in the formation and maintenance of peripheral myelin sheets and as a consequence are exclusively expressed in Schwann cells. Some examples are peripheral myelin protein 22 (PMP22), myelin protein zero (MPZ) and connexin 32 (Cx32), causing CMT1A, CMT1B and CMT1X respectively. On the other hand, axonal CMTs are frequently caused by genes involved in many different cellular processes, with a broad expression pattern not necessarily specific of neuronal cells. This has been long explained by the fact that neuronal tissue has a high degree of specialisation but a limited regenerative capacity, and both these characteristics can make neurons more sensitive to the alteration of mechanisms in common with other cell types. Another aspect that can also explain why CMTs manifest as a peripheral neuropathy, is the unique anatomy of secondary motorneurons, with a cellular body that, in humans, can be far from the periphery as much as one meter. This makes motorneurons particularly sensitive to the alteration of some cellular processes, as endosomal trafficking, axonal transport and mitochondrial dynamics.

This functional differentiation of axonal and demyelinating CMTs has to be considered only a general rule, which is not exempts from exceptions. The historical classification between CMT1 and CMT2 is recently becoming less clear, since families previously classified as

CMT1 or CMT2 based on clinical and electrophysiological data have been found to be mutated in the same gene and sometimes to carry also the same mutation. Some examples of this have been described for the genes *MPZ*, *Cx32*, *GDAP1*, *NEFL* and *DNM2*, which can cause both axonal and demyelinating forms of CMT, thus introducing additional complexity to the classification of these pathologies. This provides serious challenges for the efficient clinical application of molecular diagnosis in CMT patients and made necessary the definition of a new group of CMT, named intermediate CMT, when motor conduction velocities are found to be both in the CMT1 and CMT2 ranges.

Besides the evident difficulties to join clinical and molecular classifications, the identification of main cellular pathways involved in CMT diseases is of extreme importance for the development of an effective cure, that is still lacking. In the next paragraphs I will summarize the most frequently cellular pathways involved in axonal CMTs (Fig. 1.1).

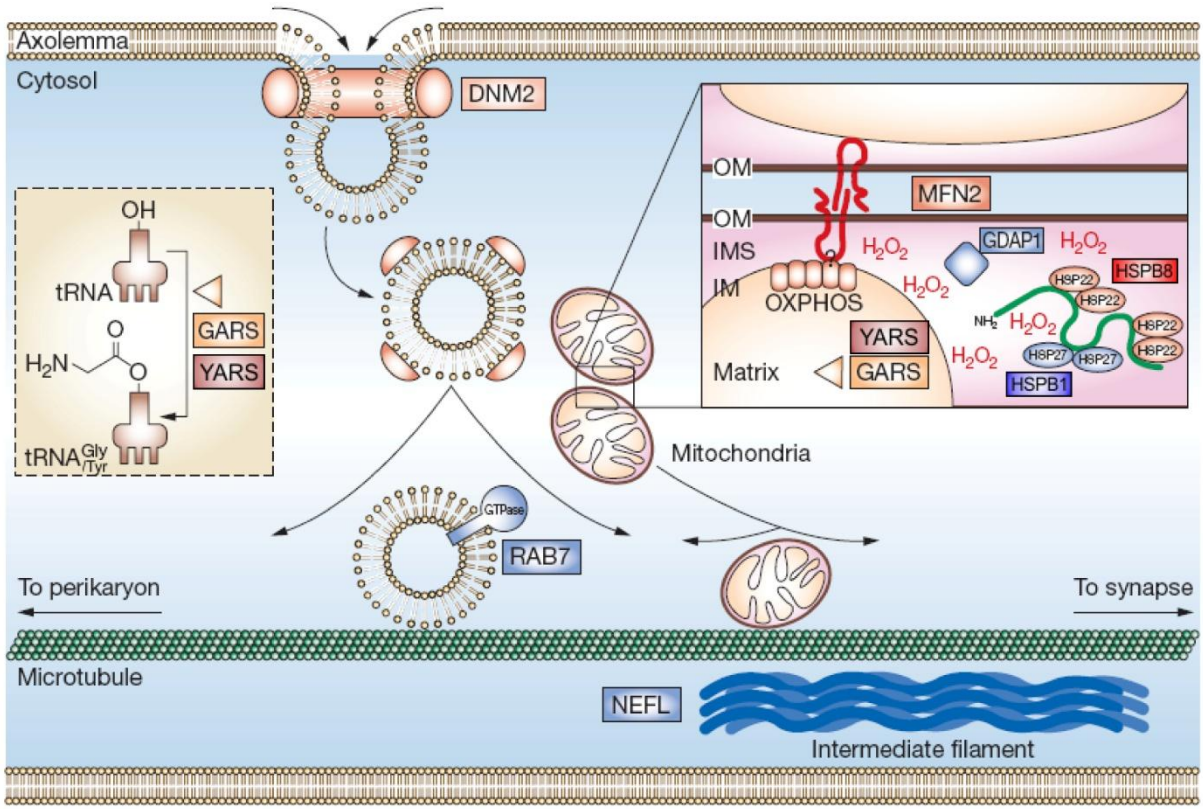

Figure 1.1: *Structure of a peripheral nerve axon illustrating the main pathways and genes involved in axonal CMTs (modified from Zuchner and Vance, 2006).*

Axonal transport and endosomal trafficking

As a consequence of their unique shape, the transport of vesicles, mitochondria and other organelles along axons is of vital importance in the maintenance of motorneuron functionality

making longest neurons more susceptible to alterations in such functions. Because of the extreme length of motor axons, motorneurons are dependent on cytoskeleton for an effective intracellular transport. Neurofilaments, the most abundant intermediate filaments in neurons, are formed by the polymerisation of three types of subunits: high, medium and light. *NEFL*, the neurofilament-light chain coding gene, was the first to be associated to an axonal CMT (14). It seems important both for the anterograde and the retrograde transport, in particular of mitochondria (15). Microtubules are also relevant for axonal transport. Anterograde and retrograde movements are mediated by the action of kinesins and by dynein-dynactin complexes respectively. A kinesin protein (KIF1B) was initially associated to CMT2A, but only one family with mutation in this gene has been so far described. Mutations in the *MFN2* gene were subsequently related to the majority of CMT2A patients (16). Interestingly mutations in *DCTN1*, coding for the motor subunit dynactin 1, are associated to distal hereditary motor neuropathy type VII (dHMNVII) (17). dHMNs are strictly associated to CMT, and can be distinguished only because sensory alterations are never present in dHMNs. Dynamin 2 (*DNM2*) is a member of the dynamin superfamily, large GTPases that are central players in the clathrin mediated endocytosis. *DNM2* causes a dominant form of CMT with axonal and demyelinating features (DI-CMTB) (18). This protein is ubiquitously expressed and plays a role in receptor-mediated endocytosis, membrane trafficking from late endosomes and Golgi complex and actin assembly (19, 20). *In vitro* experiments demonstrated that mutant DNM2 cannot locate correctly to membranes and induces disorganisation of the microtubules network (18). The RAS-associated GTP-binding proteins of the RAB family are also known to be involved in the regulation of vesicular transport, and in particular *RAB7* has been associated to CMT2B, a form with predominant sensory deficits (21).

Protein misfolding

The growing number of neurodegenerative disorders linked to alteration in protein folding demonstrates the importance of protein degradation for the correct neuronal homeostasis. Neurons express molecular chaperones, able to recognize misfolded proteins and prevent their aggregation, and co-chaperones, that sort denatured proteins between renaturation and proteasomal degradation. Small heat shock proteins are a family of conserved proteins which shares the presence of an α-crystallin domain at the C-terminus. To date ten different sHSPs (HSPB1–10) have been identified in man (22). *HSPB1* and *HSPB8* are found mutated respectively in CMT2F and CMT2L, two axonal CMTs with classical phenotypic manifestations. Interestingly, mutations in these genes were identified also in two subtypes of

distal hereditary motor neuropathy, and it is now well accepted that CMT2F is allelic to dHMNIIB and CMT2L to dHMNIIA.

Human small heat-shock proteins can form highly dynamic high-molecular-mass oligomers and are involved in many different processes. HSPB1 acts as an ATP-independent chaperone (23), but is also implicated in the maintenance of cytoskeleton structure, cell migration, metabolism and cell survival (24). HSPB8 is part of a protein complex which stimulates the degradation of protein substrates by macroautophagy, and in particular is directly involved in the recognition of misfolded proteins (25). The direct interaction between HSPB1 and HSPB8 suggests they could share a common disease mechanism (26).

RNA synthesis and processing

The glycyl-tRNA synthetase gene (*GARS*) is mutated in CMT2D (27). This gene is ubiquitously expressed and plays a leading role in RNA synthesis by covalently linking glycine with its corresponding tRNAs. GARS was the first tRNA synthetase gene that was found associated to a human disease, but to date 4 of the 36 other tRNA synthetase genes have been linked to other neurological diseases, thus indicating a central role of these genes in the nervous system development and maintenance (27-30). Notably YARS, one of these disease-causing tRNA synthetases, has been associated to an intermediate form of CMT (DI-CMTC) (29). Why the ubiquitously expressed tRNA synthetase genes are implicated in neurological disorders however is not yet clear. There is the evidence that local protein translation can occurs in axons and peripheral motor axon can be translationally active (31). As a consequence one hypothesis is that mutated tRNA synthetases cannot be transported correctly trough axons, thus causing the inhibition of peripheral protein expression.

Mitochondria dynamics alterations

Neurons are extremely sensitive to alterations in mitochondrial function, and this is mainly due to their high metabolic rate, which needs a large amount of energy to sustain ionic transmission and axonal transport (32). Recently a critical dependence on mitochondria dynamic was also demonstrated. Indeed mitochondria are highly dynamic organelles, and undergo continuous events of fusion and fission, fundamental to intermix lipids and mitochondrial DNA molecules in order to maintain a fully functional mitochondria population in cells (33). This is also demonstrated by the fact that in some of the major neurodegenerative diseases, including

Parkinson's, Alzheimer's and Huntington's disease, the disruption of mitochondrial dynamics was recognised as a key feature of the pathology (33).

Charcot-Marie-Tooth diseases were also associated to mutations in mitochondria dynamics regulators. Above all, axonal CMTs can be caused by mutations in two genes, *MFN2* and *GDAP1*, directly involved in mitochondria trafficking and morphology. Here the involvement of *GDAP1* in CMT disease will be briefly discussed, while *MFN2* functions and alterations in human diseases will be deepened in the next paragraphs.

GDAP1 is an ubiquitous protein, which is mainly expressed in the nervous system, both in motorneurons and Schwann cells (34). Bioinformatical analysis originally classified it to a subfamily of glutathione-S-transferases (GSTs), proteins associated to the detoxification of reactive oxigen species, GST-activity was never detected by in *in vitro* assays (35). Instead GDAP1 seems involved in mitochondria dynamics and it was demonstrated that this protein, located in the outer mitochondria membrane, is a regulator of mitochondrial fission (36). Interestingly, GDAP1 mutations are linked to a very broad spectrum of CMT phenotypes, with autosomal dominant or recessive inheritance and axonal, demyelinating or intermediate clinical features. In a recent review attempting to find a genotype-phenotype correlation, it was shown that recessive forms are generally more severe and with earlier onset, particularly in the presence of truncating mutations (37). However the explanation of such different phenotypic manifestations and wide intra- and inter-familial variability is still lacking.

1.3: Charcot-Marie-Tooth type 2A

1.3.1: Molecular and clinical presentation

Charcot-Marie-Tooth type 2A (CMT2A) is the most frequent form of axonal CMT. The locus associated to CMT2A was first reported in 1993 (38), and was initially linked to mutations in *KIF1B* in a Japanase kindred (39). However in any of the other CMT2 families described so far other mutations were never reported in this gene. In 2004 was finally assessed that, in the previous described kindreds with linkage in the CMT2A locus, *MFN2* gene mutations were responsible for the disease (16). Patients with mutations in *MFN2* usually have a typical axonal CMT, even if usually more severe than CMT1 (the 28% of patients with mutations in MFN2 are wheelchair dependent) (40). Nevertheless the severity of the disease can be extremely variable, and a bimodal distribution was observed: some patients have an early onset and

severe phenotype, while other present a late onset and a milder course (40, 41). A genotype-phenotype correlation explaining this distribution was never been found and this is also complicated by the fact that phenotypic variations frequently occur also in the same kindred (11).

CMT2A neuropathy in some cases can be clinically distinguished from other subtypes by the presence of complicating additional features. Optic atrophy has been described in 10-20% of affected individuals, particularly in the early-onset group. Indeed mutations in *MFN2* were associated also to the CMT variant HMSN-VI (42), but there is now general agree that CMT2A and HMSN-VI represent a unique disease (8). Another common symptom found in CMT2A patients is sensoryneural hearing loss, present in the 59% of patients (11) and found also in other forms of demyelinating CMT. Central nervous system lesions can also be present in CMT2A patients, particularly in those with early onset and severe phenotype (43, 44). The involvement of primary motorneurons and pyramidal signs was also described in some patients with the CMT subtype HMSN-V and mutations in *MFN2* (45).

1.3.2: MFN2 gene and protein structure

MFN2 is located in chromosome 1, in a genomic region extending for about 33 kilobases. In its longer form, the mRNA is built from 19 exons, of which 15 are protein-coding. A shorter *MFN2* transcript have been reported, lacking the second exon, which code for a portion of the 5' UTR. Both *MFN2* mRNAs code for a protein of 757 aminoacid residues that is located in the outer mitochondria membrane and in the endoplasmic reticulum. *MFN1*, a paralogue of *MFN2*, is located in chromosome 3 and codes for a protein of 741 aa which share with MFN2 a percentage of similarity of 77%.

1.3.3: MFN2 and mitochondria membranes fusion

Events of fusion and, in reverse, fission, are fundamental for the maintenance of mitochondria morphology. These events are mediated by a series of proteins, highly conserved from yeast to mammals, that are subdivided in pro-fusion and pro-fission. MFN1 and MFN2 are both involved in the fusion of outer mitochondria membranes (2). As their orthologue in invertebrates and yeast, named fzo, mitofusins are inserted in the outer mitochondrial membrane and share a conserved structure. They are formed by a large GTPasic domain at the N-terminal and two heptad repeats domains (HR1 and HR2) forming α-elices and involved in

colied-coil interactions. HR1 and HR2 are separated by a bipartite transmembrane domain, which allows the insertion of mitofusins in the outer mitochondrial membrane, with both N and C-terminal exposed in the cytoplasm (46, 47). (Fig. 1.2).

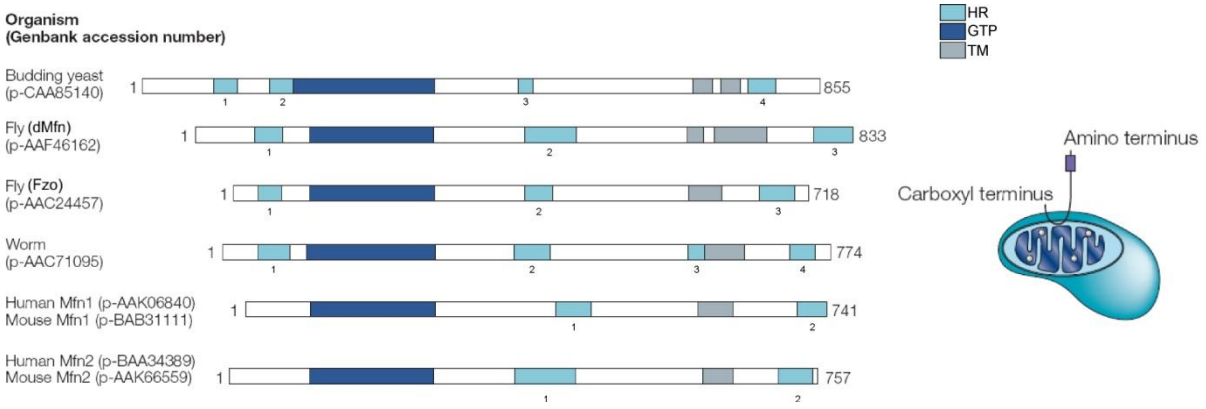

Figure 1.2: *Fzo homologues are found in a wide range of eukaryotes. They share a conserved protein structure, composed by a GTPasic domain, 2-4 heptad repeat domains (HR) and a transmembrane region (TM). Some differences in the number and positions of HR regions are present, but their functional significance is not clear. Modified from Mozdy and Shaw, 2003. (48)*

The mechanism of outer mitochondria fusion mediated by MFN1/2 involve the interaction of these proteins on opposite mitochondrial membranes. Mitofusins can form homo-dimers or hetero-dimers through the interaction of their HR2 regions. These interactions tether adjacent mitochondria prior to fusion. It was hypothesized that the hydrolysis of GTP, mediated by the GTPasic domain of the two proteins, could provide biomechanical energy for outer membrane fusion (49).

Since mitochondria are double membrane-bound organelles, fusion is a particularly complex process and fusion of inner mitochondria membranes must follow that of the outer membranes. OPA1, is another highly conserved dynamin related protein that, contrary to mitofusins, is inserted in the inner membrane of mitochondria, with the C-terminal exposed in the intermembrane space. OPA1 acts during the phases of mitochondria inner membrane tethering and fusion, in a similar way to that described for mitofusins and, being able to interact with MFN1, is also involved in coordinating the fusion of outer and inner membranes (50, 51). Human *OPA1* is a large gene that originates several so called “long isoforms” by alternative splicing. These isoforms can be further modified by proteolytic cleavage, originating “short isoforms” that lack the TM domain and are able to diffuse in the intermembrane space.

Fission depends on the activity of dynamin-related proteins as well. In mammals two proteins are mainly involved in this process: dynamin-related protein 1 (DRP1), and FIS1. DRP1 is a

cytosolic GTPase, while FIS1 is inserted in the outer mitochondrial membrane. Through its tetratricopeptide repeat motifs (TPR), FIS1 interacts directly with DRP1 and targets it into large foci at the sites of mitochondria fission (52, 53). The understanding of the mechanisms of mitochondria fission were better clarified in yeast, where other proteins, beyond the orthologues of FIS1 (Fis1) and DRP1 (Dnm1), have been identified to contribute to mitochondria fission (54). Probably, as for mitochondria fusion, the mechanisms of fission in mammals are similar to that described in yeast and other proteins, as the already mentioned GDAP1, may be involved in the process.

The great dependance of neurons on mitochondria fusion and fission is demonstrated by the fact that mutations in several genes involved in these processes can lead to disorders of the nervous system. As previosly said, MFN2 and GDAP1 are both associated to CMT disease. Alterations of inner mitochondria membrane fusion can also induce neuropathy. In fact OPA1 mutations cause the most frequent cause of autosomic dominant optic atrophy (55) and paraplegin, a protease that cleaves OPA1 (56), is associated to a recessive form of hereditary spastic paraplegia that is frequently complicated by the presence of cerebral and optic atrophy (57). Moreover, a mutation in *DRP1* was identified in a newborn with a lethal syndrome characterised by microcephaly, absence of tendon reflexes and pail optic disks (58).

1.3.4: Mitofusin 1 and 2 have not completely redundant functions

Even though the mitofusin/fuzzy onions (Fzo) protein family is present from yeast to humans, the appearance of two mitofusins orthologues with ubiquitous expression has been described only in the vertebrate evolutive line. Indeed *Drosophila melanogaster* genome codes for two mitofusin like proteins: fzo and dmfn. However the expression pattern, more similar to that of vertebrates mitofusins, and the higher similarity, make dmfn the direct homologue of mitofusins rather than *Drosophila* fzo (59).

In all vertebrates analysed, mitofusin 1 and mitofusin 2 share a very high sequence similarity, but their function is far from be totally overlapping. First of all, although they are considered both ubiquitary proteins, their expression pattern is quite different. In rat the two proteins are expressed at a comparable level in liver, kidney, and adrenal glands, but show differences in brain, where Mfn2 is highly expressed and Mfn1 is present in traces, and heart and testis, where Mfn1 predominates (Fig. 1.3) (2). In man a similar expression pattern was described: mRNA of both mitofusins was detectable at high levels in several tissues, but *MFN2* mRNA

resulted specifically enriched in skeletal muscle and heart and that of *MFN1* in pancreas and liver (47).

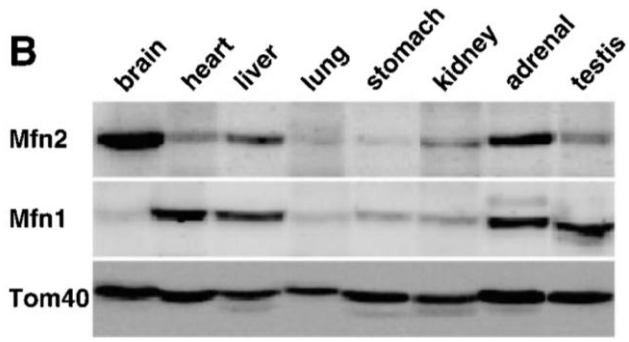

Figure 1.3: *Tissue expression of rat* Mfn *proteins. The total proteins prepared from indicated tissues of adult rat were subjected to immunoblotting using anti-rat Mfn2 (top) or Mfn1 (middle). An immunoblot against the mitochondrial protein Tom40 was used as a loading control (lower stripe) (2).*

Another difference between MFN1 and MFN2 concerns the GTPase functional domain. An active domain is essential for the function of both proteins, but *in vitro* studies demonstrated that MFN1 has a high GTPase activity but a low GTP affinity, while the contrary is true for MFN2. This implies that homotypic interactions of MFN1 are 100-fold higher than that of MFN2. It was speculated that MFN1 and MFN2 could be involved in different steps of mitochondria fusion: MFN1 should mainly induce the first step of mitochondria tethering, while MFN2 may be involved in the fusion process (60). An involvement of MFN1 in the coordination of outer and inner mitochondria membranes was also reported, as *in vitro* experiments demonstrated that MFN1 but not MFN2 is necessary for OPA1 function. (51).

The importance of mitofusins in development is demonstrated by the fact that in mouse the complete knock-out (KO) for either *Mfn1* or *Mfn2* results in embryonic death (61). Although both KO-mice die in midgestation, some distinctive phenotypic features in embryos and embryonic fibroblast derived cell lines (MEF) can be identified, thus leaning towards a differentiation of mitofusins function.

Heterozygous KO-mice are fertile and show any alteration, but in homozygosity the absence of mitofusins results lethal in both KO-lines, although at different stages. In Mfn1-KO live embryos can be recovered up to embryonic day (e) 10,5, but are completely resorbed by e12,5. Mfn2-KO show earlier lethality, since full viable embryos can be see only until e9,5, and are resorbed by e11,5. Interestingly KO-embryos show different developmental alterations. In Mfn2-KO defects of placenta are ascribed as the major cause of perinatal death. In fact at e9,5 Mfn2-KO embryos are only slightly smaller and show no obvious malformations, while the giant cells of trophoblast, the polyploid cells that give rise to the placenta, are reduced in quantity due to a diminished number of endoreplication cycles. This was not observed in Mfn1-KO embryos, that at e10,5 are significantly delayed in development and malformed, but

without morphological defects in trophoblasts. To assess the involvement of placenta defects in determining the unviable phenotype of mitofusin-KO mice, some conditional KO lines, where Mfn1 or Mfn2 are not depleted only in the trophoblasts, were developed. Surprisingly the conditional Mfn1-KO resulted vital and fertile, and survived through adulthood with no evident defects, thus demonstrating that indeed also Mfn1-KO lethality is due to a placental defect. On the contrary, conditional Mfn2-KO dies by postnatal day 17 and shows severe defects in movement and balance. These alterations were ascribed to defects in the development of cerebellum, particularly of Purkinje cells, which appear to have less branched and shorter dendrites and nuclear clustering of mitochondria. Since Purkinje cells have a high expression of Mfn2 but a very low presence of Mfn1, and given that their alterations in the conditional Mfn2-KO can be rescued with the same strength both by Mfn1 and Mfn2, it was inferred that the loss of mitofusin function in general, rather than the specific loss of mitofusin 2, was responsible for the phenotype (62). We can also argue that tissues where Mfn1 expression is lower, as neuronal tissues, are more sensible to the decrease of Mfn2 activity.

As for the effects on mitochondria morphology, some differences can be evidenced in KO-derived MEF cells (61). The loss of either Mfn1 or Mfn2 causes mitochondria fragmentation, but at a higher degree in Mfn1-KO cells. Very importantly, similarly to what happens in Purkinje cells, the mitochondrial fragmented phenotype of Mfn2-KO MEFs can be completely restored by the over-expression of both Mfn1 and Mfn2. Intriguingly, although both proteins are expressed in wt MEFs, in Mfn1-KO cells the tubular shape of mitochondria is completely rescued by Mfn1, but of only the 25% by the over-expression of Mfn2, thus implying that mitofusin 1 has a higher fusion capacity and that mitofusin 2 can have some distinct functions (61). However the importance of the integration of both Mfn1 and Mfn2 for the tubulated mitochondria morphology maintenance and particularly the significance of the formation of functional etero-dimers of Mfn1 and Mfn2 was also demonstrated. Indeed some Mfn2 CMT2A causing mutations lack mitochondrial fusion activity when expressed in MEFs lacking both Mfn1 and Mfn2, but show substantial fusion activity in cells expressing only Mfn1. This cooperation occurs *in trans* by the formation of hetero-dimers of Mfn1 and mutated Mfn2 (63), and a similar complementation was found also in yeast, where a fzo1 mutated in the GTPase domain could cooperate with one mutated in a HR region to promote mitochondrial fusion (64). This suggests that each subunit of the mitofusins oligomer need not be fully functional to provide function to the complex and further stresses the importance of MFN1 expression for

the manifestation of mitochondria alterations in cells with a lowered activity of MFN2, both due to MFN2 mutations or ablation.

1.3.5: Mitofusin 2 roles beyond fusion

As speculated by the mentioned complementation studies performed on knock-out MEF cells, in recent years it was demonstrated that MFN2 has a role not only in mitochondria membrane fusion, but also in mitochondria movement along microtubules, endoplasmic reticulum-mitochondria thetering and signaling. Here the state of art about these novel MFN2 functions and their possible relation CMT2A pathogenesis will be briefly treated.

Mitochondria movement

In a first work, Baloh and collegues reported that in cultured dorsal root ganglion neurons (DRG) the expression of disease-associated MFN2 mutant proteins induced alterations in mitochondria distribution, which resulted clustered in the soma or at the neuronal terminals. They also proved that the altered distribution of mitochondria is consecutive to a defect in mitochondria transport, which is however not dependent on a decreased ATP production (65). Interestingly a defect of mitochondria distribution in axons was reported also CMT2A patients. Electron microscopy of sural nerve biopsies shows the presence of distal clustering of fragmented mitochondria and a corresponding decrease of mitochondria along axons (40, 66, 67). In 2010 a direct interaction of MFN2 with the Miro/Milton motor protein complex was demonstrated (68). Miro is an outer mitochondrial membrane protein involved, together with the adaptor protein Milton, in the attachment of mitochondria to the motor proteins kinesin and dynein (69). MFN2 is able to interact with both Miro and Milton in a specific manner not dependent on fusion. As a consequence the absence of MFN2, or the expression of disease-related allele, specifically disrupts mitochondria movement in axons (68).

ER-mitochondria tethering

MFN2 is also involved in the endoplasmic reticulum (ER) and mitochondria juxtaposition. Indeed MFN2 is also expressed in the ER membranes, and is particularly enriched in the sites of contact with mitochondria. In MEF cells, ablation of Mfn2 disrupts ER morphology and detaches mitochondria from ER-membranes, thus demonstrating the importance of Mfn2 omodimers and Mfn1-Mfn2 heterodimers in the ER-mitochondria tethering (70). Contacts between ER and mitochondria are physiologically important in many cellular processes, since

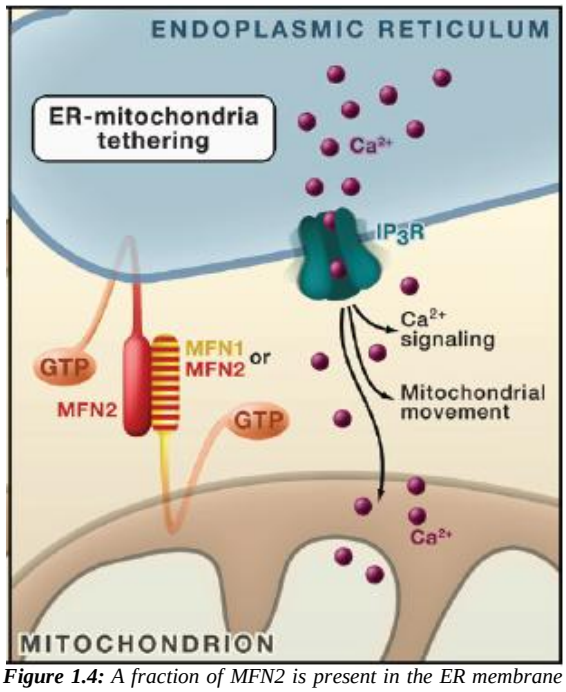

Figure 1.4: *A fraction of MFN2 is present in the ER membrane and assembles with MFN1 or MFN2 at the mitochondrial surface to tethes ER to mitochondria. ER-mitochondria juxtapositionis required for efficient Ca++ uptake into mitochondria and may have important implications for cell signaling and mitochondrial movement (1).*

they allow the regulation of Ca^{++} level in cells. In Mfn2 deficient MEFs, mitochondrial Ca^{++} uptake is indeed reduced, proving that a close apposition of the two organelles is crucial during Ca^{++} signalling. This may have important implications in many other cellular processes in which Ca^{++} signalling is involved, first of all the induction of apoptosis. Intriguingly Ca^{++} is also important for the regulation of kinesin-mediated mitochondrial motility, as an increase of Ca^{++} induces a conformational change in Miro, which becomes able to interact directly with kinesin and induce arrest of mitochondria movement (71).

Mitofusin 2 as a signalling protein

MFN2 acts not only as a tethering molecule, but has also signalling functions. Indeed MFN2, but not MFN1, has a p21Ras binding site at the extreme N-terminal, before the GTP-binding domain (72). MFN2 over-expression is able to induce cell cycle arrest by inhibition of the Ras-MAPK-ERK pathway. This was also demonstrated *in vitro* by the fact that hyperproliferating vascular smooth muscle cells (VSMCs), derived from spontaneously hypertensive rat arteries, show a down-regulation of MFN2 expression. In these cells the artificial over-expression of MFN2, and thus the inhibition of Ras pathway, is able to induce cell cycle arrest. This effect of MFN2 is however independent on its function in mitochondrial fusion (72) and ER-mitochondria tethering (73), but suggests a possible contribution of MFN2 in proliferative cardiovascular disorders and potentially other proliferative diseases as cancer. Intriguingly a mutation in MFN2 in a kindred with recurrent strokes occurence was identified (74) and two patients with MFN2 mutation causing a neuropathy with pyramidal signs showed also vasomotror troubles (75).

Project aims

Mutations in mitofusin 2 gene (MFN2) account for the most common variant of axonal Charcot-Marie-Tooth disease (CMT2A), an inherited disorder of the peripheral nervous system. This pathology is characterised by phenotypic variability and reduced penetrance and, even if more than 80 MFN2 mutations have been described, a clear genotype-phenotype correlation was not identified. Mitofusin 2 is localised in the outer mitochondria membranes and endoplasmic reticulum. It is a multifunctional protein, and its main functions are the tethering of mitochondria prior to fusion, the ER-mitochondria juxtaposition and the axonal transport of mitochondria. Both in vitro and in vivo studies have been performed in order to clarify the mechanism of action of MFN2 mutations. In vivo studies resulted particularly complicated in mouse, and future investigations would certainly benefit of new models of the disease. Very interesting indications may come from the zebrafish (Danio rerio), an animal model that recently proved to be an excellent tool for the study of neurological disorders. In order to contribute to the identification of a genotype-phenotype correlation and evaluate new models of the disease, with this project I propose to:

a) Perform a genetic screening of MFN2 gene in a cohort of patients affected by axonal CMT. This analysis will be conducted by direct sequencing, and MLPA (multiplex ligation-dependent probe amplification), in order to evaluate both point-mutations and MFN2 gene rearrangements.
b) Evaluate zebrafish as a model for CMT2A. First, to study the role of mfn2 gene in the development of zebrafish neuromuscular system, I will perform knock-down experiments of this gene using a morpholino-oligo. Then I will evaluate the ability of human MFN2 transcript to complement for the loss of zebrafish mfn2. This will allow to assess if human and zebrafish proteins are functionally conserved. In order to elucidate the mechanism of action of MFN2 mutations, I will also study the CMT2A disease causing mutation R94Q using zebrafish as a model. In particular, by performing rescue experiments with the mutated transcript, I will evaluate if this allele has a loss of function activity. On the other hand, over-expression experiments will be performed to evaluate the gain of function activity of the R94Q allele.

Chapter 2: Analysis of MFN2 mutations in CMT2A patients

2.1: Background

2.1.1: MFN2 mutation distribution in CMT2A patients and inheritance patterns

To date more than 80 disease causing mutations have been described in *MFN2*. As illustrated in figure 2.1, most of them cluster in the GTPasic domain and in the region linking this domain with the HR1 region. However some mutations in or around the HR regions, even much rarer, have also been found in CMT2A patients. Most mutations are missense and with a dominant inheritance. Phenotypically a surprisingly high percentage of non-penetrance associated to an elevated variability in the phenotypic expression, also among people of the same kindred, was reported. A total of 4 nonsense and 2 frameshift mutations have also been described. Interestingly 3 of these mutations were found to have a recessive inheritance pattern and were reported in patients with compound heterozygous *MFN2* mutations. Indeed 8 cases of recessive inheritance of MFN2 mutations were reported so far (40, 66, 75-77).

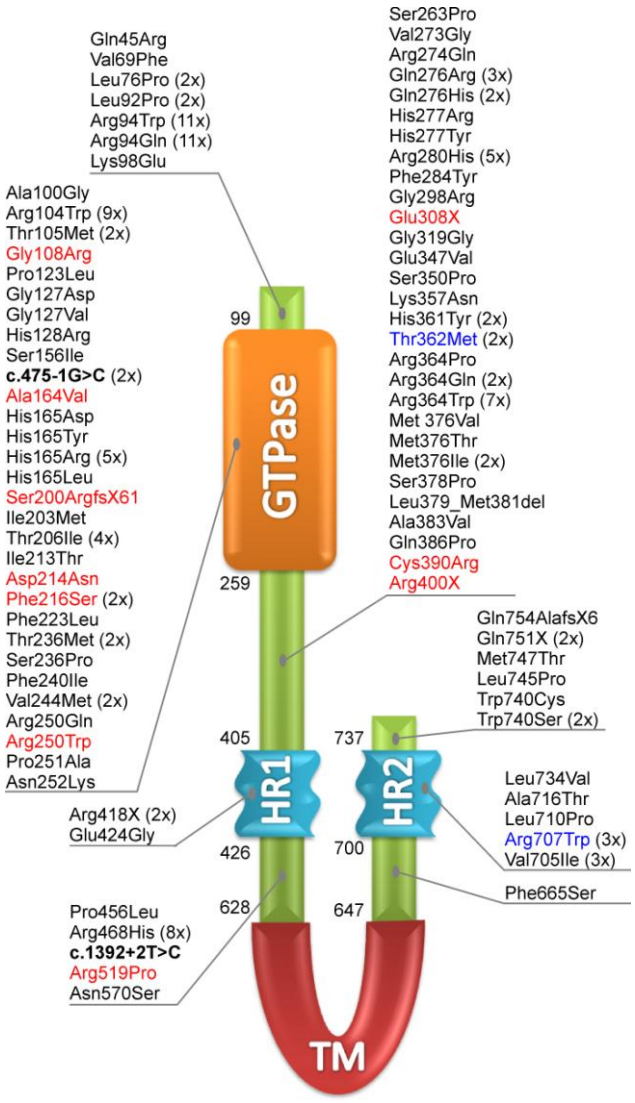

Figure 2.1: *Schematic representation of the human* MFN2 *protein. Mutations found in CMT2A are indicated with their corresponding frequency. Abbreviation: HR; heptads repeated region, TM; transmembrane domain. In red are mutations found only in homozygous or heterozygous state, in blue that found both recessively and dominantly inherited. In bold are indicated intronic mutations on splicing-sites.*

Some positions of the protein appear to be more frequently mutated and mutations in these sites were reported several times in independent works. Above all the arginine at position 94 appears particularly prone to mutations, being the substitutions R94Q and R94W described 11 times each. Since R94Q and R94W were reported several times in patients with a *de novo* mutation, it is reasonable that 94 position represents indeed a mutational hot spot (78).

2.1.2: Phenotype-genotype correlation hypothesis

Although the severity of the phenotype induced by *MFN2* mutations and the presence of complicating additional features can be extremely variable among patients (see paragraph 1.3.1), on the basis of age at onset and severity of the disease, two main clinical groups can be identified. In the first group are included patients with an early onset, generally before 10 years, and a severe phenotype, frequently complicated by other symptoms, especially optic atrophy. The second group comprise patients with a later onset, after 10 years, and a milder course of the disease (40). Interestingly pyramidal signs were reported preferentially in patients with mild or moderate forms of CMT2. This is possibly due to a masking effect of pyramidal signs when an important peripheral motor neuropathy is present (75). Even if this clinical subclassification is, with rare exceptions, always observed, it does not reflect an evident genotypic-phenotypic correlation. For example it is reported that mutations located in the GTPasic domain or in the HR regions are able to induce similar phenotypes. The only exceptions are the mutation R418X (40) and P456L. The nonsense mutation R418X is located in HR1 and it potentially causes the expression of a truncated form of MFN2 lacking the transmembrane domain (TM), which therefore would not insert in the outer mitochondrial membrane. *In vitro* studies demonstrated that a mutant form of MFN2 deprived of the TM domain is able to act as a dominant negative allele (79). Interestingly the patient bearing the R418X shows an extremely severe CMT2 phenotype, characterised by onset in infancy, wasting of distal and proximal muscles and vocal cord paresis. However no functional studies have been performed on this mutation that can support the hypothesis that it acts with a dominant-negative mechanism. The other mutation, P456L, positioned between HR1 and TM, was found in a patient with early onset cerebral stroke. The patient showed any clinical or electrophysiological sign of neuropathy. The father, from who she inherited the *MFN2* mutation, showed white matter lesions probably due to unawared stroke events, and similarly to his daughter, has no signs of motorneuron alterations at ENG (74).

The only observation supporting the existence of some genotypic-phenotypic correlation in CMT2A is the fact that individuals with homozygous or compound heterozygous MFN2 mutations have the tendency to manifest a more severe phenotype. Indeed, even if CMT2A was originally reported as an autosomal dominant disease, in the last years is growing the evidence that *MFN2* mutations are recessively inherited in a significant number of families. To date a total of six kindred with recessive inheritance have been reported (40, 66, 75, 76). The proband, usually a son of two unaffected parents, tends to have an extremely early onset and a severe phenotype. The parents are typically unaffected, although sometimes can have some subclinical signs. Some mutations, are found only in homozygous or heterozygous state, thus meaning they may have a real recessive inheritance. Other mutations, as for example T362M, were found also to have dominant inheritance. Nevertheless, when present in heterozygosity, T362M cause a mild phenotype, but when associated to other missense mutations (A164V) it causes an extremely early onset and severe disease.

Altogether these results demonstrate the difficulties in determining a genotype-phenotype correlation and stress the importance of deeper studies of the molecular mechanisms through which different *MFN2* mutations can induce CMT2A disease.

2.1.3: Mechanism of action MFN2 mutations

Several *in vitro* studies were conducted with the aim to identify the mechanism of action through which mutations in *MFN2* gene leads to CMT2A disease.

In the only extensive functional study published so far, Detmer and Chan analysed 9 *MFN2* diseases causing mutations using KO-MEF cells and they first hypothesized that different molecular mechanisms could be responsible for the effect of different *MFN2* mutations (63). This hypothesis is based on the observation that in the absence of both mitofusins, a moderate over-expression of some mutations is able to recover the fragmented mitochondrial tubules with the same strength of wt *MFN2*, while other mutations result non-functional. Intriguingly all the non-functional alleles are in position conserved in MFN1 and MFN2, thus suggesting a possible explanation for their different ability to recover mitochondria fragmentation in double KO-MEFs. They also observed that in cells expressing only the non-functional alleles, the over-expression of *MFN1* but not *MFN2* is able to recover the phenotype. In an elegant series of complementation studies, they demonstrated that *MFN1* is able to cooperate with mutant *MFN2* to promote mitochondria fusion through the formation of functional hetero-oligomers in

trans, in a way that is independent on the presence of a fully functional GTPase domain. This effect, observed also in yeast *fzo1*(64), underlies the importance of *MFN1* for the phenotypic manifestation of *MFN2* mutations and supports the hypothesis that tissues expressing less MFN1 are more prone to suffer mitochondrial dynamics alterations in the presence of mutated MFN2.

The work of Detmer and Chan is somewhat limited by the fact that they screened cells expressing mutant *MFN2* only for mitochondria alterations, while recently an involvement of MFN2 in axonal transport of mitochondria and ER-mitochondria tethering was verified.

In the works where Baloh and Misko demonstrate a role of MFN2 in mitochondrial axonal transport (65, 68), an analysis of the effects of some disease related *MFN2* mutations on mitochondria transport was also performed. They showed that in wt-DRG neurons, the expression of mutated *MFN2* induces proximal and distal clustering of mitochondria, similarly to what observed in patients. Interestingly the mutations R94Q an L76P, that Detmer described as fusion "uncompetent" and "competent" respectively, have a similar effect on the alteration of mitochondria movement (65). Misko further demonstrated that *MFN2* mutations do not disrupt the interaction of MFN2 with Miro and Milton proteins, and propose that the disruption of mitochondrial transport could be caused by an altered regulation of the kinesin transport apparatus (68).

Informations about the capacity of mutations in *MFN2* to alter ER-mitochondria tethering are available only for the R94Q mutation. De Brito and Scorrano demonstrated that, contrary to wt MFN2, R94Q cannot complement the ER morphological alterations of *Mfn2*-KO cells, nor recover ER-mitochondria tethering (70).

All these results are promising and we could speculate that possibly *MFN2* mutations act by inducing ER-mitochondria detachment. This alters Ca^{++} exchange, which is necessary for the correct activity of the motor proteins involved in mitochondria movement. However many questions about the mechanism of action of *MFN2* mutations remain to be elucidated. In particular it is not explained why mutations can have different phenotypic manifestations and why some are active only in heterozygous or homozygous state. Some important clues may come from the generation and study of animal models.

2.1.4: Animal models of CMT2A

Attempts to model CMT2A disease were made uniquely in mouse. As discussed in chapter 1.3.4, the complete knock-out of either *MFN1* or *MFN2* is lethal mainly due to placental defects (61). Intriguingly the conditional *MFN1*-KO, in which mitofusin is expressed only in the placenta, is vital and phenotypically normal, while that for *MFN2* shows motor abnormalities, which were however ascribed to alterations in cerebellum, rather than in the peripheral nerves (62).

Some mouse models expressing *MFN2* disease related mutations were also developed. A first attempt to model *MFN2* mutations was the generation of a mouse knock-in line for the common mutation R94Q (63, 80). Surprisingly heterozygous mice are vital and healthy, without any sign of neuropathy, while homozygous animals have severe movement defects and die by the third week after birth, hence much later than the complete *Mfn2*-KO. In addition alterations of mitochondria morphology in MEF cells derived from homozygous animals were not detected, and this was explained by the fact that in these cells Mfn1 is able to interact with $Mfn2^{R94Q}$ to complement the phenotype (63).

The absence of evident alterations in heterozygous mice expressing R94Q could also be justified by the differences between human and murine motorneurons: in humans with CMT only longer neurons are affected, whereas in mouse, characterised by shortest motorneurons than man, the effect of *MFN2* mutations could probably not disclose phenotypically. For this reason the authors derived also a mouse transgenic line overexpressing the mutation T105M (80). In this model the transgene ($Mfn2^{T105M}$) is driven by the HB9 promoter in order to overexpress the mutant protein only in the peripheral nervous system. HB9-$Mfn2^{T105M}$ mice show several phenotypic alterations that recapitulate some of the motor defects observed in CMT2A patients (abnormal gait, foot deformities, reduced number of motor axons, calf muscles atrophy). These defects are present only in homozygous animals, while heterozygous have only a slightly shortened tail, but retain a normal motor capacity. Alterations in the distribution of mitochondria along axons were also evident and aggregated mitochondria uneven distributed along axons could be noticed in homozygous animals. All these defects are congenital and indeed the HB9 promoter is expressed embryonically coincident with motor neuron formation and during the whole fetal life, but decreases dramatically by three weeks of age. The absence of a control transgenic line, overexpressing the wild type construct, and the fact that in cells the over-expression of MFN2 induces apoptosis (81), arose the suspect that the dose dependent phenotype of this transgenic mouse could be a side effect of the over-expression of the protein, rather than of the mutation itself.

Recently Cartoni and colleagues developed an alternative transgenic mouse model for the mutation R94Q. Also in this transgenic line the mutation is expressed specifically in the nervous system, but it is driven by the neuron specific enolase promoter (NSE). Compared with Hb9, NSE is active in the whole neural tissue starting embryonic day 13, but continues to function also after birth (82). The NSE-Mfn2^{R94Q} line shows several motor and phenotypic alterations reminding CMT2A disease. Interestingly, as the previously described model, the expression of the phenotype is dose dependent and was detected only in the homozygous animal. However a control transgenic line overexpressing the wild-type construct shows any phenotypic alteration. Thus it is reasonable to hypothesize that the phenotypic alterations found in NSE-Mfn^{R94Q} are a direct consequence of the expression of the mutation. An interesting feature, which was not observed in the previous models, is that the phenotype is evident starting 5 months after birth, thus mimicking further the degenerative feature of CMT2A disease. As described in the HB9-Mfn2^{T105M} line, a strong phenotypic variation among siblings of the same genotype can also be observed, probably due to slightly different levels of transgene expression. Finally the observation that in motorneurons with diameter smaller than 3,5 μm there is a distal accumulation of mitochondria, as observed in CMT2A patients, suggests that indeed defects in the retrograde movement of mitochondria could be the cause of the pathology.

Altogether these mouse models contributed to the understanding of the mechanisms by which mutations in *MFN2* leads to CMT2A. However many questions are still unresolved, and only the study of the genotype-phenotype correlations of *MFN2* mutations and the development of new animal models could finally lead to a complete comprehension of CMT2A disease.

2.2: Materials and methods

2.2.1: Patients analysed

In the present study a cohort of 25 patients diagnosed with axonal Charcot-Marie-Tooth disease where analysed for mutations in MFN2 gene. 13 patients were diagnosed in Padua Hospital (Clinica Neurologica) or were directed to our laboratory by the UILDM association branch of Padua. The remaining came from other hospitals of northern Italy. Elettroneurography was conducted on all patients, except patient 9 who was too young to perform the exam. A positive familiar history can be traced for 17 probands. All patients included in the study gave informed consent to carry out the genetic test.

2.2.2: Blood DNA extraction

Genomic DNA was isolated from blood samples using a modified protocol from (83). Briefly whole blood samples were diluted 1:4 with N-N solution (NaCl 0,9%, Nonidet 0,1%) to lyse erythrocytic membranes. Lymphocytes are recovered by a centrifugation at 6000 rpm for 30 min performed at 4°C. Cells are then resuspended in 4 ml of TEN solution (TrisHCl 10mM, EDTA 2 mM pH8, NaCl 400 mM) and 600 µl of SDS 10% and lysed 3 hrs at 80°C. The *salting-out* of proteins and cellular debris is performed by adding 1 ml of a NaCl saturated solution. The supernatant containing the genomic DNA is recovered by centrifugation at 6000 rpm for 10 min. To purify the DNA, 1 volume of chloroform is added and, after a centrifugation at 6000 rpm for 10 minutes, the supernatant aqueous phase containing the DNA is recovered and precipitated by adding 1 volume of isopropanol. DNA is recovered by centrifugation and washed 2 times with cold ethanol 70% solution, then resuspended in 300-500 µl of sterile TE solution (Tris HCl 10 mM pH 8, EDTA 1mM). The concentration and purity of DNA is then measured with NanoDrop 2000 (Thermo Scientific) and the integrity is evaluated by gel electrophoresis in 1% agarose gel. DNA is then stored at 4°C.

2.2.3: PCR amplification of MFN2 gene exons

The amplification of the coding regions of *MFN2* gene was performed by PCR using primers pairs designed on the intronic flanking regions of each exon. Since *MFN2* has 2 transcript variants, for reference we referred to isoform 1 (NM_014874) that has a longer 5'UTR.

Exon	Primers	Fragment length	DMSO	Ta	Program	Taq
1	**F: ccatgatgcagtgggagtc** R: gcttgactgcatcccagac	426	-	60	N	A
2	**F: ttgtttggcttgaaacctga** R: ctaagcaaccagcgaaatcc	423	-	60	N	A
3	**F: tgacctgagatccccatattc** R: atggcagttcccttgtcttc	483	-	60	N	A
4	**F: gccaccatagaggatctgga** R: cctggaacgttctgtgacct	377	-	60	N	A
5	**F: actggcaacattgcactgaa** R: tctcccattcacctccacag	397	-	60	N	A
6	**F: gtggaagaagaaagggtagc** R: gttgagcccatctgaaaggt	384	-	60	N	A
7+8	**F: caggtctgttctcagcagga** **R: cactagatccaggggtgcag**	489	-	60	TD	A
9	F: catgcccagcctcttatgac **R: gcctctctgctcttctcagc**	372	-	60	N	A
10+11	**F: ctgagaaggggatgctgaga** R: tgggagcccagagactca	579	-	60	TD	A
12	**F: tacctgggaaggggaagg** R: acagggccacaactttcttc	400	-	60	N	A
13+14	**F: aggctgctggtttgagagg** R: cagaacctgaaggtatcgagt	668	-	60	N	A
15	**F: atccctggcagtagctggta** R: ggaggcagggtacagactga	379	-	60	N	GO
16	**F: agccactctgtgtccctgtt** R: cagtggactgtggagtgtgg	371	-	61	N	FS
17	F: gaaacatgaaggctccttgg **R: acgatgcttaggacccagtg**	425	-	60	N	GO
18	**F: gctgctggcagggatataga** R: ccagcccatggtacacatct	399	8% v/v	60	N	A
19	**F: ggatgatgtaagggtgtgtgtc** R: tgcttcattctcttggcagt	300	-	60	N	A

Table 2.1: *Primers used to amplify human MFN2 gene, dimensions of amplification product and Taq and PCR conditions used. In bold are indicated the primers used for sequencing. Ta= annealing temperature; N=standard PCR program; TD=Touchdown PCR program; A=AmpliTaq Gold; GO=GO Taq; FS=FastStart Taq.*

Primers were designed with Primer3 (v. 0.4.0) using default settings. Conditions such annealing temperature (Ta), time of denaturation, annealing and extension phases, number of cycles, adding of DMSO and selection of Taq polymerase to be used were adjusted empirically. In some cases, to avoid the amplification of aspecific products, a touchdown

amplification program was used (84). Primer pairs and amplification conditions are described in table 2.1 while in table 2.2 are described the PCR programs used. All the PCR amplifications were conducted using AmpliTaq Gold (Applied Biosystem), GO Taq (Promega) or FastStart Taq (Roche) with the reaction mixes listed in table 2.3. PCR products were tested on a 2% agarose gel before sequencing.

A) Standard PCR program		
temperature	**time**	
95 °C	2-10 min	
95 °C	45"	x 33
Ta	45"	
72 °C	45"	
72 °C	10 min	
15 °C	5 min	

B) Touchdown PCR program		
temperature	**time**	
95 °C	2-10 min	
95 °C	45"	x 10
(Ta+10)-1 °C every cycle	45"	
72 °C	45"	
95 °C	30"	x 26
Ta	30"	
72 °C	45"	
72 °C	10 min	
15 °C	5 min	

Table 2.2: *details of PCR programs used .A) standard PCR program; B) touch-down PCR program.*

A) AmpliTaq Gold	
DNA (50ng/µl)	1 µl
Buffer 10X	1,5 µl
$MgCl_2$ (25mM)	1,5 µl
dNTPs (1mM)	3 µl
primer F+R (10 pmol/µl)	0,5+0,5 µl
MilliQ H_2O	6,9 µl
AmpliTaq gold (5U/µl)	0,1 µl

B) GO Taq	
DNA (50ng/µl)	1 µl
Buffer 5X (w $MgCl_2$ 7,5 mM)	3 µl
dNTPs (1mM)	1,5 µl
primer F+R (10 pmol/µl)	0,5+0,5 µl
MilliQ H_2O	8,42 µl
GOTaq (5U/µl)	0,08 µl

C) FastStart Taq	
DNA (50ng/µl)	2 µl
Buffer 5X (w $MgCl_2$ 20 mM)	1,5 µl
dNTPs (1mM)	2,5 µl
primer F+R (10 pmol/µl)	0,5+0,5 µl
MilliQ H_2O	7,9 µl
FastTaq (5U/µl)	0,1 µl

Table 2.3: *composition of PCR mixes used. A)Mix fof AmpliTaq Gold; B) Mix for GO Taq polymerase; C) mix for FastStart Taq.*

2.2.4: Direct PCR sequencing

To eliminate the unincorporated primers and dNTPs which could interfere with the sequencing reaction, 1 µl of ExoSAP-IT® solution (USB), containing exonuclease I and shrimp alkaline phosphatase, is added to 2,5 µl of freshly made PCR and incubated at 37 °C for 15 min and then at 80 °C for 15 min to inactivate the enzymes. At the end of the purification reaction, the sequencing primer (10 pmol) is added to the PCR and the sample is dried at 60 °C and sent to BMR genomics (www.bmr-genomics.it) to perform the sequencing reaction. Sanger sequencing was carried out using Applera BigDye version 3.1 and the automated sequencers ABI 3730XL and ABI 3100. The electropherograms were analysed with Chromas Lite version 2.01 and Seqman Pro 7.1.0 and aligned to the RefSeq of human *MFN2* isoform 1 (NM_014874). All nucleotidic differences were compared to dbSNP database (http://www.ncbi.nlm.nih.gov/projects/SNP). Differences in the coding sequence of MFN2 that were not reported as polymorphisms were analysed in at least 100 healthy subjects using Restriction Fragment Length Polymorphism (RFLP), when possible, or direct sequencing.

2.2.5: MLPA analysis of MFN2

Multiplex Ligation-dependent Probe Amplification (MLPA) is a relatively new method used to identify alterations in DNA copy number of up to 40 sequences in a single reaction (85). This method uses specific probe pairs that hybridize to genomic DNA in correspondence of every single exon of the gene to be analyzed. The probe pair consists of a short left probe (L) with a hybridization sequence specific for the target gene at the 3' end and a common 19 nucleotides sequence that is recognized by the reverse PCR primer, at the 5' end (Fig. 2.2). The long right probe (R), conversely, has the hybridization sequence at the 5' and the forward primer recognition sequence at the 3' end. In the R probe, between the hybridization sequence and the primer recognition sequence is included a stuffer sequence of different length for each probe pair. The probes are designed to hybridize adjacently to the target DNA and after ligation is possible to perform a semiquantitative multiplex PCR to amplify the derived fragments taking advantage of the common primer recognition sequences. Since the reverse primer used is fluorescently labelled and the stuffer sequence has different lengths for every probe pair, after PCR is possible to separate by capillary electrophoresis the fragments to obtain an electropherogram in which at every length correspond a probe pair that hybridize to a known exon and with a peak area that is proportional to the amount of that exon sequence in the

genomic DNA of the patient analyzed. Heterozygous deletions will appear as a reduction of 35-50% of the corresponding relative peak area. However the presence of point mutations in the vicinity of the ligation site will also cause the reduction of peak area. For this reason is always necessary confirm the absence of nucleotide substitutions by sequencing.

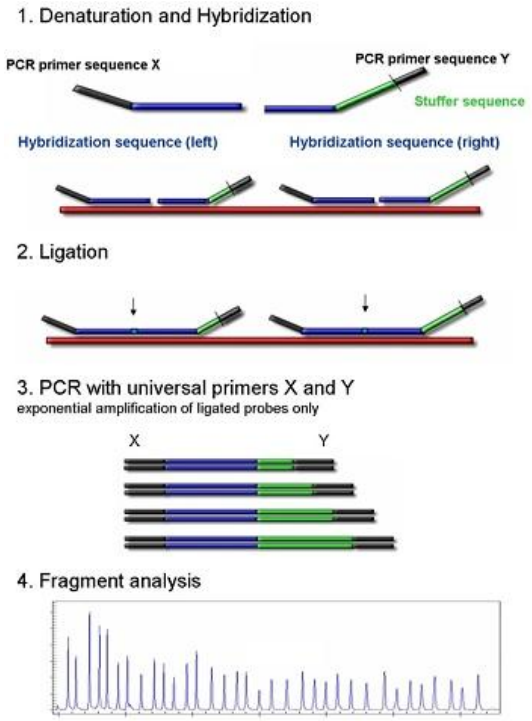

Figure 2.2: *step-by-step representation of Multiplex Ligation-dependent Probe Amplification (MLPA) procedure.*

To analyse if rearrangements of *MFN2* gene could be responsible of the disease in CMT2A patients that resulted negative by sequencing, MLPA analysis was performed with the MLPA kit P143 by MRC-Holland that allows the simultaneous detection of copy number variations in *MFN2* and *MPZ*, that is associated to CMT type 1B. The kit contains the probes for all the 19 exons of *MFN2* and for the 6 coding exons of *MPZ* and 10 control probes located in other human genes on different chromosomes. The reaction was performed according the manufacturer and the statistical analysis on electropherogram peak areas was conducted with the Coffalyser V6 software (MRC-Holland).

2.2.6: RFLP analysis of control DNA for nonpolimorphic changes found in MFN2 gene

Restriction Fragment Length Polymorphism (RFLP) was used to analyse the DNA of control subjects for the presence of *MFN2* non-polymorphic variations found in patients. DNA was

amplified with the primer pairs corresponding to the exon bearing the substitution, and restriction enzymes with the recognition site over the mutation (tab. 2.4) were used to digest the DNA. 5µl of PCR product were digested with 1-2 U of enzyme in the appropriate restriction buffer. The reaction was performed at the optimal reaction temperature of the enzyme for 2 hours. Then digested product were tested in a 2% agarose gel. At least 100 individuals were analysed for each mutation.

Restricion enzyme	**mutation**	**Wild-type fragments**	**Mutated fragments**	**Reaction temperature**
XmnI	c.987_989delAAG	147/431	578	37 °C
HpaII	c.2213C>T	118/182	300	37 °C
BsaJI	c.281G>C	377	261/116	60 °C

Table 2.4: *restriction enzymes used in the RFLP analysis of DNA from healthy control subjects. The fragment lenghts obtained from the wild-type and mutated allele are shown.*

2.3: Results

2.3.1: Screening of MFN2 gene in patients affected by CMT2A

Screening of *MFN2* gene was performed on all CMT2 patients. Only one affected proband was analyzed when a family with segregation of CMT2 disease was under study. The genetic analysis was performed on all the other family members for which the DNA was available, only when a nonpolimorphic substitution or a known mutation was found in the proband. In table 2.4 are summarised the major clinical and phenotypic features of the patients analysed, together with the results obtained by sequencing of MFN2 gene. Mutation in MFN2 gene were found in 5 subjects among the 25 CMT2 patients (20%). In the following paragraphs are illustrated in detail the results obtained for the patients 5, 7, 10, 21, 24, 26 and their relatives that were found mutated in MFN2

Patient ID	Sex	Age onset	Inheritance	UL involvement	MNCV (m/s)	Other symptoms	Mfn2 Mutation, status	Previous reported
1	M	<3 y	AD	-	40	-	-	
2	M	31 y	AD	-	43	-	-	
3	F	<29	AD	-	40	-	-	
4	F	?	AD	-	42	-	-	
5	F	<6 y	S	+	>38	OA	p.E329del, HZ	no
6	F	<31 y	AD	-	36,8	-	-	
7	M	9 y	AD	-	>38	-	p.A738V, HZ	no
8	F	<45 y	AD	-	42 m/s	-	-	
9	F	<7 y	na	-	NA	HL, WMA	-	
10	M	16 y	AD	+	>38	-	p.R94P, HZ	no
11	M	<48 y	S	-	4	-	-	
12	F	7 y	AD	+	35	-	-	
13	M	<11 y	AD	-	44	-	-	
14	F	<27 y	AD	+	>38	-	-	
15	F	<9 y	S	-	41	-	-	
16	F	46 y	S	+	45	-	-	
17	F	50 y	AD	-	40	RP	-	
18	M	10 y	S	+	47	-	-	
19	M	<18 y	S	-	45	-	-	
20	F	<45 y	AD	-	40	-	-	
21	F	<35 y	na	+	38 m/s	-	p.H165R, HZ	(40, 41, 86)
22	M	<1 y	S	+	>38	D	-	
23	F	<35 y	AR	-	40	-	-	
24	M	3 y	AR	+	NE	OA, RF, FMA, D, HL	p.[K38del] +[T362M], CHZ	no, (41)
25	M	5 y	AD	-	55	HL, OA, E	-	

Table 2.5: *Clinical findings of CMT2 patients analysed. Abbreviations: AD: autosomal dominant; AR: autosomal recessive; S: sporadic; na: not available; ne: not evocable; HL: Hearing Loss; D: dysphonia; OA: optic atrophy; RP: Retinitis Pigmentosa; RF: Respiratory failure; E: epilepsy; FMA: facial muscle atrophy; WMA: white matter alterations; HZ: heterozygous; CHZ: compound heterozygous.*

Patient 5

The patient showed difficulty in walking and muscular asteny from 1 year of age. She was operated to lengthen the Achilles tendon at the age of 6 and 18 years. Over the years she suffered of a gradual hypotrophy of lower limb distal muscles and from the age of 34 she started to show weakness of right hand muscles. EMG evidenced a severe axonal sensorymotor neuropathy of lower limbs, with a consistent peripheral denervation. Bilateral optic atrophy was diagnosed at the age of 38 and caused a severe loss of visual acuity. Her parents are referred healthy and nonconsanguineous.

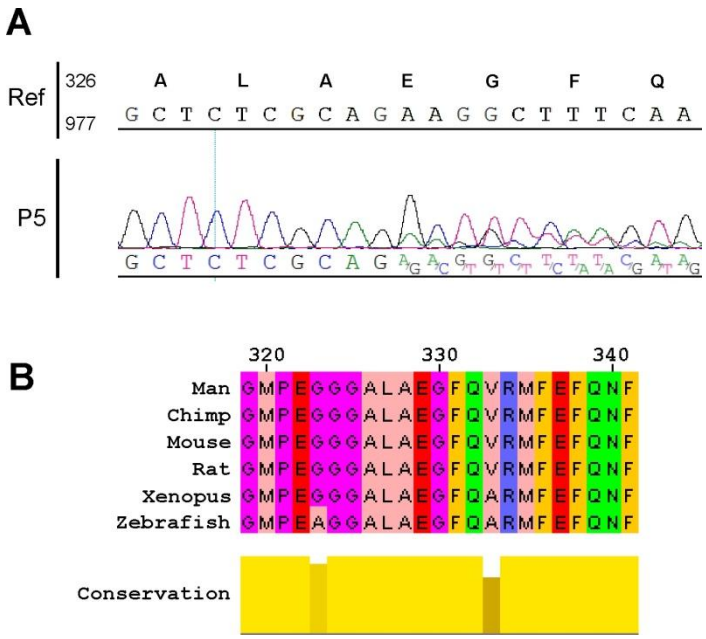

Figure 2.3: *A) electropherogram obtained by sequencing of exon 10 of MFN2 in patient 5; B) alignment of* MFN2 *proteins of various organisms illustrating the conservation at aminoacid residue 329.*

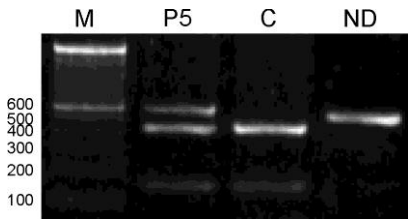

Figure 2.4: *RFLP analysis for the identification of c.987_989delAAG MFN2 mutation using XmnI restriction enzyme. P5; patient 5, C, not mutated control; ND, not digested PCR product.*

The sequencing of MFN2 revealed a heterozygous in frame deletion of 3 nucleotides in exon 10 (c.987_989delAAG) which result in the aminoacidic deletion p.E329del in a conserved position of the protein between GTPasic domain and coiled coil region HR1(Fig. 2.3).

Since this variant was never been reported in literature, the DNA from healthy control subjects was analysed. Given that the deletion causes the loss of a sequence recognition site for the restriction enzyme XmnI, RFLP technique was used (Fig. 2.4). None of the 200 chromosomes analysed resulted bearing the mutation and it is reasonable to conclude that the p.E329del deletion is the disease causing mutation in patient 5.

Patient 7

The proband (III-3) showed walking difficulty from the age of 9 and was operated to correct pes cavus at the age of 15. The EMG show the reduction of compound motor action potential amplitudes (CMAP) in both sensory and motor nerves and is compatible with a sensorymotor neuropaty of axonal nature. Also the sister (III-2) and the father (II-2) showed difficulty in walking, as well as other relatives related through their father (I-1, II-3 and II-4).

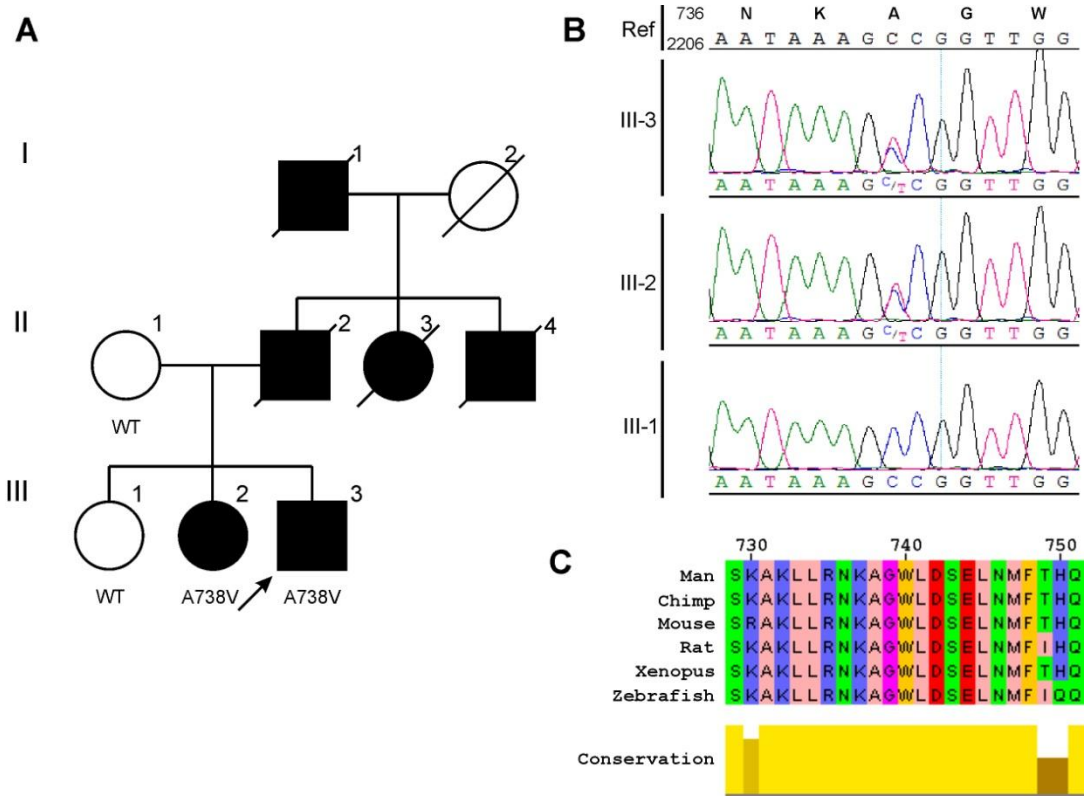

Figure 2.5: *A) family pedigree of patient 7. B) Electropherogram obtained by sequencing of exon 19 of MFN2 in patient 7 and in the indicated other members of the family; C) Alignment of* MFN2 *proteins of various organisms illustrating the conservation at aminoacid residue 738.*

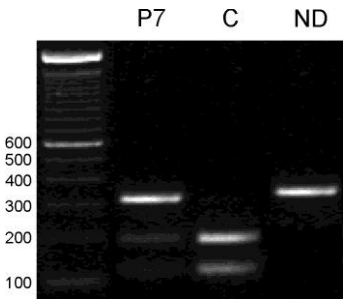

Figure 2.6: *RFLP analysis for the identification of c.2213C>T MFN2 mutation using HpaII restriction enzyme. P7; patient 7, C, not mutated control; ND, not digested PCR product.*

In the proband and in his affected sister (III-2) was identified a heterozygous single nucleotide substitution in exon 19 of MFN2 (c.2213C>T), leading to the missense mutation p.A738V (Fig. 2.5). The c.2213C>T substitution was not found in the unaffected sister (III-1) and in the mother (II-1) of the proband. The DNA from the other members of the family was not available.

Also this mutation was never proviously reported in literature and the analysis of the DNA of unaffected subjects by RFLP using HpaII restriction enzyme revealed that none of the 200 chromosomes

analysed bears the substitution (Fig. 2.6). For this reason we can conclude that A738V is the mutation causing CMT2A in this family.

Patient 10

The proband (III-2) showed difficulty in walking from the age of 16 years. The disease progressively worsened into a severe flaccid tetraparesis associated to distal hypotrophy and mild alterations of sense in the lower limbs. EMG evidenced a marked motor and sensory polineuropathy. Subject III-1 is also affected from the age of 15 years and has the same symptoms observed in the proband. The mother (II-2), is mildly affected, shows only *pes* cavus, while the aunt (II-3) has the same clinical picture of the proband, with a milder phenotype.

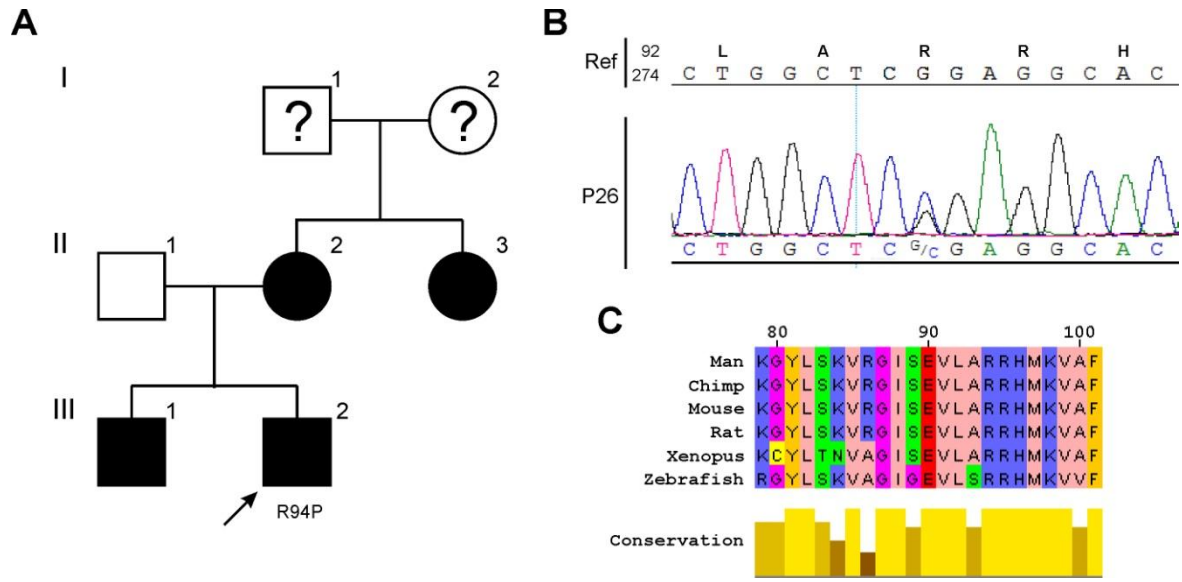

Figure 2.7: *A) family pedigree of patient 10. B) Electropherogram obtained by sequencing of exon 4 of MFN2 in patient 10; C) Alignment of* MFN2 *proteins of various organisms illustrating the conservation at aminoacid residue 94.*

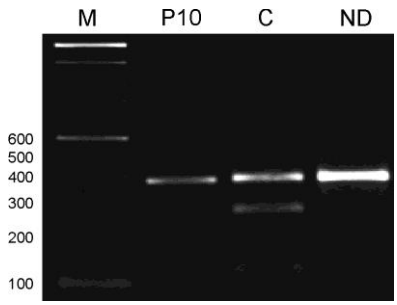

Figure 2.8: *RFLP analysis for the identification of* ***c.281G>C*** *MFN2 mutation using BsaJI restriction enzyme. P10; patient 10, C, not mutated control; ND, not digested PCR product.*

Only the DNA of the proband was available for this family. The analysis revealed the presence of the heterozygous substitution c.281G>C in exon 4 leading to the missense mutation p.R94P (Fig 2.7).

This undescribed mutation was not present in 300 healthy subject chromosomes analysed with RFLP using the restriction enzyme BsaJI (Fig 2.8). For this reason and considering that codon 94 is considered a mutational hot spot of *MFN2*, we can conclude that p.R94P is the causing mutation in this patient.

Patient 21

The patient underwent neurological investigations because affected by carpal tunnel syndrome. Through EMG study she was diagnosed a mild peripheral neuropathy involving both upper and lower limbs with a slightly reduced nerve conduction velocity.

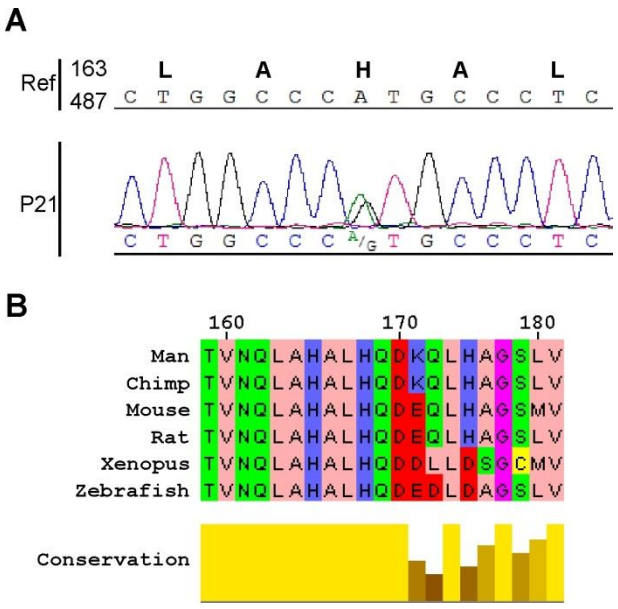

Figure 2.9: *A) Electropherogram obtained by sequencing of exon 6 of MFN2 in patient 21; C) Alignment of* MFN2 *proteins of various organisms illustrating the conservation at aminoacid residue 165.*

The sequencing revealed the mutation c.494A>G in heterozygosity in exon 6 that leads to the aminoacidic substitution p.H165R (Fig. 2.9). This mutation was previously reported in 4 unrelated kindreds with autosomal dominant inheritance (40, 41, 86).

Patient 24

The patient experienced frequent fallings and hyposteny of lower limb muscles from the age of 3 years and became wheelchair dependent from the age of 12. The disease was slowly progressive and later involved also the upper limbs and facial muscles. Also the respiratory muscles were involved and she uses a ventilator during the night from the age of 29 years. In the same period she was also diagnosed a bilateral optic atrophy. She suffers of sensorineural hearing loss from the age of 36. The EMG evidenced a nearly complete denervation of both upper and lower distal muscles. Two brothers (II-1 and II-4) of the proband show a similar clinical picture, while the parents (I-1 and I-2) and a sister (II-3) are referred healthy.

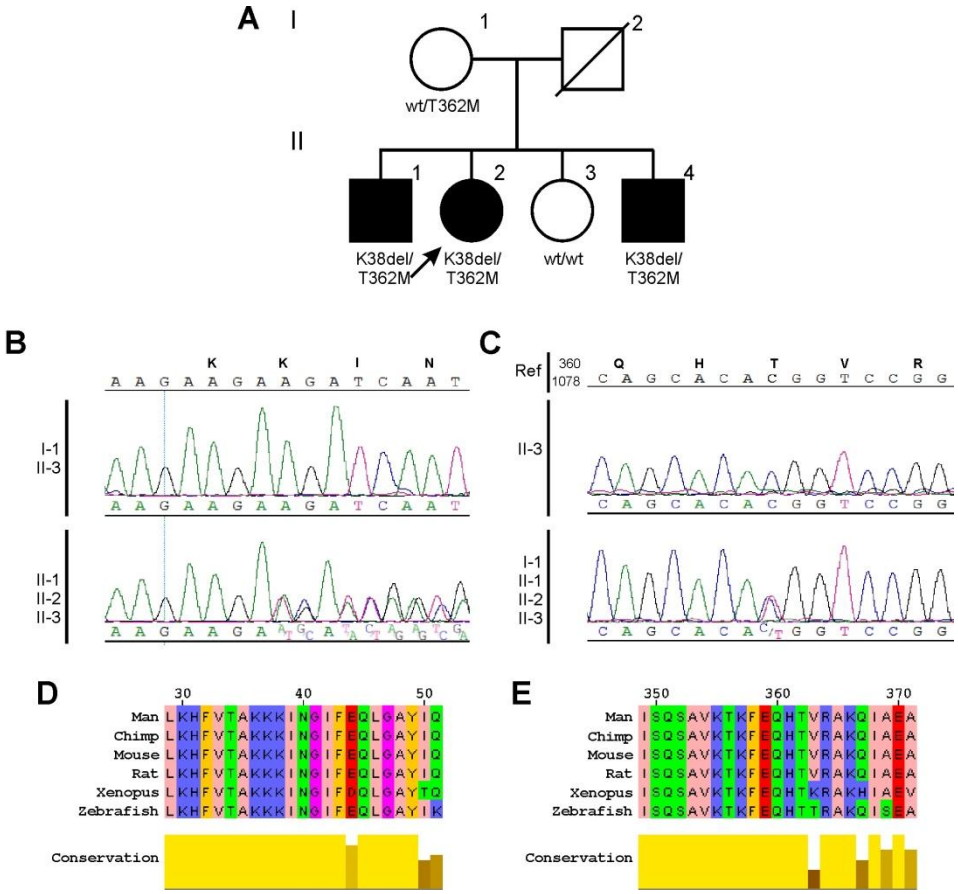

Figure 2.10: *A) family pedigree of patient 24. Electropherograms obtained by sequencing of exon 3 (B) and exon 11 (C) of MFN2 in the indicated subjects of the family of patient 10; Alignment of* MFN2 *proteins of various organisms illustrating the conservation at aminoacid residues 38 (D) and 362 (E).*

The sequencing revealed the presence of two *MFN2* mutations in *trans* in the proband (II-2) and in the other affected members of the generation II (Fig. 2.10). One is a previously reported missense mutation (c.1085C>T) leading to the aminoacidic substitution p.T362M (41), that was inherited from the mother. The other is an unreported 3 nucleotides in frame deletion (c.113_115delAGA) leading to the mutation p.Lys38del, that was probably inherited from the father, of which the DNA was not available. This mutation was not found in 400 healthy subjects analysed by sequencing.

2.3.2: MLPA analysis

Direct sequencing is a very sensible method for the identification of single nucleotide changes and small insertions and deletions. However it is inadequate for the detection of large genomic rearrangements involving entire exons or genes. Recently is growing the idea that relatively small rearrangements involving few exons can be an important cause of disease. A first case of a patient with CMT2A bearing deletion involving exons 7 and 8 of *MFN2* was just described

(77). For this reason we further analysed the DNA of subjects that resulted not mutated by sequencing of *MFN2* gene, using MLPA technique. We also performed the MLPA analysis on 5 healthy subjects as a control. A statistical analysis of the resulting electropherograms was performed with the program Coffalyser. A heterozygous deletion should give a reduction of the peak area corresponding to the probe annealing to that exon of about the 35-50% compared to that of a control subject, and a similar gain should be noticeable in the case of a duplication. A loss of a peak, instead, constitutes a homozygous deletion. None of the analysed patients showed any deletion or insertion in *MFN2*

.

Chapter 3: Effects of down-regulation of MFN2 and analysis of R94Q mutation effect in zebrafish

3.1: Background

3.1.1: Zebrafish as a model organism

In the last 15 years the tropical freshwater fish *Danio rerio*, commonly known as zebrafish, has been stated as the leading vertebrate model for developmental studies. As early as the 1930s, this little teleost have been appreciated by developmental scientists for the ease of maintenance, the exceptional spawning ability, the short generation time and the rapid external development, which, unlike other vertebrate models, allow the observation and the manipulation of the very first developmental stages. More recently the evolution of genetic techniques, as cloning, mutagenesis and transgenesis, previously amenable only in other more common animal models as *Drosophila* and mouse, prompted the use of this fish in other fields of biology, and in particular for the study of human diseases.

Zebrafish is easily maintained in specialized facilities in water kept within a 25-28,5 °C temperature range. Spawning can be induced easily, by regulating feeding and the light-dark cycle. It is an extremely prolific animal and each female can generate clutches of 100-200 eggs, which are externally fertilised by the male and can be easily recovered at the bottom of a spawning chamber. Embryos are transparent and development can be followed *in vivo* and in real time. Organogenesis is particularly rapid: at 24 hours post fertilisation (hpf) most organ primordials have formed and by 48-72 hpf larvae hatches and are able to move and react to stimuli (Fig. 3.1).

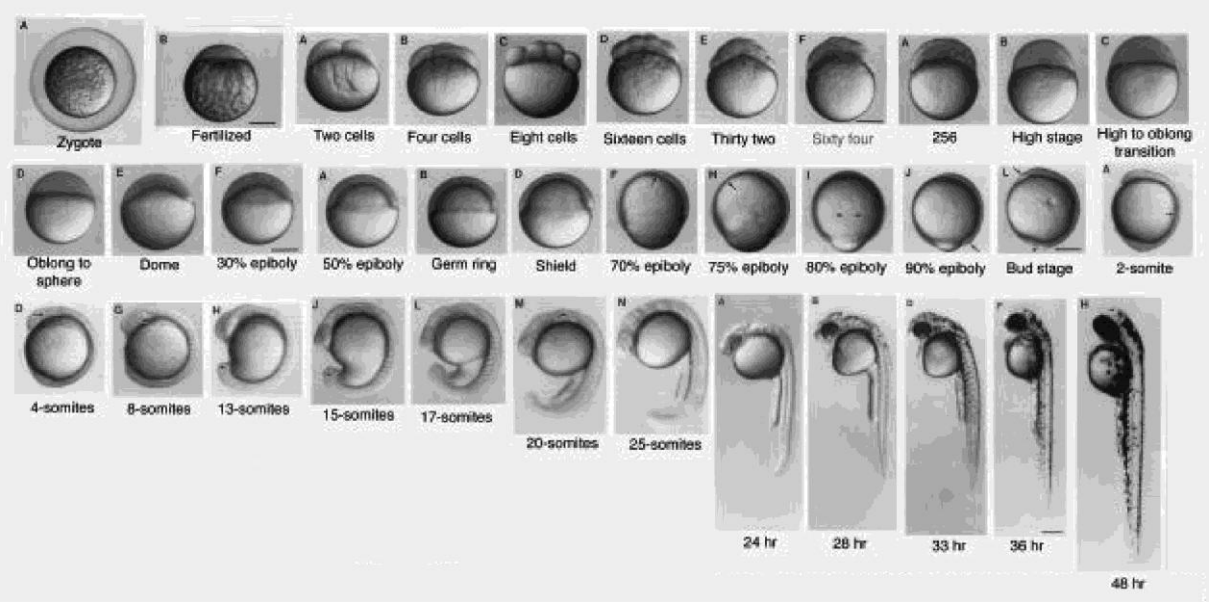

Figure 3.1: *representation of developmental stages of zebrafish embryos from 1 cell stage to 2 days post fertilization. Modified from Kimmel et al (1995).*

Despite the 400 million of years of evolution, it was found that many human genes have an orthologue in zebrafish. Bioinformatical analysis on the zebrafish genome, whose sequencing project, sponsored by the Sanger institute, started in 2001 and is now in completion, showed also that extensive chromosomal regions retain a well conserved sinteny (88). Interestingly, it was shown that zebrafish genome contains more genes than that of humans, and this is a result of a duplication that probably occurred 100-400 million years ago (89, 90). As expected by the genetic similarity, man and zebrafish organs are remarkably similar at morphological, physiological and molecular level.

All this characteristics made zebrafish an invaluable animal model for the study of several human disease, from cancer (91) to Alzheimer (92), and this was also recognized by the NIH through the establishment of the Trans-NIH Zebrafish Coordinating Committee in 1997. As research is ongoing, scientists can rely on increasingly genetic and genomic informations, which are collected in the *Zebrafish Model Organism Database* (ZFIN) available on the web (http://zfin.org). This provides an integrated representation of mutants, genes, genetic markers, mapping panels, publications and community resources.

Being little and particularly permeable to any small molecule dissolved in the water, zebrafish is also well-suited for use in chemical screens and in the last years this stimulated the beginning of several drug screening programs that can count on a growing number of chemical libraries (93). Hence zebrafish potentials in the field of human diseases go far beyond the

modelling of pathology and potentially it could reach also a fundamental role in pharmaceutical drug discovery.

3.1.2: Genetic analysis using zebrafish

Similarly to the widely used invertebrate models *Drosophila* and *Caenorhabditis*, zebrafish is particularly suitable to forward genetics approaches. However in the last years, with the advent of genomic era and the sequencing of zebrafish genome, now in completion, many reverse genetics strategies have also been developed, that can make this little teleost a fundamental complement of studies in mammal models. Here will be discussed briefly the many genetic technologies that have been developed over the years, with particular attention on the more recent reverse genetic approaches.

Forward genetic

Forward genetic analysis relies on the availability of mutant libraries and efficient and rapid mutagenesis screening methods. Although exceptionally successful in invertebrates, this approach has been historically of limited use in mammals model systems.

The zebrafish, unlike most vertebrate organisms, lends itself remarkably well to forward genetic approaches. The ease of keeping many fishes in a small space, the large brood size, the diploid genome, and the reasonably short life cycle, render large-scale genetic screens practical and economical. Forward genetics is driven by phenotypes: mutagens, as ethylnitrosourea (ENU), are employed to produce random changes in the DNA and the phenotypic consequences are assayed. Zebrafish is resistant to ENU toxicity and the phenotypic consequences of mutations can be easily screened under the microscope. Two large scale mutagenesis screening were performed, which focused on early development and led to the identification of 1800 mutants. They represented a great achievement and deserved the definition of an “accomplishment of historic proportions” in Science (94) and a special issue of Development (95). Random mutagenesis using retroviral methods has also been successfully carried out in zebrafish (96, 97). This method, although lower in efficiency than ENU mutagenesis, has the advantage to tag each insertion event, thus facilitating the mapping of the mutation. These forward-genetic screening recovered also numerous mutants in genes orthologues to that involved in human diseases. In some instances, the phenotype of the mutant was so similar to that of man that could be identified by a candidate gene approach. One example is the zebrafish mutant *sapje*, which display several muscular defects that phenocopies

the alterations found in patients with Duchenne muscular dystrophy and it was found to be due to a nonsense mutation in the orthologue of human dystrophin gene (98).

Reverse genetics

Reverse genetic is driven by genes and studies the phenotypic consequences of the disruption or over-expression of the gene of interest. The major limitation is the fact that it relies on the knowledge of the genomic location of genes and the possibility to alter their expression in a site-directed way. With the advent of genomic era and the sequencing of zebrafish genome, informations about zebrafish genes are now easily recovered. Further, besides the absence of a gene targeting technique by homologous recombination similar to that of mouse, many ways to specifically knock-down or induce the expression of genes have been developed in this model organism.

Zebrafish embryos develop externally and during the first four cellular divisions the blastomeres are open to the yolk. This allows the delivery of nucleic acid molecules directly in the fertilised egg through microinjection. In this way transient interference or over-expression of genes is easily achievable and, being the first developmental stages of zebrafish fast, the effects can be rapidly screened. To induce the down-regulation of the gene of interest, the most widely used technique is the microinjection of antisense morpholino phosphorodiamidate oligos (morpholinos or MOs), antisense nucleic acid analogs in which a morpholine moiety replaces the pentose ring (Fig. 3.2). Due to their small size and altered chemistry, MOs are more stable and do not trigger the immune response of the organism.

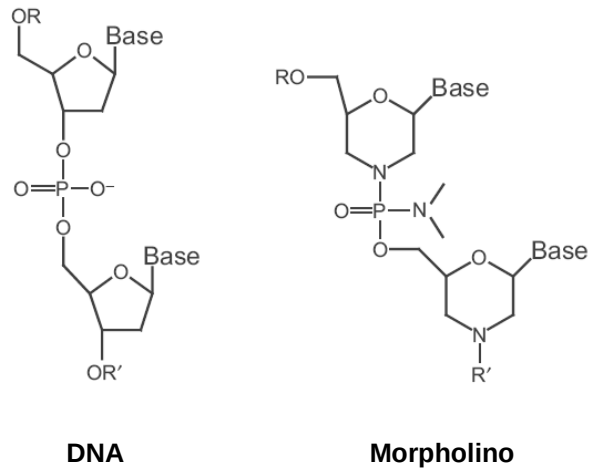

Figure 3.2: *Comparison of the chemical structure of DNA (A) and morpholino (B) molecules.*

MOs, that typically are long 25 bases, can be designed on translational start sites (TSS), in order to block translation, or on splicing sites, to cause the mis-splicing of mRNA and consequently the induction of mRNA decay (NMD). In both cases the effect will be a dose dependent reduction of the translation of the gene of interest and the generation of a functional knock-down embryo,

commonly known as “morphant”. Since MOs are resistant to nucleases, their activity will be decreased over time only by the effect of dilution resulting from cell division. Depending also on the expression levels of the targeted gene, a consistent knock-down can be achieved up to 7 dpf. The choice between translation blocking and splice-modifying MOs is dependent on the purposes of the experiment and on the and needs of the investigator. Translation blocking MOs binds to TSS and sterically block the attachment of ribosomes. They have the advantage to be active on both maternal and zygotic mRNAs, but, since they do not cause the degradation of mRNAs, immunologic methods, particularly Western blot, have to be used to check their efficacy. This is sometimes hampered by the fact that antibodies that cross-react in zebrafish are rarely available. Splice modifying MOs, on the contrary, act by sterically interfering with the spliceosome. Unfortunately the effect of a splice MO is not predictable basing only on its sequence, and MOs on donor or acceptor splice sites can both trigger intron retention, exon skipping or activation of cryptic splice sites. Nonetheless the effect will be in most cases the introduction of a premature stop codon in the mRNA with the consequent induction of NMD. This is particularly advantageous since allows the monitoring of MO efficacy simply by RT-PCR. Contrary to translation-blocking, splice-modifying MOs are not active on maternal transcripts, and thus the knock-down effect will be evident only from the midblastula transition, when maternal mRNA is degraded and the zygote start to express its own genes (99-101).

Despite general high specificity, morpholinos can sometimes show non-specific effects, due to the presence of contaminants or, more frequently, to the off-target of other genes. (102). For this reason morpholino experiments need several controls to be sure that the phenotype obtained is really consequent to the knock-down of the gene of interest. The most frequent control used is the injection of a “mismatch” MO, which typically has 4 mismatches in the sequence, or a random-sequence MO. With the injection of these control-MOs it is possible to check only for non-specific morpholino effects and not for the more frequent off-targeting. A more reliable way to control the off-targeting, although more expensive, is the use of two or more independent MOs to demonstrate that they are able to induce equivalent knock-down phenotypes. Arguably, the most convincing morpholino control of all is the phenotypic rescue, as this approach directly addresses the issue of specificity. For some genes, the knock-down phenotype can be efficiently reversed by restoring the gene product of interest via co-injection of the corresponding mRNA. While this is particularly easy when using splice-modifying MOs, some modifications of the mRNA have to be introduced when working with TSS-

binding MOs, in order to avoid the binding of the MO to the injected mRNA. This can be achieved by removing the 5' untranslated region of the mRNA, by introducing silent mutations into the annealing site of the MO or using mRNA from other organisms. Although such rescue experiments are compelling, they are sometimes not easily achievable. This is particularly true for genes with highly localized expression patterns or in cases where outcome is sensitive to precise protein levels. The result is that frequently an amelioration rather than a complete rescue of the morphants' phenotype is obtained (103).

Similarly to knock-down approaches, also the over-expression of genes is readily feasible in zebrafish by microinjection. As morpholinos, plasmid DNA or 5'-capped mRNA are injected in 1-4 cell stage embryos. When using plasmid DNA is possible to regulate the expression of the transcript by using different promoter to drive the expression of the gene. However the expression will start only after the mid-blastula transition and, since plasmids distribute unequally between cells due to their bigness, there will cause invariably a mosaic expression.

By contrast, mRNA distributes generally better and leads to a far more homogenous distribution of the protein, with translation initiating shortly after the time of injection. However, as in practice the mRNA often becomes asymmetrically localized, it is common to trace the distribution of the gene product within the embryo. This can be achieved by co-injecting an easily detectable tracer such as GFP or LacZ or by tagging the molecule of interest, for example with a series of Myc-epitopes, to allow direct antibody detection of the ectopic protein. This last method however can interfere with normal protein function and much care has to be taken to avoid non-consistent results.

Altogether these methods have proven to be invaluable in dissecting early developmental events. However MOs are inactivated by dilution and mRNA are also gradually degraded upon injection, and this limits their use only to the study of processes occurring in the first developmental stages.

In the last years several methods have been developed to address this limitation and to balance for the absence of a site-directed mutagenesis methods in zebrafish. The isolation of mutant alleles of orthologues of human gene can be achieved by TILLING (induced local lesions in genomes). This strategy rely on traditional ENU mutagenised libraries, that are then screened for the presence of mutation in the desired genes by high-throughput screening (104). This method is nonetheless expensive and labour intensive, and for this reason TILLING programmes are limited to a few centres around the world. Anyway mutant lines are usually

made freely available to the scientific community and some project, as the Zebrafish Mutation Resource of the Sanger institute (http://www.sanger.ac.uk/Projects/D_rerio/mutres/), accept request of other laboratories for the search of mutations in specific genes.

A new reverse genetic approach that is currently object of intense investigations is known as "genome editing" and is based on the use of zinc finger nucleases (ZFNs). Engineered ZFNs are able to introduce a double-strand break (DSB) in a specific genomic target sequence, that is then repaired by the cell through non-homologous end joining (NHEJ) or homology-directed repair (HDr). Since NHEJ rapidly ligates the two broken ends with the occasional gain or loss of genetic information, it is possible with this method to introduce small insertion or deletion and create null alleles of the gene of interest. While the insertion of mutations mediated by NHEJ repair is accidental, by exploiting HDr it is possible to select the mutation to introduce. This can be achieved by providing, in conjunction to the ZFN, a donor DNA molecule containing the desired mutation, which can be both a substitution and a little rearrangement. This approach, developed in tissue culture systems and applied with some success in whole organisms, including *Caenorhabditis* and *Drosophila* (105), has now been shown to be highly efficacious in zebrafish. Although the methods for selecting the appropriate zinc fingers require optimization, this opens up the possibility to generate mutant alleles of any gene of interest in zebrafish, thus opening new important perspectives in the study of human diseases using this animal model.

Transgenic approaches

Transgenesis can be exploited for a variety of tasks (analysis of regulatory elements, gene over-expression, tracing of cellular lineages) and, in contrast to other gene over-expression techniques, can be used to gain spatial and/or temporal gene expression control, removing the embryo-to-embryo variability associated with the injection of molecules into fertilized eggs. Many advances has been made in the last years, and now several techniques, based on the use of enzymatic approaches, transposons, and retroviruses, have been implemented to increase the efficiency of transgenes insertion into the zebrafish genome. At present probably the most common methods are that based on the use of transposons, particularly the *Tol2*, a transposable element originally isolated from the genome of the medaka fish. The natural *Tol2* element is autonomous and codes for its own transposase. If the transposase is provided *in trans*, only short sequences of respectively 200 and 150 base pairs from the left and right of *Tol2* are essential for its insertion in the genome. In this way almost any DNA molecule up to 10 Kb can

be inserted between the two terminal sequences and injected into fertilized eggs together with the transposase mRNA to induce its integration (106). *Tol2*-mediated transgenesis allows a frequency of insertion of up the 50%, and usually with a single insertion. The efficiency of integration, joined to the prolific nature and rapid development of zebrafish, has led in the last years to the development of several transgenic lines. Particularly useful are those expressing fluorescent proteins under control of tissue-specific promoters, that turned useful for the *in vivo* study of gene expression patterns during development (107).

3.1.3: Zebrafish in the field of neuromuscular disorders

Zebrafish proved to be a useful tool to dissect a wide range of human pathologies, but probably one of the most interesting and promising application is the study of neurological disorders. Facilitated by the small dimensions and transparency, neuronal patterning, pathfinding and connectivity of neurons in the in the CNS have all been deciphered and were found to correlate with that of humans (108, 109). Further, by use of *in situ* hybridisation, immunohistochemistry and, more recently, transgenic lines, it is possible to identify spinal motor axons an monitor them during development (110). Then, although the physiology and development of neurons is similar to that of human, during the first days of development, zebrafish has a relatively simple neuromuscular system. This facilitates the microscopic observation of axonal outgrowth in zebrafish models of neurological diseases.

Spinal motorneurons develop in two distinct “waves”. During gastrulation (9-10 hpf) “primary motorneurons” start to differentiate. They have large cell bodies (around 10 μm in diameter) and can be uniquely identified by the positions of their cell body within the spinal cord hemisegment. Initially only 3 motorneurons per hemisegment are present: Caudal Primary (CaP), Middle Primary (MiP) and Rostral Primary (RoP). Growth cones of all primary motorneurons leave the spinal cord approximately at 18-24 hpf and extend ventrally on the medial surface of the ventral myotome, between the myotome and the notochord. This is defined as “common pathway”, since all primary motorneurons extends axons along this region. The distal end of the common pathway is delineated by a group of specialised cells, the “muscle pioneers”, which define the nascent horizontal myoseptum, which separate dorsal from ventral myotomes. This is an intermediate target for primary motorneurons and it represents a choice point, because only after having reached this area, primary motorneurons start to differentiate their pathway in order to innervate non-overlapping territories of

myotomes. CaPs continue to extend their axons along the ventral myotomes, MiPs invert the growth direction and move dorsally between the spinal cord and the dorsal myotome, while RoPs extend laterally within the future horizontal myoseptum (Fig. 3.3).

After primary motorneurons, secondary motorneurons differentiate. They have smaller cell bodies (7 μm of diameter) and appear at 14-15 hpf, but start to extend their axons at 26 hpf. They are more numerous and approximately 30 secondary motorneurons are present per hemisegment. However their axons extend along that of primary, in order to form the dorsal and ventral motor nerves.

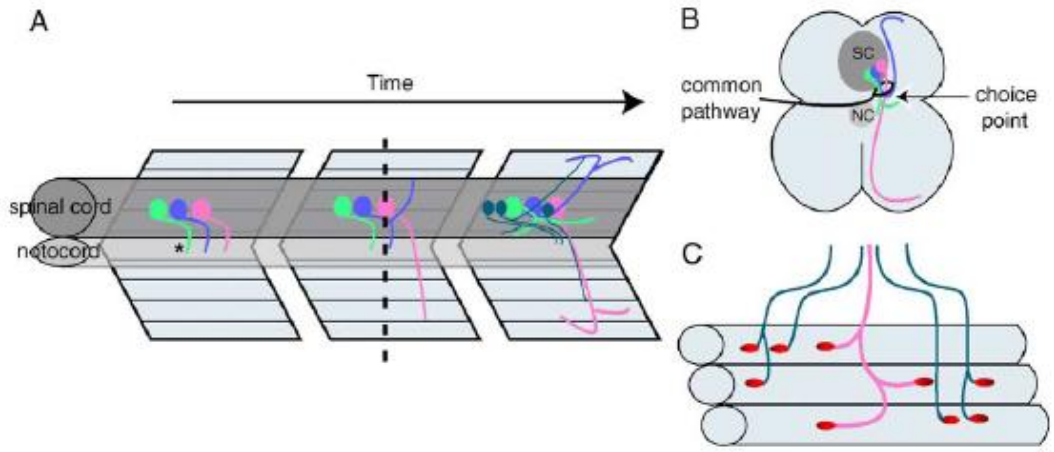

Figure 3.3: *Neuromuscular synaptogenesis in wild-type zebrafish. (A) Primary motor neuron axons CaP (pink), MiP (blue), and RoP (green) exit the spinal cord through the ventral root and extend along the common pathway to the choice point (asterisk) located at the horizontal myoseptum. At the choice point, axons pause and then proceed to innervate a cell-appropriate territory. At later time points, MiP retracts its ventral axon, the dorsal MiP and ventral CaP axons reach the edge of the myotome and turn laterally, and RoP elaborates an axonal arbor laterally near the horizontal myoseptum. Beginning ca. 5 h after primary motor axons, secondary motor axons (dark blue) exit the spinal cord and extend into the periphery. (B) Cross-section at 24 hpf illustrating the medial location of the common pathway, choice point, the initial medial projections of MiP and CaP, and the lateral turn of these axons at the edge of the myotome (SC, spinal cord; NC, notochord). (C) The mature pattern of muscle fiber innervation consists of several neuromuscular synapses distributed along the length of each fiber. Muscle fibers are multiple innervated by one primary motor neuron (pink) and several secondary motor neurons (dark blue). From Panzer et al (2005).*

Some examples of successful application of zebrafish models on neuromuscular disorders are the results recently obtained in the study of spinal muscular atrophy (SMA) and hereditary spastic paraplegia. Similarly to CMTs, SMA affects secondary motorneurons, but the consequent denervation induces both distal and proximal atrophy and leads to paralysis and death. It is recessively inherited and due to mutations causing the aploinsufficiency of *SMN* gene. Morphants and zebrafish lines bearing nonsense mutations in the *SMN* orthologue show several alterations of axonal outgrowth in the peripheral nervous system, thus phenocoping the human disease. A fine analysis of the neuromuscular system revealed that the loss of *Smn* in zebrafish induce a specific decrease in the synaptic vesicle protein SV2, thus demonstrating that Smn has a role in the maintenance of presynaptic integrity (111). Mutations in spastin gene

(SPG4) are one of the more common cause of hereditary spastic paraplegia, a neuromuscular disorder in which the degeneration of primary motor axons in the corticospinal tract induce progressive lower limb spasticity. The knock-down of SPG4 orthologue in zebrafish do not alter the differentiation of motorneurons, but inhibit their correct. It was demonstrated that this defects was due to the alteration of microtubules stability in axons, thus providing a new light into the comprehension of the molecular mechanism leading to hereditary spastic paraplegia (112, 113).

3.2: Materials and methods

3.2.1: Zebrafish keeping and maintenance

In this work zebrafish from the GT strain (114) were used. Zebrafish are maintained and raised in 5 l tanks with freshwater at 28 °C with a 12 hr light/12 hr dark cycle. Embryos are obtained by natural mating according the indications of the zebrafish book (115) and raised at 28 °C in Petri dishes containing fish water. Embryo older than 24 hpf that had to be analysed with i*n situ* hybridisation or at fluorescence microscope were treated with an inhibitor of pigment formation from 24 hpf to the time of analysis by adding the tyrosinase inhibitor 1-phenyl-2-thiourea (PTU) to fish water.

Fish Water 50 X:
5 g/l instant ocean
7,9 g/l $CaSO_4$
1 g/l $NaHCO_3$

Fish Water 1 X:
Dilute 50x solution in ddH_2O and add 0.2 mg/l of methylene blue

PTU 100 X
0.3% 1-phenyl-2-thiourea in 10 X PBS.
Dilute 10 X in fish water w/o methylene blue and store at 4 °C protected from light. Dilute at working concentration in fish water 1 X w methylene blue before use.

3.2.2: Bioinformatical analysis on zebrafish genome

To identify the zebrafish *MFN2* orthologue, a research in GenBank sequence database using protein BLAST program (116) was performed. As query the sequence of the human MFN2 protein (NP_055689) was used. To better clarify the identity of the zebrafish sequences retrieved with BLAST and evaluate the evolutionary relationship between mitofusins, a multialignment with the aminoacidic sequences of mitofusin 1 and 2 of other organisms was carried out using ClustalW (117). A phylogenetic tree was generated with the maximum likelihood method using the program Phylogeny (118) and the identity of the zebrafish mitofusins was finally confirmed by sinteny analysis made comparing the up to date assemblies of human and zebrafish genomes using UCSC Genome Browser (119).

BLAST
http://blast.ncbi.nlm.nih.gov/Blast.cgi

ClustalW
http://www.ebi.ac.uk/Tools/msa/clustalw2/

Phylogeny
http://www.phylogeny.fr

UCSC Genome Browser
http://genome.ucsc.edu/

3.2.3: RNA extraction from zebrafish embryos and tissues

RNA extraction from whole embryos and tissues was performed with TRIzol® reagent (Invitrogen). 1 ml of TRIzol® was added every 50-100 mg of tissue in 1,5 ml tubes. For zebrafish embryo RNA extraction, at least 20 embryos were used. Tissues/embryos were homogenised with a sterile pestle for 1.5 ml microfuge tubes and incubated at RT for 5 min. To separate RNA from DNA and proteins, 0,2 ml of chloroform every 1 ml of TRIzol® was added and samples were energically mixed with a vortex. Phase separation was performed by centrifugation at 12000 x g for 15 min at 4 °C and the superior aqueous phase containing the RNA was transferred into a new tube. RNA was precipitated adding 0,5 ml of isopropanol for every ml of TRIzol® used. Samples were incubated at -20 °C for 15 minutes and RNA was pelleted by centrifugation at 12000 x g for 15 min at 4 °C. Pellet was then washed once with 75% ethanol in DEPC water, air-dried and resuspended in 50-100 μl of DEPC water. RNA was then quantified with NanoDrop 2000 (Thermo Scientific).

3.2.4: cDNA synthesis

Total RNA retrotranscription was performed with ImProm-II™ Reverse Trascriptase (Promega) using random primers according the manufacturer instructions. Briefly a mix A containing RNA and random primers was prepared, denatured at 70 °C for 5 min and immediately chilled on ice. Then a mix B containing the transcriptase (RT), the nucleotides and the appropriate buffer was added and retrotranscription was conducted at 42 °C for 1 h. In table 3.1 the reaction mixes and temperature reaction conditions are shown.

MIX A	
RNA	500 ng
Random primers (500 ng/µl)	1 µl
nuclease free H_2O	to 5 µl

MIX B	
nuclease free H_2O	5,6 µl
Buffer 5X	4 µl
MgCl (25 mM)	2,4 µl
dNTPs (10 mM)	1 µl
RNasin (40 U/µl)	1 µl
ImProm-II™ RT	1 µl

Reaction program	
25 °C	5 min
42 °C	1 h
70 °C	15 min
15 °C	5 min

Table 3.1: *reaction mixes used for RNA retrotranscription and reaction program used.*

3.2.5: Semiquantitative PCR for evaluation of zebrafish Mfn2 expression

A rough estimation of zebrafish mfn2 expression level was obtained performing a semiquantitative PCR using AmpliTaq Gold® DNA Polymerase (Applied Biosystem). Zebrafish *mfn2* cDNA was amplified with a forward primer in exon 2 and a reverse primer in exon 5. Amplification of a fragment of the housekeeping gene β-actin 1 was used for normalisation. In table x.y are shown the primers and the PCR cycling conditions used.

Gene	Primers	cDNA fragment length	Ta	Number of cycles
mfn2	F: GCGCCTACATCAAAGAAAGC R: CAGCATCCAAATCCTCATCC	387	60	26
β-actin 1	F: TGTTTTCCCCTCCATTGTTGG R: TTCTCCTTGATGTCACGGAC	558	55	22

Table 3.2: *PCR primers used for semiquantitative RT analysis of zebrafish mfn2 and β-actin mRNA.*

3.2.6: In situ hybridisation

Cloning of Mfn2 probe

To synthesize the probe used for in situ hybridisation, a fragment of 554 bp of zebrafish *Mfn2* cDNA was cloned into the plasmid pCRII-TOPO (Invitrogen). Total zebrafish RNA was obtained from 5 dpf embryos (see paragraph 3.2.3) and retrotranscribed using ImProm-II™ reverse transcriptase (Invitrogen) (see paragraph 3.2.4). A region spanning exons 2-6 of zebrafish *Mfn2* cDNA was PCR amplified using AmpliTaq Gold (Applied Biosystem) and the

primers Forward: GCGCCTACATCAAAGAAAGC and Reverse: GACTCTGAATTGGCCACCAG with an annealing temperature of 58 °C using a normal PCR cycling program (see paragraph 2.2.3). The obtained fragment was cloned into pCRII-TOPO vector (Invitrogen), which contain SP6 and T7 promoters at the opposite ends of the cloning site and allow blue-white colony screening. Top10 chemically competent *E. Coli* (Invitrogen) were transformed and plated on LB-Agar plates containing kanamycin spread with 40 mg/ml X-Gal, to permit the blue-white colony screening. Plasmid DNA was prepared from white colonies grown in kanamycin added LB-broth using PureYield Plasmid Miniprep (Promega), and the direction of insert was determined by sequencing with M13 forward (TTGTAAAACGACGGCCAGT) and M13 reverse (CAGGAAACAGCTATGACC) primers. The selected construct (pCRII-zMFN2-probe) contained the *Mfn2* fragment cloned in direct sense, so that the antisense probe can be transcribed with T7 and the sense probe with SP6 RNA polymerase (Fig. 3.4).

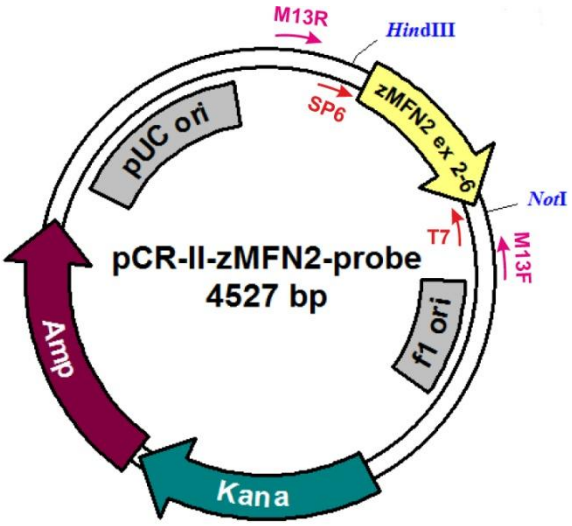

Figure 3.4: *plasmid map of pCR-II-zMFN2-probe used for the synthesis of sense and antisense probes employed in whole mount in situ hybridisation.*

LB-Broth

10 g/l bacto tryptone
5 g/l bacto yeast extract
10 g/l NaCl
To pH 7.0 with NaOH
Autoclave immediately and store at 4 °C
Add the antibiotics before use

Kanamycin	20 µg/µl
Ampicillin	50 µg/µl

LB-Agar plates

15 g/l agar in LB-broth.
Autoclave, use immediately or store at 4 °C until use.

For selective plates add the antibiotic immediately before preparing the plates
Kanamycin 20 µg/µl
Ampicillin 50 µg/µl
Store the plates at 4 °C protected from light.

X-Gal stock solution
X-Gal 40 mg/ml in DMF (N, N Dimethylformamide)
Mix until completely dissolved. Store at -20 ºC protected from light.

Synthesis of Mfn2 antisense and sense probes

The synthesis of *Mfn2* digoxigenated antisense and sense probes to be used for *in situ* hybridisation was performed with T7 and SP6 RNA polymerases respectively (Ambion). 5 µg of pCRII-zMFN2-probe plasmid DNA were linearized using HindIII to transcribe the antisense probe with T7 and with NotI to transcribed the sense probe with SP6. Restrictions were performed using 20 units of enzyme in a 50 µl reaction volume and incubating at 37 °C for 3 h. 1 µl of restricted plasmid was loaded into a 1% agarose gel together with the undigested plasmid to check the completion of the digestion. The linearized plasmid was then purified and concentrated with the kit DNA Clean Up (Zymoresearch) using an elution volume of 6 µl and quantified with NanoDrop 2000. To synthesize the DIG-probes, a reaction containing 1 µg of linearized plasmid, the DIG-NTPs and the RNA polymerase (SP6 or T7) together with RNAsin to inhibit the RNAses, was setted up (see tab 3.3). The reaction was incubated 2 h at 37 °C.

DIG-RNA probes synthesis reaction	
Linearised plasmid	1 µg
T7/SP6 Buffer 10X	2 µl
DIG-NTP 10X	2 µl
RNAsin (35 U/µl)	1 µl
T7/SP6 polymerase (10 U/µl)	2 µl
DEPC H_2O	to 20 µl

Table 3.3: *mix reaction used for the synthesis of DIG-RNA probes to be used for in situ hybridisation.*

When the reaction was completed, the template plasmid DNA was removed by adding 1µl of TURBO DNase (Ambion) and incubating at 37 °C for 15 minutes. RNA probes were then purified with MEGAclear columns by Ambion, gel quantified and stored at -80 °C.

Hybridisation reaction

In situ hybridisation was performed on whole embryos to analyse the expression of *Mfn2* during zebrafish development (87). The hybridisation was performed in parallel with the antisense and sense probe as control. Embryos are obtained by natural mating and staged according (120). Embryos above 24 h of development are manually deprived of their chorion and fixed in PFA 4% ON at 4 °C or 2 h at room temperature and stored at -20 °C in absolute methanol. Embryos are then rehydrated in solution at decreasing concentration of methanol in PBS.

Permeabilisation: it is necessary only for embryo with more than 1 day of development. It is performed with a proteinase K solution at 10 µg/ml according this scheme:

- 1 h for embryos older than 3 days
- 30 minutes for 2 days embryos
- 15 minutes for 1 day embryos

Embryos are then postfixed in 4% paraformaldehyde solution (PFA) for at least 20 minutes.

Prehybridisation: the samples are prehybridised with Hybridisation Mix solution (HM) for 2-5 h at 65 °C

Hybridisation: HM solution is substituted with a HM solution added with the RNA dig-labelled probe (0,75 ng/µl). Incubation was performed ON at 65°C.

Washes: were performed at hybridisation temperature according this scheme:

- HM 75%, 2X SSC 25%, 15 min
- HM 50%, 2X SSC 50%, 15 min
- HM 35%, 2X SSC 75%, 15 min
- 2X SSC, 15 min

Final wash was performed at RT with 0,2 X SSC (2x 30 min)

Preincubation: samples are transferred in 100% PBT by a series of incubations at RT in solutions at decreasing concentration of SSC in PBT:

- 75% 0,2 X SSC 25% in 1X PBT, 10 min
- 50% 0,2 X SSC 50% in 1X PBT, 10 min

- 25% 0,2 X SSC 75% in 1X PBT, 10 min
- 1 X PBT, 10 min

Embryos are then incubated for 2 h at RT in a block solution containing 2% sheep serum, 200mg/ml BSA in PBT.

Anti-Dig antibody incubation: Samples are incubated ON at 4 °C in 300-400 µl of anti-digoxigenin antibody in PBT (1:5000, Roche).

Washes: antibody solution is removed and samples are washed in PBT solution (6 times for 15 min) and then in staining buffer (3 times for 5 min)

Staining: embryos are incubated in staining solution at RT in the dark and monitored under the microscope the staining is sufficiently intense. To block the reaction embryos are washed in stop solution. Samples are then post-fixed in 4% PFA in PBS.

Hybridisation Mix (HM)
Formamide 60%; 5X SSC; 0.1% Tween-20; Heparin 50 µg/ml; tRNA 500 µg/ml; to pH 6 with citric acid. tRNA and heparin are added only to the prehybridisation and hybridisation HM solution and not in HM washing solution.

1X SSC
150 mM NaCl; 15 mM citric acid in DEPC H_2O.

PBT
1% Tween-20 in 1X PBS

Staining buffer
100 mM Tris-HCl pH 9.5; 50 mM MgCl2; 100 mM NaCl; 0.1% Tween-20

Staining solution
225 mg/ml NBT; 175 mg/ml BCIP in staining buffer.
(NBT: for 50 mg/ml stock solution: 50 mg Nitro Blue Tetrazolium in 0,7 ml Dimethyl-formamide anhydre, to 1 ml with water. BCIP: for 50 mg/ml stock solution: 50 mg 5-Bromo 4-Chloro 3-Indolyl Phospate, to 1 ml with anydrous dimethyl-formamide)

Stop solution
EDTA 1 mM in PBS 1X pH 5.5

3.2.7: Design of Morpholino oligonucleotide against Mfn2 and PCR verification of morpholino effect

Basing on the Mfn2 sequence obtained with the bioinformatical analysis, a morpholino oligonucleotide against the acceptor splice site of intron 2 of zebrafish *Mfn2* was designed (MO-mfn2: GTTTCTGTTAAAGGGAAAACGGGCA). As control a oligo morpholino

without any annealing sequence on zebrafish trascriptome was also synthesized (MO-Ctrl: GTTAATACCAGGATTAGATTGATTG). Both morpholinos were produced by Gene Tools, resuspended in DNAse/RNAse free water at a final concentration of 1 mM and stored at 4°C.

To verify the effect on *Mfn2* splicing and expression, a semiquantitative PCR on cDNA obtained from MO-mfn2 and MO-Ctrl injected embryos was performed using the same primers and PCR conditions described in paragraph 3.2.5.

3.2.8: Production of MFN2 mRNA

Human MFN2 cloning and mutagenesis

Human *MFN2* cDNA fused to SV40 poly(A) signaling sequence was PCR amplified with iProof High-Fidelity DNA polymerase (Biorad) from pCI-HA-hMFN2 (gently provided by Scorrano L.) using the primers Forward: CATATGTCCCTGCTCTTCTCTCG and Reverse: CCTAGGAAACGTCTATCAGGGC in order to eliminate the HA tag. According manufacturer instructions PCR product was cloned into pCR-bluntII-TOPO vector (Invitrogen), which contain T7 promoter sequencing at the 3' end of the cloning site. Since the integration of the insert disrupts the cytotoxic protein ccdB gene, only positive colonies can survive (Fig. 3.5).

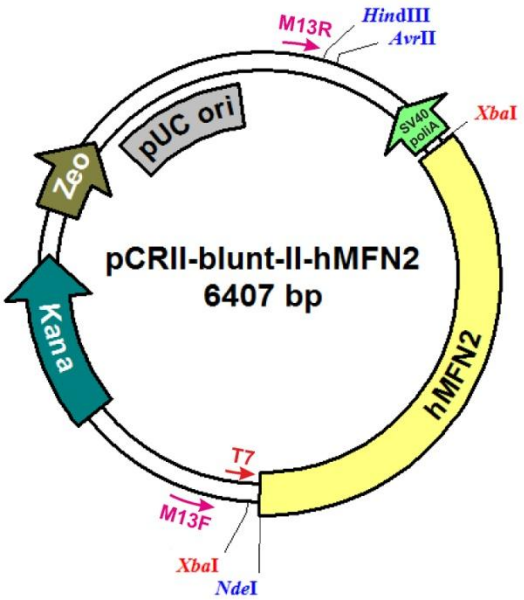

Figure 3.5: *plasmid map of pCR-blunt-II-hMFN2 used for the synthesis of human capped mRNA to be used in zebrafish injection experiments.*

After preparation of plasmid DNA, the direction of insert was determined by sequencing with M13 forward (TTGTAAAACGACGGCCAGT) and M13 reverse (CAGGAAACAGCTATGACC) primers and with primers internal to the human *MFN2* cDNA sequence.

Mutagenesis was performed on pCR-bluntII-hMFN2 to introduce the common mutation R94Q (c.281G>A) found in CMT2A patients. A modified protocol from (121) was used. Briefly a mutagenesis reaction was performed with iProof High-Fidelity DNA polymerase (Biorad) using a single primer. The mutagenesis primer bears the desired nucleotide substitution in the middle with at least 10 flanking residues and was designed to have a high Tm (>72 °C). In table 3.4 are listed the mutagenesis reaction conditions.

A

Primer name	**Sequence**	**Tm (NN)**
Mut-hMFN2-	GGTGCTGGCTC**a**GAGGCACATGA	73,4

B

Mutagenesis reaction	
Plasmid	1 µl
Buffer (5X)	5 µl
dNTPs	5 µl
Mutagenesis	1,25 µl
H_2O	13 µl
Taq iProof	0,25 µl

C

Cycling program		
98 °C	1 min	
98 °C	10 sec	X 30
68 °C	30 sec	
72 °C	2 min	
72 °C	10 min	
15 °C	5 min	

Table 3.4: *primers (A), mutagenesis mix reaction (B) and cycling program (C) used for to introduce the c.281G>A mutation in plasmid pCR-blunt-II-hMFN2. Melting temperature (Tm) was calculated with the nearest neighbor method.*

At the end of the mutagenesis reaction, the plasmid template DNA, that is methylated, is digested for 1 h at 37 °C with 1 µl of DpnI restriction enzyme, which cleaves only methylated dsDNA. 2 µl of digested product are used to transform TOP-10 chemically competent cells (Invitrogen) according the manufacturer instructions and plated in kanamycin LB-Agar plates. The insertion of the nucleotide substitution was confirmed by sequencing with primers internal to the insert.

In vitro transcription of MFN2 mRNA

To synthesize wild-type and mutated forms of human *MFN2* RNA, 5 µg of the plasmids pCR-bluntII-hMFN2 and the mutagenised pCR-bluntII-hMFN2^{R94Q} and pCR-bluntII-hMFN2^{T105M} were linearised with HindIII using 20 units of enzyme in a 50 µl reaction volume and incubating 3 h at 37 °C. The linearised plasmid was loaded on a 1% agarose gel, to verify if the digestion was completed, and purified with DNA Clean Up kit (Zymoresearch). The transcription reaction was conducted with T7 RNA polymerase with MEGAscript® T7 kit (Ambion). The reaction, containing the template DNA, the NTP/CAP and the T7 polymerase (see Tab. 3.5) was incubated at 37 °C for 2 h.

Capped mRNA transcription reaction	
Linearised plasmid	1 µg
T7 Buffer 10X	2 µl
NTP/CAP 2X	10 µl
T7 enzyme mix	2 µl
DEPC H_2O	to 20 µl

Table 3.5: *reaction mix used for the synthesis of human MFN2 capped mRNA*

The template DNA was digested adding 1 µl of TURBO DNase (Ambion) and incubating 15 min at 37 °C. The transcripts were then purified with MEGAclear columns (Ambion) and gel-quantified. To verify the correct length and the integrity of the transcripts, 100 ng of RNA were loaded in a formaldehyde agarose gel together with a RNA ladder. The gel was post-stained incubating it for 30 min in agitation in staining solution and visualized under an UV transilluminator.

Formaldehyde 1% agarose gel
Agarose 1% w/v
MOPS 1X
Formaldehyde 0,6 M
In DEPC water

Running buffer 1X
MOPS 1X
Formaldehyde 0,2 M

MOPS 10X
MOPS 0,4 M
NaOAc ($3H_2O$) 0,1 M
EDTA 10 mM

Staining solution
Dilution 3 X in water of GelRed Nucleic Acid Stain 10000 X (Biotium). Store RT protected from light.

3.2.9: Microinjection of zebrafish embryos

Embryos at 1-2 cells stage were injected with morpholino and mRNA solutions using a microinjector connected to a micromanipulator. Injecting needles were made from 1 mm glass capillaries with a horizontal micropipette puller programmed with 630 heat, 75 pull, 25 velocity, 50 time. Freshly laid eggs were aligned onto the long side of a microscope slice put on a Petri dish and injected with approximately 10 nl of solution.

Morpholino and/or the mRNA to be injected were diluted in Danieau solution, that is better tolerated by embryos than water, and added with phenol red as an injection tracer. The composition of the working solution used for injections are illustrated in table 3.6.

A) MO-mfn2
MO-mfn2 (0,75 µg/µl)
Danieau 1X
Phenol red 2%

B) *MFN2* mRNA
mRNA 25 ng/µl
Danieau 1X
Phenol red 2%

C) Rescue
MO-mfn2 (0,75 µg/µl)
mRNA 1 ng/ µl
Danieau 1X
Phenol red 2%

Table 3.6: *composition of the solution used for zebrafish embryos injections. A) solution used to down-regulate mfn2 with MO-mfn2 morpholino; B) solution used for the over-expression of human mitofusin 2; C) solution used for rescue experiments.*

Before use the injected solutions are heated for 5 min at 65 °C and then placed on ice. This allows the denaturation of secondary structures and ameliorate the efficiency of both morpholino and mRNA.

Danieau 10 X
50 mM NaCl, 0.7 mM KCl, 0.4 mM $MgSO_4$, 0.6 mM $Ca(NO_3)_2$, 5 mM HEPES, pH 7.6

Phenol red 10 X
0.2 % phenol red in PBS 1 X

3.2.10: Histological analysis on injected embryos

Acetylated tubulin immunohistochemistry

An immunohistochemistry against the pan-neural marker acetylated tubulin was performed to analyse the motorneurons of zebrafish embryos. 48 hpf embryos, previously treated with PTU to avoid pigments formation, were manually dechorionated and fixed in 4% PFA in PBS for 2 h at RT or at 4 °C ON. They were permeabilized with absolute methanol ON at -20 °C and then incubated in cold acetone for 7 min at -20 °C. They were rehydrated in solutions at decreasing concentration of methanol in PBS and washed at RT in agitation with PBTX (3 times for 10 min and 3 times for 30 min).

Embryos were then incubated with the primary mouse anti-acetylated tubulin antibody (Sigma) diluted 1:1000 in PBTX. Incubation was performed for 48 h at 4 °C.

At the end of the incubation, embryos were washed again with PBTX (3 times for 10 min and 3 times for 30 min) and incubated ON at 4 °C with the secondary antibody diluted 1:100 in PBTX. Depending on the need, an anti-mouse tetramethylrhodamine or Alexa Fluor® 488 conjugated (both from Invitrogen), were used. Samples were then washed again with PBTX (3 times for 10 min and 3 times for 30 min), embedded in 1,5% low-melting agarose gel and mounted on microscope slides and analyzed with a Leica DMR microscope equipped with a Leica DC500 digital camera. Images were processed with ImageJ and CorelDRAW X5 softwares.

PBTX
1% Triton X-100 in PBS.

Phalloidin staining

In order to examine the muscular system of treated and untreated zebrafish larvae, we performed a staining with fluorescent phalloidin that binds to F-actin, which is particularly abundant in muscle fibres. Whole 48 hpf embryos were fixed in PFA 4% and permeabilized in PBTX 2% overnight at 4 °C. Unspecific binding sites were blocked incubating the samples in blocking solution for 10 minutes. The incubation with tetramethylrhodamine B isothiocyanate-conjugated phalloidin (Sigma) diluted 1:100 in PBTX was performed 3 h at RT. Embryos were then washed 3 times for 10 min and 3 times for 30 min in PBTX, embedded in low melting 1,5% agarose and visualised with a Nikon Eclipse E600 microscope equipped with a Biorad radiance LE 2000 laser scanning system. Z-stack images were generated by scanning segments

located above the yolk sack extension, centred on the 12th somite. ImageJ was used to measure muscle fibres diameter.

PBTX 2%
2% Triton X-100 in PBS

Blocking solution
1% BSA (Bovine Serum Albumin)
1% DMSO (Dimethyl Sulfoxide)
In 1X PBS

Synaptic vesicles and acetylcholine receptor staining

To analyse the correct development of neuromuscular junctions (NMJ) in zebrafish embryos, a staining of acetylcholine receptors (AChR) and synaptic vesicles was performed. To mark synaptic vesicles we used a mouse sv2 primary antibody (DHSB, Iowa) together with an anti-mouse Alexa Fluor® 488 conjugated secondary antibody. The acetylcholine receptors were visualised with α-bungarotoxin (BTX) Alexa Fluor® 555 conjugated (Invitrogen). Embryos are fixed in PFA and permeabilized ON at 4 °C with PBTX 2%, then they are incubated ON at 4°C with the sv2 primary antibody diluted 1:50 in PBTX. Larvae are then washed 3 times for 10 min and 3 times for 30 min in PBTX to remove the primer antibody, and then incubated in PBTX ON at 4 °C with the green anti-mouse secondary antibody (1:100) and the red BTX (1:200). Embryos are then washed again and mounted on microscope slides embedded with low melting agarose. Visualization was performed with a confocal microscope and Z-stack images were analyzed with ImageJ software.

3.2.11: Behavioural analysis on injected embryos

To evaluate the motor capability of MO-Ctrl, MO-mfn2 and rescued embryos, a simple behavioural assay was used (122). Embryos were allowed to develop to 2 dpf and manually dechorionated at least 3 hours before the experiment. To assess their motor ability, they were gently touched with a mounted needle at the dorsal tip of the tail for at least three times. Fishes were scored as “normally responding” if they can swim for a distance of at least 3 times their length, as ‘‘impaired” if they vibrated, turned around or swim for a short distance, and as “unresponding” if they did not react after three stimulations.

3.2.12: Statistical analysis

Statistical analysis were performed using GraphPad Prism version 5.00 with a confidence interval of 95%. Chi square test was used to analyze the data obtained from the analysis of mortality, phenotype and movement of zebrafish injected larvae, while t-test and ANOVA were used to analyse the data obtained from the measurement of muscle fibres.

3.3: Results

3.3.1: Identification of zebrafish mfn2 and analysis of its expression pattern

Identification of mitofusin 2 gene in zebrafish and conservation analysis

To identify zebrafish *mfn2*, a similarity search was performed in GenBank using the program BLAST and the human MFN2 protein sequence (NP_055689) as query. Three entries with a high similarity were found. The one with the highest score (NP_001121726.1) is the zebrafish mfn2 RefSeq (also named in zebrafish LOC567448), located in chromosome 8, while the others are that of mfn1 (NP_956941.1), in chromosome 11, and a hypothetical protein annotated as mitofusin 1-like (XP_002660753). The identity of the two zebrafish mitofusins was confirmed by reconstructing the maximum likelihood phylogenetic tree, which was calculated using the mitofusins sequences from other organisms. As can be seen in figure 3.6, this analysis confirms the evolution of vertebrates' mitofusins from an ancestral gene, which appear to be more similar to the ubiquitous dmfn of *Drosophila* than to the fzo gene found in the same organism.

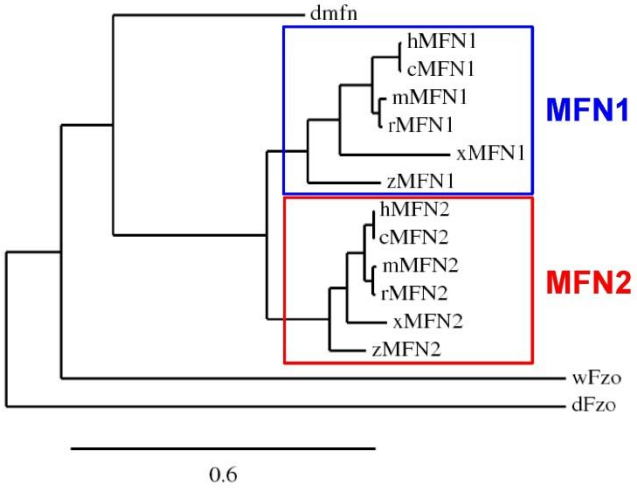

Organism	MFN1	MFN2
Man (h)	NP_284941	NP_055689
Chimp (c)	XP_001167765	XP_514395
Mouse (m)	NP_077162	NP_573464
Rat (r)	NP_620432.1	NP_570964
Xenopus (x)	NP_001016189	NP_001084869
Zebrafish (z)	NP_956941	NP_001121726.1
	Invertebrates mitofusin-like proteins	
	Fzo	**dmfn**
Drosophila (d)	NP_732840	NP_572320
Caenorhabditis (w)	NP_495161	-

Figure 3.6: *The unrooted tree was generated using the web-based pipeline provided by Phylogeny.fr. The horizontal bar at the bottom of the tree represents a distance of 0,6 substitutions per site. The RefSeq of the sequences used for the analysis are listed in the table on the right.*

Genomic regions surrounding mitofusin 2 gene in man and zebrafish, analysed with UCSC Genome Browser and the most recent genome assemblies available, revealed that the synteny with genes near the 5' end of mitofusin 2 is retained (Fig. 3.7 A). In addition the two mitofusin 2 genes of man and zebrafish have maintained the same exons organisation in man and zebrafish and codes for proteins of the same length (see Fig. 3.7 B).

A

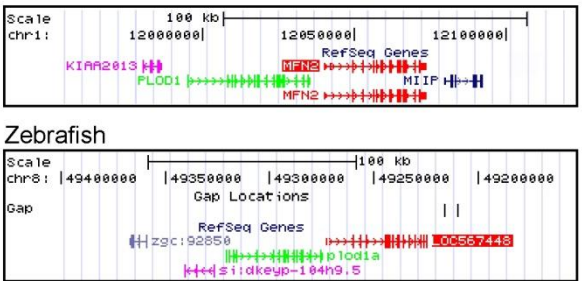

B

Organism	Chromosomic localisation (strand)	Gene size (bp)	cDNA RefSeq (lengh)	Protein RefSeq (lengh)	Coding exons number
Man	1 (+)	4685	NM_014874 (4685 bp)	NP_055689 (758 aa)	17
Zebrafish	8 (-)	2327	NM_001128 254.1 (2327 bp)	NP_00112172 6.1 (758 aa)	17

Figure 3.7: *A) Genomic regions surrounding mitofusin 2 genes in man and zebrafish. Mitofusins are in red and the surrounding genes are coloured in function of their orthology. Synteny conservation is evident at the 5' terminus. It is not possible to analyse the 3'end for the presence of 2 gaps in the zebrafish genome. B) Comparison of mitofusin 2 genes, mRNAs and proteins in man and zebrafish. Note that the different cDNA length is due to the incomplete sequencing of the UTR regions in zebrafish mfn2.*

Subsequent to the genomic and genetic analysis, a comparison between human, mouse and zebrafish mitofusin 2 proteins was performed, in order to evaluate the conservation degree at the aminoacidic level (Fig. 3.8). The multi-alignment demonstrates that zebrafish mfn2 shares the same percentage of similarity (92%) and identity (83%) with human and mouse proteins. The higher conservation is observed in the functional domains and in particular in the transmembrane region.

Figure 3.8: *Multiple sequence alignment of human, mouse and zebrafish mitofusin 2 polypeptides. In colour are evidenced the domains of the proteins: GTPase, GTPasic domain; HR1, coiled coil region 1; TM, transmembrane domain; HR2, coiled coil region 2.*

Expression of mfn2 in zebrafish: semiquantitative RT-PCR analysis

A semiquantitative RT-PCR analysis of *mfn2* mRNA was performed on whole embryos at different developmental stages and in different adult zebrafish tissues.

RNA was extracted from embryos between from 2 cells to 5 dpf. cDNA was normalized for the housekeeping β-actin gene. As shown in figure 3.9, zebrafish m*fn2* was found expressed in all stages analysed. Since the early embryo is transcriptionally silent until blastula, the presence of *mfn2* transcript at 2 and 64 cells indicates that *mfn2* has a maternal expression, and that *mfn2* mRNA is present in mature form in the unfertilized eggs.

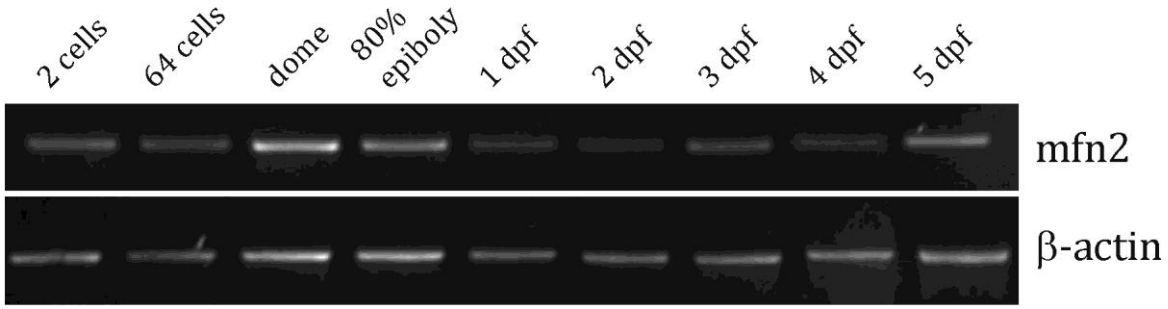

Figure 3.9: *semiquantitative RT-PCR analysis of Mfn2 transcript in zebrafish at different stages of development from 2 cells to 5 days post fertilisation (top panel). Total cDNA was normalised against β-actin gene (lower panel).*

It is known that in humans *MFN2* is expressed ubiquitously, but is enriched in some tissues (47). To verify if the pattern of expression of zebrafish *Mfn2* resembles the same pattern observed in man, semiquantitative RT-PCR was performed on RNA extracted from different adult zebrafish tissues and organs. *Mfn2* resulted ubiquitously expressed, but is particularly enriched in the heart and skeletal muscles, and, at a lower level, in the brain and eyes (Fig. 3.10). A very low amount of mRNA was found in swim bladder, liver, ovary and gut.

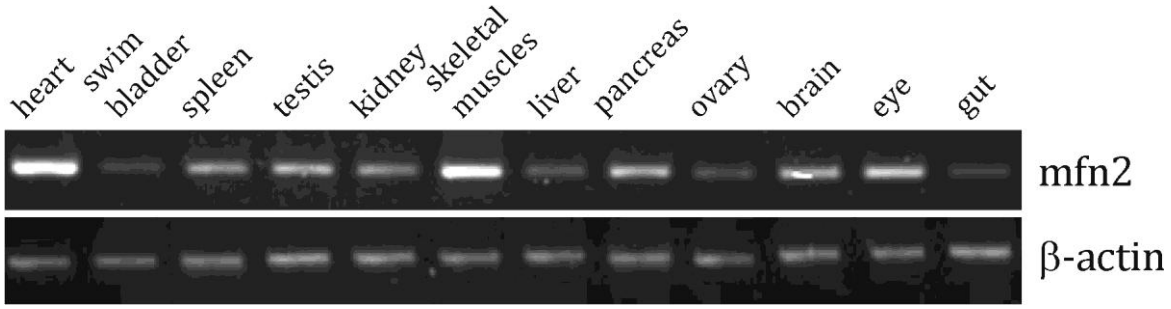

Figure 3.10: *semiquantitative RT-PCR analysis of Mfn2 transcript in different adult zebrafish tissues (top panel). Total cDNA was normalised against β-actin gene (lower panel).*

Expression of mfn2 in zebrafish: in situ hybridisation

To investigate more deeply the expression pattern of zebrafish *mfn2*, we performed a whole mount *in situ* hybridisation (WISH) on zebrafish embryos and larvae at different developmental stages. The antisense probe used was synthesized from the plasmid pCRII-zMFN2-probe and is complementary to a region of *mfn2* cDNA comprised between exon 2 and 6. To assess the specificity of the hybridization, a sense probe was used in a parallel control experiment at all stages and no staining was detected in any embryo.

With this analysis it was possible to locate precisely the sites of *mfn2* expression in embryos from 2 cells to 48 hours post fertilisation. As can be seen in figure 3.11, *mfn2* mRNA is maternally expressed and ubiquitous until the completion of somitogenesis (Fig 3.11 A-C), but by 24 hpf (Fig 3.11 D-F) it starts to be upregulated in the anterior part of the embryo, mainly in the midbrain, in the growing ganglion cell layer of the retina, in the ventral mesenchyme and along the midline of each miotome. Between 48 and 96 hpf, *mfn2* mRNA localize mainly in cortical brain neurons but remarkable signals are also retained in the otic vesicle, heart and gut (Fig 3.11G-I).

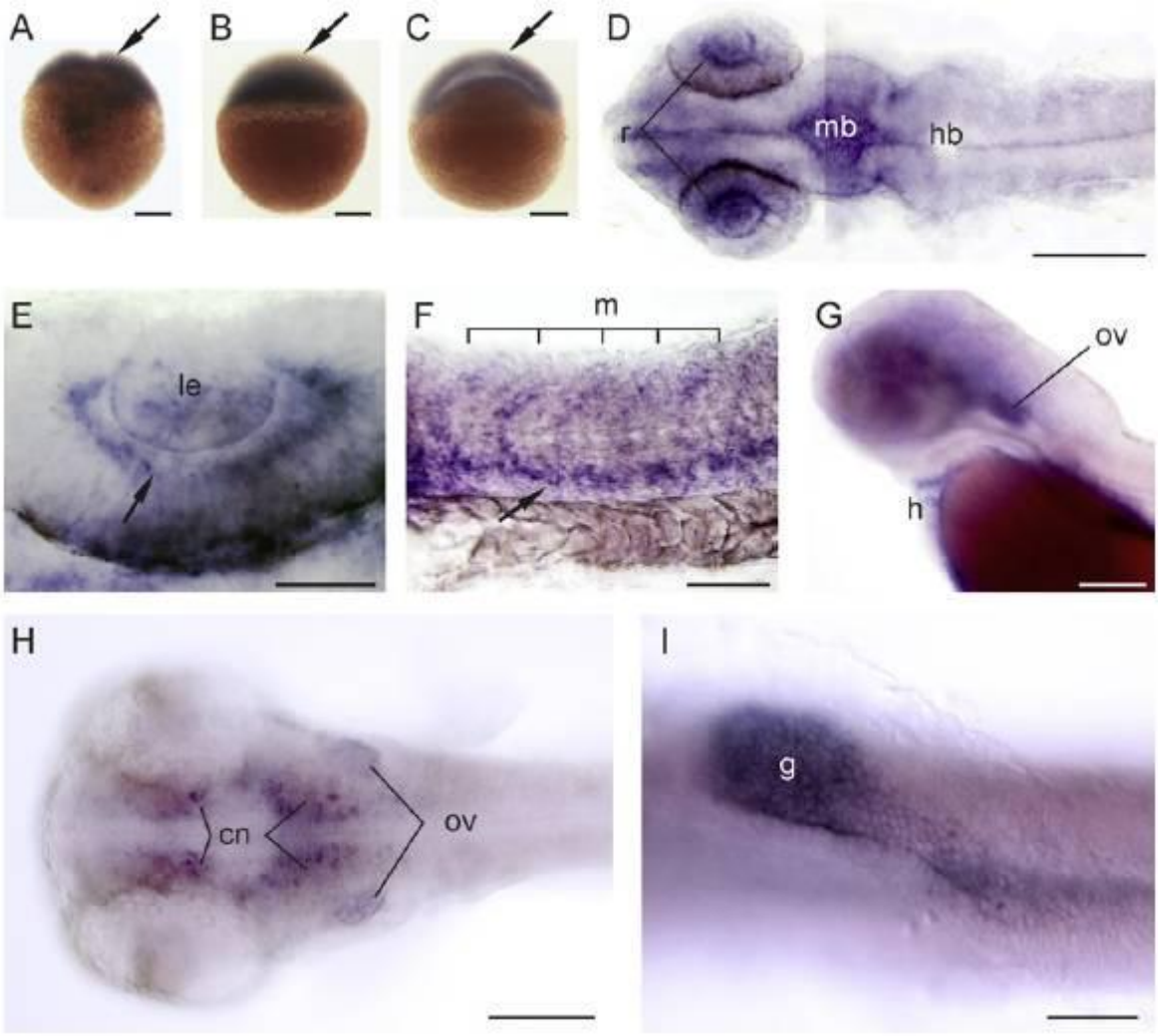

Figure 3.11: *Mitofusin 2 (mfn2) localization by in situ hybridization during zebrafish embryonic development. Maternal mfn2 mRNAs are already detectable at the two cell (A) and dome stage (B). Ubiquitous expression is seen from 50% epiboly (C) and throughout somitogenesis (not shown). (D–F) At 24 h postfertilization (hpf) mfn2 transcripts are mostly localized in the cephalic region of the embryo with faint gapped signal in the hindbrain (hb) and intense hybridization staining in the midbrain (mb) and retina (r), especially in the region (see arrow in E) in more close contact to the developing crystalline lens (le). (F) The presence of mfn2 is evident also in ventral mesenchyme (arrow in F) and along the midline of each miotome (m). At 48 hpf (G) the presence of mfn2 persists in the head and in the eye but can be also detected in the heart (h) and in the otic vesicles (ov). (H and I) At 4 days post-fertilization the expression pattern is mainly restricted to the encephalic region (H), in cranial neurons (cn) and otic vesicles (ov). (I) High levels of mfn2 transcripts are also detectable in the gut (g). Animal pole to the top in A–C; anterior to the left in D–I. Dorsal view in D, E, and H. Ventral view in I. Lateral view in F and G. Scale Bar is 200 μm except for E, F, and I (50 μm).*

3.3.2: Analysis of mfn2 down-regulation effects in the first stages of zebrafish development

Splice-modifying morpholino design and evaluation of its effect on *mfn2* splicing

Since it is known that in mouse the complete knock-out of *Mfn2* is embryonically lethal and given that fertilised oocytes undergo rapid mitochondria movement during the first developmental stages (123), we decided to use a splice-modifying MO against *mfn2* (MO-mfn2) to avoid the possibility of a complete lethality of the morphant embryos. Given that in zebrafish *mfn2* exon 1 and exon 2 are 5'UTR-coding, MO was designed in the most upstream position of the protein-coding mRNA, which is the acceptor splice site of intron 2. To induce the down-regulation of mfn2, zebrafish embryos at 2-4 cell stage were injected with MO-mfn2. In order to control for unspecific effects induced by the injection of MO, each experiment was performed in parallel with a control morpholino (MO-Ctrl) with no complementary RNA targets. To verify the effect of MO-mfn2, total RNA was extracted from 48 hpf embryos injected with increasing doses of the morpholino and semiquantitative RT-PCR was performed. This analysis revealed that MO-mfn2 acts by inducing the skipping of exon 3, thus introducing a premature stop codon in exon 4 (Fig 3.12). The strength of this effect appears to be dose dependent up to 7,5 ng. At this dose, which was used for all the subsequent experiments, the reduction of the wild-type transcript was of about the 70%.

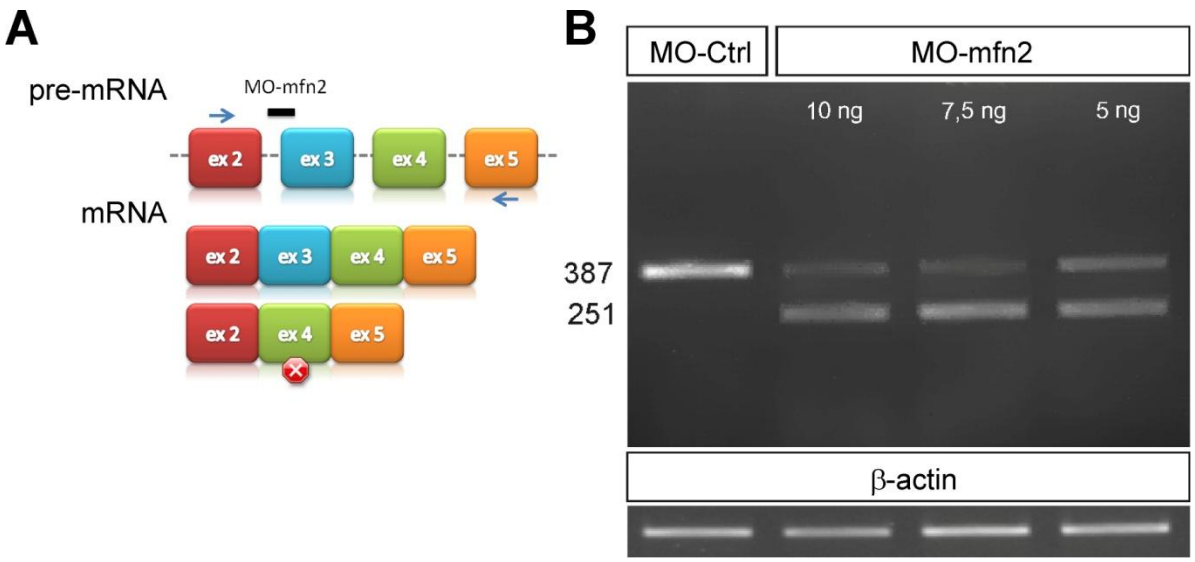

Figure 3.12: *A) site of annealing and effect of MO-mfn2 on zebrafish mfn2 mRNA. Arrows indicate the annealing sites of the primers used in the semiquantitative RT-PCR. B) Result of the semiquantitative RT-PCR on embryos injected with MO-Ctrl and different doses of MO-mfn2. MO-mfn2 injected embryos have an additional lower band compared to that of controls. Sequencing confirmed that the extra-band is an incorrectly spliced transcript lacking exon 3. This induces a frameshift in the sequence and the introduction of a premature stop codon in exon 4.*

Effects of *mfn2* knock-down on early zebrafish development

The first evident effect of *mfn2* down-regulation was a reduced vitality of MO-mfn2 injected embryos (64%) as compared to controls (90%) (Fig 3.13 D). The surviving larvae, although slightly delayed in growth, do not show evident morphological alterations until 48 hours post fertilisation (hpf). At this stage the 99% of MO-mfn2 injected larvae (Fig 3.13 E) show a characteristic phenotype, and morphants were classified according the severity of the alterations into 3 groups (Fig 3.13 A-C):

- Normal: with no evident morphological alterations
- Mild: showing curved tail, irregular somites, facial prognathism, underdeveloped eyes and brain ventricles oedema
- Severe: presenting shortened body axis, little head with encephalic necrosis, ventral expansion of the yolk and trunk oedema.

Mfn2 morphants appeared also severely impaired in their motor ability, as is in the case of CMT2A patients. To quantify this feature, MO-injected embryos were allowed to develop to 2 days post-fertilization and motility defects were scored with a behavioural assay. While the 96% of control larvae can react to the stimulus by swimming, the majority of morphants didn't react (31%) or reacted in a weaker way (52%) (Fig 3.13 F).

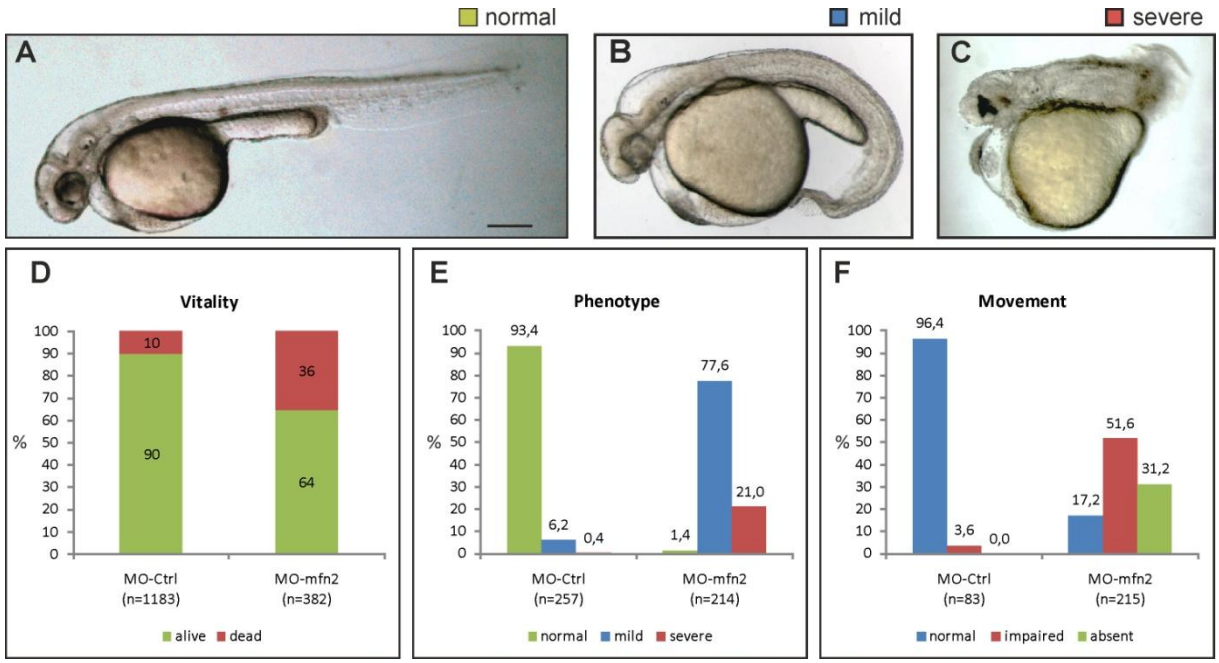

Figure* 3.13: effects of mfn2 knock-down on zebrafish embryos at 48 hpf. A) At 48 hpf MO-Ctrl injected embryos show no apparent phenotypic abnormalities, while at the same stage MO-mfn2 treated larvae display a mild (B) or a severe (C) phenotype. Histograms showing the vitality (D), the phenotype distribution (E) and motility test reaction (F) in control embryos (MO-Ctrl), and in larvae injected with an anti-mfn2 morpholino (MO-mfn2). All the differences found between controls and morphants were tested with Chi-square test and resulted statistically significant ($p < 0.0001$).*

Evaluation of motorneurons alterations in *mfn2* morphants

Considering that *mfn2* morphants showed evident motor abnormalities, we decided to determine whether the reduced levels of mitofusin could cause growth defects in motorneurons. Embryos were microinjected with either MO-mfn2 or MO-Ctrl and analysed by immunohistochemistry against the pan-neural marker acetylated-tubulin. Abnormal length and structure of ventral extending nerves innervating the somitic muscles, which are formed by the fasciculation of caudal primary motor neurons (CaPs) and secondary motorneurons, were analysed in 48 hpf larvae. Motor neurons were scored as "altered" when axons branched above the horizontal myoseptum or when they appeared truncated or missing. The presence of these defects was evaluated in trunk motorneurons above the yolk extension in both sides of each larva. From this analysis were excluded the embryos with a severe phenotype because of the complete disorganization of their nervous system.

When morphologically normal or mildly altered embryos were analysed, a significant difference in motorneurons organization between MO-mfn2 and MO-Ctrl treated embryos was observed. In 74% of MO-Ctrl injected larvae, microtubule staining demonstrated that motor neurons spread normal axonal projections along the centre of each somite. In contrast, in the trunk of *mfn2* morphant embryos, axons were less intensely stained, the ventral projecting nerves were abnormally developed and in 67% of MO-mfn2 treated larvae at least one branched, truncated or missing nerve was identified (Fig. 3.14).

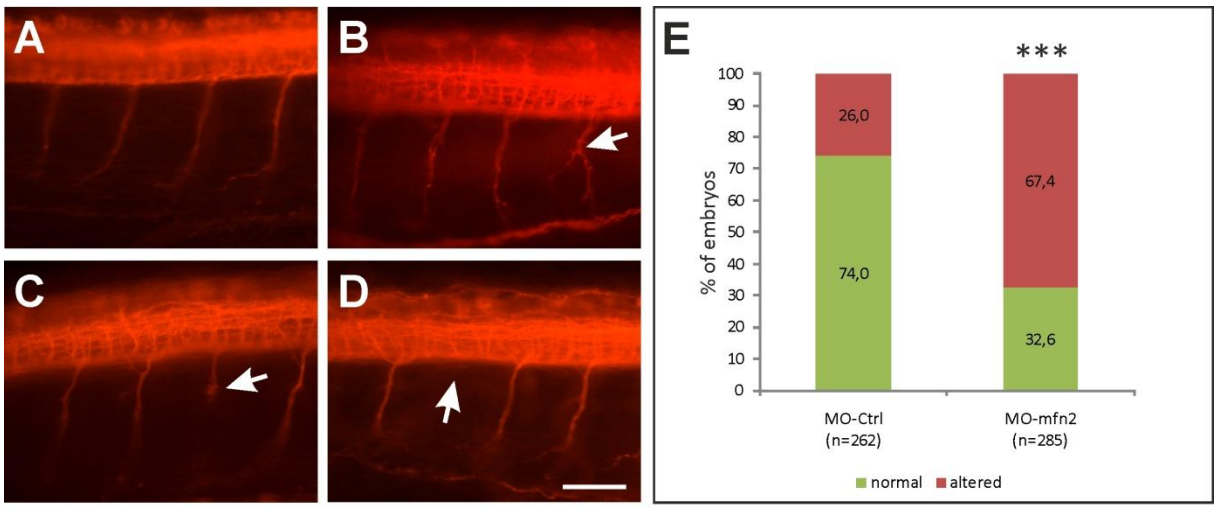

Figure 3.14: *Immunohistochemistry of 48 hpf embryos with anti-acetylated tubulin antibody. A) Lateral view of an MO-Ctrl embryo. MO-mfn2 injected embryos displayed several types of motor neuron alterations (arrows): premature branching (B), truncation (C) and failed extension (D). Scale bar: 50 μm. E) Trunk motor neurons at the level of the yolk extension were evaluated and embryos were considered altered if at least one misshaped motor neuron was present. No statistically significant difference between control (MO-Ctrl) and rescued embryos (MO-mfn2+hMFN2-wt) was observed. Significance was determined by Fisher's exact test. ***p < 0.0001.*

Analysis of neuromuscular junctions in mfn2 morphant larvae

The formation of neuromuscular junction (NMJ) is a key event in the development of neuromuscular system. It was recently demonstrated that the aggregation of acetylcholine receptor clusters (AChR) occurs in muscle fibres before the contact of neurons. After the elongation of neurons, only the AChR clusters that are contacted by the growth cone can form functional NMJs, while the others rapidly disappear. In zebrafish AChRs start to pre-pattern at 16 hpf, in advance of the extension of CaP motorneurons, and are stabilised by 20 hpf, when the elongation of primary motorneurons is almost completed (124). Since the incorrect formation NMJs can cause movement defects, we performed an analysis of NMJ formation in *mfn2* morphant larvae. The analysis was performed on 48 hpf larvae, since at this stage the NMJs should be completely developed. To analyse the innervation of muscles, axon terminals were stained in green by immunohistochemistry with sv2 antibody, which binds to synaptic vesicles, while acetylcholine receptors were marked with a red fluorescent α-bungarotoxin (BTX). Embryos were then mounted laterally and visualised with a confocal microscope (Fig. 3.15). This analysis revealed that in mfn2 knock-down larvae the arborisation of intact CaPs motorneurons is highly diminished (Fig. 3.15 A and A'). Acetylcholine receptors are greatly reduced (Fig. 3.15 B and B') and the colocalisation with the signal of sv2, indicating the formation of a functional neuromuscular junction, is present only in a small area of the mid-region of some somites, (see arrows in Fig. 3.15 B'). Notably the colocalisation of sv2 and AChRs appear reduced also in fully elongated nerves, in which there is a complete depletion of AChR in the distal regions (see fig. 3.15 A''-B'').

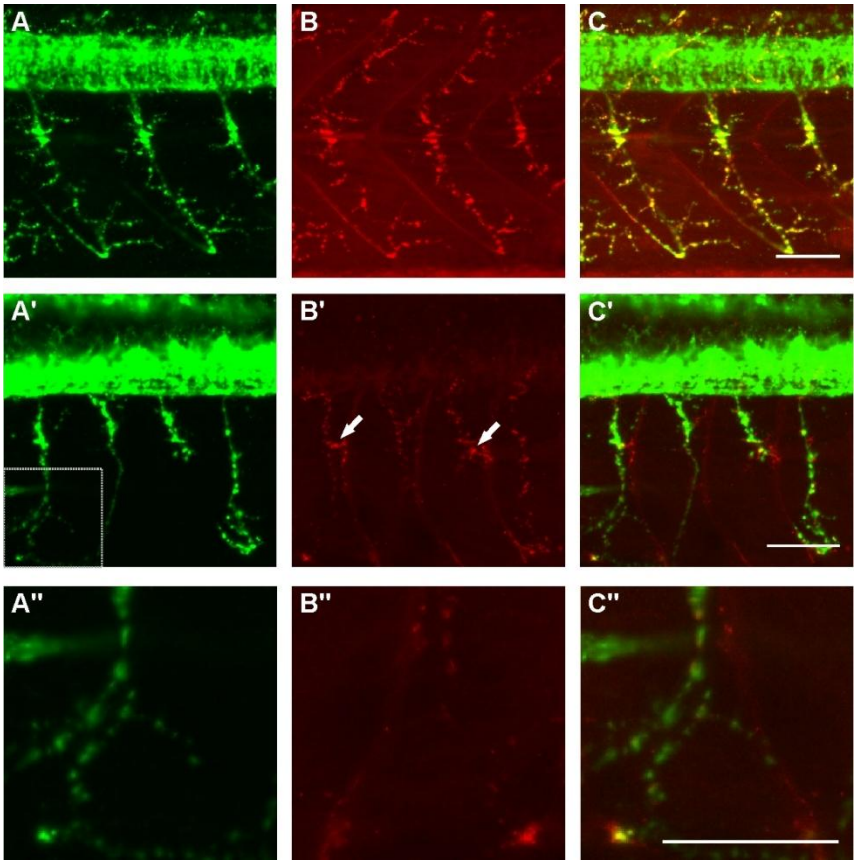

Figure 3.15: *Effect of mfn2 depletion on neuromuscular synapse formation on 48 hpf larvae. Zebrafish embryos were injected with MO-Ctrl (A–C) and MO-mfn2 (A'-C'), and stained for synaptic terminals, with sv2 antibody (green), and Acetylcholine receptors (AChR, red), with bungarotoxin (BTX) at 48 hpf. A) In 48 hpf control larvae caudal primary motor neurons (CaP) completely extended in the mid of each myotome and started to form many arborizations to contact the myofibres. A') In MO-mfn2 injected larvae, CaP motor neurons appeared disorganized and with less arborizations. BTX staining of controls embryos (B) showed the presence of AChR in the mid of each somite, in regions where the CaP's arborizations contact the muscular fibres (see merge panel in C). On the contrary, in mfn2-MO-injected larvae (B'), BTX staining was severely reduced, with a high presence of AChR cluster only in the mid of each somite (arrows in B') and along the myosepta. AChR are totally absent from the distal regions of fully elongated motorenurons (see A''-C'', which are the enlargement of the grey box in A'). Scale bar 50 μm.*

Effects of *mfn2* knock-down on somitic muscles

Considering the defects observed in the neuromuscular junctions formation in mfn2 morphants, and given that CMT2A patients suffer of a degeneration of muscular fibres that is secondary to denervation, an analysis of muscular fibres diameter was performed on MO-mfn2 injected larvae at 48 hpf. Muscle fibres were stained with fluorescent phalloidin, which binds to actin filaments, mounted laterally and visualized at confocal microscopy. An evident disorganization of the muscle myosepta structure, that appears U-shaped rather than V-shaped, was observed in 48 hpf MO-mfn2 injected larvae (Fig. 3.16 A-A'). The analysis of muscle fibres diameter revealed that, consistently with the pathology, mfn2 depletion determine also a reduction in the size of muscle fibres (2.4 ± 0.04 μm vs. 4.2 ± 0.1 μm) which in addition appear irregularly aligned and joined less tightly (Fig. 3.16 B).

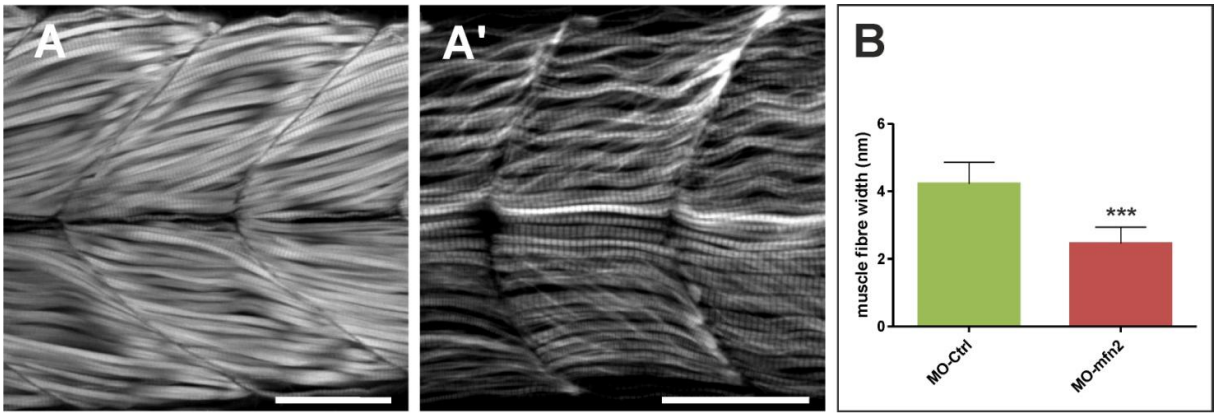

Figure 3.16: *Knock-down of mfn2 in zebrafish induces somitic and muscular alterations. MO-mfn2 and MO-Ctrl injected embryo were fixed at 48 h hpf and stained with phalloidin-tetramethylrhodamine that binds to F actin in muscle cells. Confocal microscopy confirmed the alterations of the shape of somites which compared with controls (A), appeared thinner and U-shaped in morphants (A'). Further analysis of the muscular fibres revealed that in MO-mfn2 treated embryos the width of the single myofibres is significantly smaller than in controls (B). Images in A and A' were centred in the 12th somite and resulted from the merge of 2 images taken at 2 µm of distance. Scale bar 50 µm. Significance was determined by t test with Welch correction. ***p < 0.0001.*

3.3.3: MO-mfn2 rescue with human and R94Q mutated *MFN2* transcripts

The effect of morpholinos can be sometimes due to their off-target effect on other genes. For this reason when working with MOs it is important to include some experiments in order to control for such events. The use of a control-MO, with no target in the zebrafish transcriptome, is common to evaluate a toxic effect of the morpholino molecule. To specifically control the off-target other methods have to be used. The conclusive evidence of the specificity in a knock-down experiment using morpholinos is the phenotypic rescue with the mRNA of the knocked-down gene.

Since human and zebrafish mitofusins share a high sequence similarity, we decided to performed rescue experiments using the human *MFN2* transcript. In this way we will be able also to determine if the human mitofusin 2 can complement the function of the endogenous zebrafish mfn2, and thus assess if the two proteins share the same functions. In parallel to the rescue experiments with the wild-type human *MFN2* mRNA, we performed also the rescue with a *MFN2* transcript bearing the mutation R94Q in the GTPasic domain. This mutation is one of the most frequent found in CMT2A patients. It is generally associated to an early onset and severe phenotype and has a high penetrance. However the mechanism of action (gain or loss of function) of this, as of other mutations, is not clear. Rescue experiments with the R94Q mutated transcripts will help to assess if this mutation *in vivo* can act via a loss of function mechanism.

Vitality, morphological phenotype, movement and percentage of embryos with motorneurons alterations were analysed in morphants rescued with human wild-type (hMFN2-wt) or mutated (hMFN2-R94Q) *MFN2* mRNA.

The coinjection of MO-mfn2 with hMFN2-wt significantly increased the vitality of larvae (p-value=0,0033) since the percentage of embryos dying at 48 hpf passes from the 36% of morphants to the 20% in hMFN2-wt rescue. On the other hand, hMFN2-R94Q was not able to increase the vitality, and causes a percentage of lethality not significantly different to that observed in morphants (Fig 3.17 A).

Although the injection of hMFN2-wt cannot completely rescue the phenotype of MO-mfn2 morphants, a statistically significant difference in the distribution of phenotypes between morphants and hMFN2-wt injected embryos was observed (p-value<0,0001). hMFN2-wt causes an amelioration of the phenotype, reducing the percentage of embryos with a mild and severe phenotype and inducing an increase of normal embryos which passed from a percentage of 1,4% in morphants to the 23,2% in hMFN2-wt rescue. Rescue with hMFN2-R94Q can also ameliorate the phenotype of morphants, but at a lower degree than hMFN2-wt. hMFN2-R94Q causes an increase of normal embryos to only the 8,3% and do not significantly modify the percentage of embryos with a severe phenotype (Fig. 3.17 B).

Movement alterations were evident in the 82,8% of morphants. Rescue performed with hMFN2-wt reduce this percentage to 67,5%. Wild-type transcript acts by increasing the percentage of normally responding embryos, which passes from the 17,2% of morphant to the 32,5% (p-value=0,0016). Surprisingly hMFN2-R94Q could also ameliorate the motor abilities of morphants. This effect seems to be as strong as that of hMFN2-wt, since no statistically significant differences can be noticed in the distributions of motility-phenotypes between hMFN2-wt and R94Q rescued larvae (Fig. 3.17 C).

The most evident effect of hMFN2-wt transcript was noticed at the level of motorneurons. The coinjection of hMFN2-wt with MO-mfn2 was able to completely rescue the percentage of embryos with altered motorneurons found in morphants (67,4%) to a percentage (35,3%) not significantly different to that of MO-Ctrl injected larvae (26%). Interestingly hMFN2-R94Q did not rescue these defects, leading to a percentage of embryos with motorneurons alterations of 58%, not significantly different from that of morphants (p-value=0,1999).

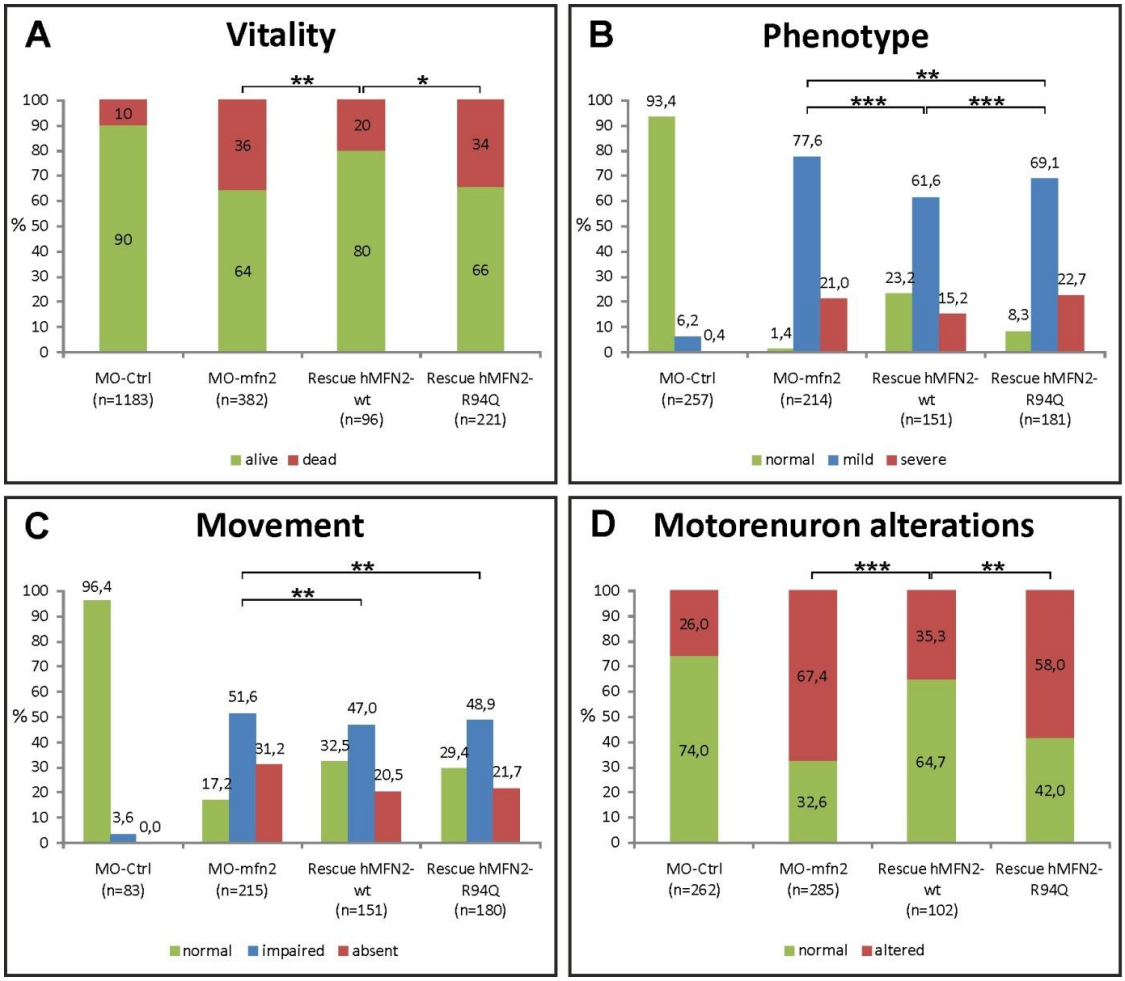

Figure 3.17: *analysis of vitality (A), phenotype (B), movement (C) and motorneuron alterations (D) in morphants rescued with human wild-type (hMFN2-wt) or mutated (hMFN2-R94Q) mRNA. The results obtained for controls (MO-Ctrl) and morphants (MO-mfn2) are shown as comparison. A) Analysis of vitality of embryos at 48 hpf. While hMFN2-wt is able to completely rescue the vitality, hMFN2-R94Q do not ameliorate significantly this characteristic giving a distribution not significantly different from that of morphants. B) hMFN2-wt transcript significantly ameliorate the phenotypic alterations found in morphants. Also hMFN2-R94Q display an effect, causing a distribution significantly different to that of morphants, but it result less effective than hMFN2-wt. C) Movement defects found in morphants are partially rescued by the coinjection of hMFN2-wt with MO-mfn2. Rescue performed with hMFN2-R94Q resulted as efficient as with the wild-type transcript. E) Motorneuron alterations are completely rescued by hMFN2-wt since no statistical differences between rescue hMFN2-wt and MO-Ctrl were found with chi-square test. On the contrary, hMFN2-R94Q do not rescue the motorneuron alterations found in morphants, being the distribution of rescue hMFN2-R94Q not significantly different compared to that of morphants.*
*(***p < 0.0001; **p < 0.001; *p < 0.01).*

3.3.4: Analysis of the gain of function effects of wild-type and mutated *MFN2* in zebrafish

Through the analysis of the effects of hMFN2-R94Q rescue we were able to evaluate if the R94Q mutation retains some functionality in the absence of *mfn2*, and thus the possibility that in patients it acts via a loss of function mechanism. To assess if it has also a gain of function effect, we injected high doses of the mutated mRNA in fertilized zebrafish eggs, in order to overexpress the protein during their development. We titrated the dose of mRNA and we decided to use a dose of 250 pg of mRNA per embryo, which was the higest tolerated dose of

the wild-type transcript. As a control, since mRNA is rapidly degraded, a semiquantitative RT-PCR using primers specific for the human MFN2 mRNA was performed, in order to verify the retention of the mRNA after 48 hpf, the time of the analysis (Fig. 3.18). As a control, for each experiment a batch of embryos was injected in parallel with water or with the same amount of the wild-type transcript.

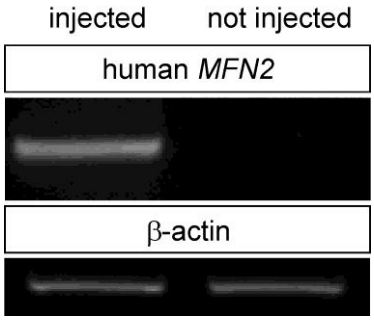

3.18: *Semiquantitative RT-PCR analysis performed to evaluate the presence of the human transcript at 48 hpf in embryos injected with 250 pg of hMFN2. cDNA obtained from injected embryos was amplified using primers specific for the human sequence. β-actin amplification was used as a control.*

Development of larvae injected with water, hMFN2-wt or R94Q was monitored over 2 days post fertilisation. Phenotypically, larvae overexpressing wt or R94Q mitofusins were morphologically not distinguishable from water-injected larvae and showed the same survival rate. In addition, in contrast with morphant embryos and CMT2A patients, hMFN2-R94Q overexpressing larvae showed at 48 hpf the same movement ability observed in hMFN2-wt and water injected control larvae.

Even though morphologically MFN2 R94Q overexpressing embryos display any alteration, it is still possible that subtle motorneuronal and muscular alterations are present but are unable to induce a gross phenotypic defect in the first developmental stages. For this reason we analysed the structure of ventral motor nerves by immunohistochemistry with an anti-acetylated-tubulin antibody. As can be seen in figure 3.19, any difference in the development of motorneurons was evidenced.

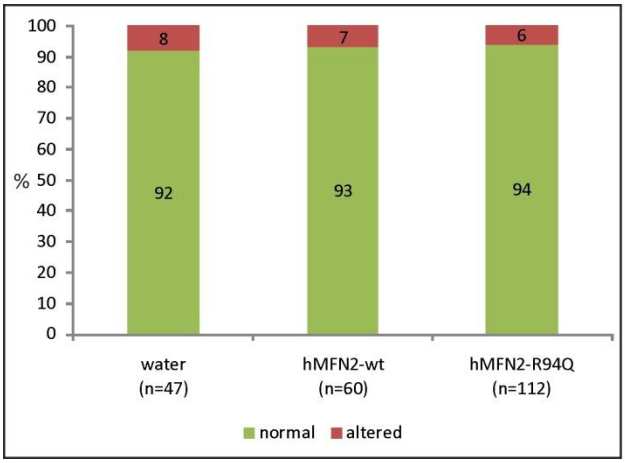

Figure 3.19: *analysis of motorneuron alterations in water, and 250 pg hMFN2-wt and hMFN2-R94Q injected larvae at 48 hpf. No alterations were evidenced in the differently injected embryos.*

To further analyse the effects of R94Q over-expression in the neuromuscular system, we performed the analysis of neuromuscular junction by staining motorneurons in green with sv2

antibody and AChR in red with a fluorescent BTX. Once again no overt differences were demonstrated between larvae injected with water, hMFN2-wt or hMFN2-R94Q mRNA (Fig. 3.19).

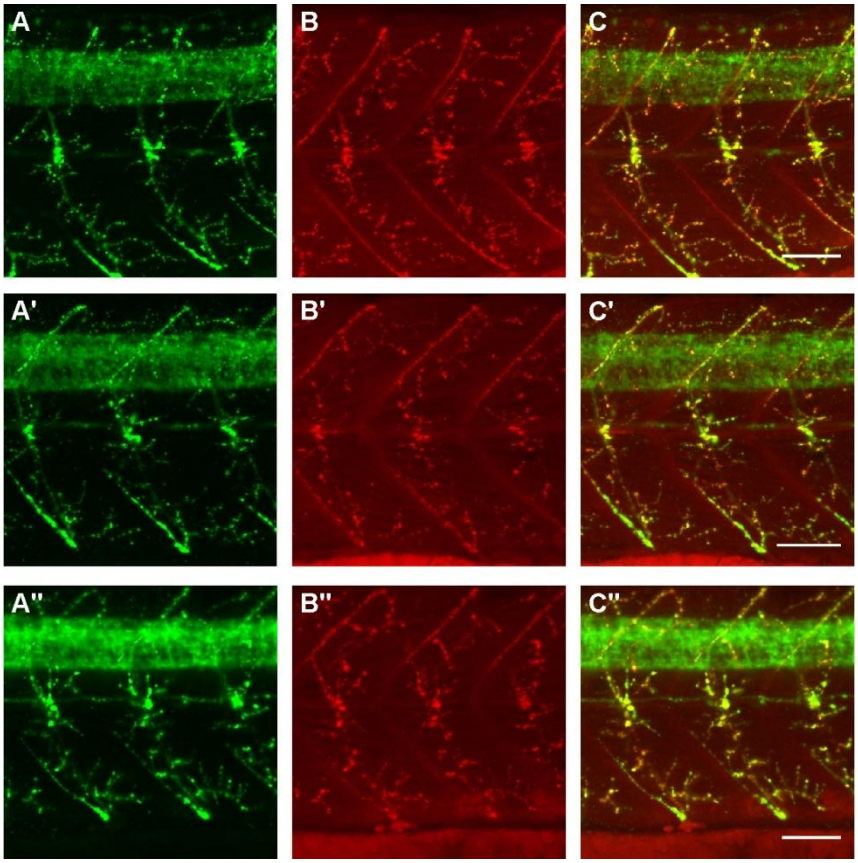

Figure 3.20: *Analisys of the neuromuscular junction of water and 250 pg hMFN2-wt and hMFN2-R94Q injected larvae at 48 hpf. In green are synaptic terminals stained with sv2 antibody, in red the acetylcholine receptors marked with a fluorescent bungarotoxin. No differences between water (A-C), 250 pg hMFN2-wt (A'-C') and hMFN2-R94Q (A''-C'') injected larvae were evidenced.*

Finally an analysis of somitic muscle fibres was performed after staining with fluorescent phalloidin. Somitic muscles appear normally developed both in hMFN2-R94Q and wt injected larvae and the analysis of muscular fibres thickness revealed no significant reduction of their diameter (Fig. 3.20).

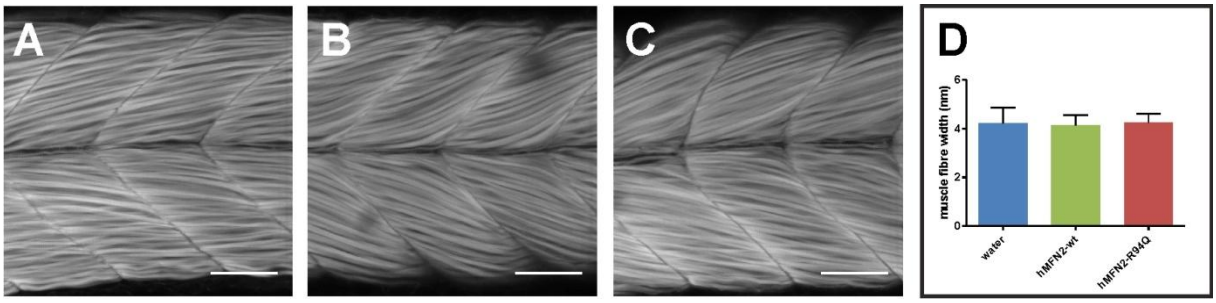

Figure 3.21: *A-C) somitic muscles of 48 hpf injected larvae stained with fluorescent falloidin and visualised at confocal microscope. Differences in the structure of muscles was not evidenced in water (A), 250 pg hMFN2-wt (B) or hMFN2-R94Q (C) injected larvae. The analysis of muscle fibres diameter was performed in differently treated embryos, but no statistical differences were found with t-test.*

Chapter 4: Discussion

Charcot-Marie-Tooth neuropathies (CMT) are a group of genetically heterogeneous diseases of the peripheral nervous system. They present with progressive distal muscles weakness, followed, during the disease course, by muscle atrophy. Alterations of sensory nerves are also present and differentiate CMTs from other related hereditary neuropathies. With a median prevalence of 1:2500, they are the most common hereditary pathology of the peripheral nervous system and have been found world-wide in all races and ethnic groups. These diseases can be extremely disabling, since patients slowly lose their use of lower and, frequently, upper limbs and represent a serious medical problem for which an effective medical treatment is still lacking. On the basis of electrophysiological criteria, CMTs are subdivided into demyelinating (CMT1) and axonal (CMT2) forms. Several genes and loci have been associated to many different demyelinating and axonal subtypes of CMT. In some cases different mutations in the same gene are able to cause both CMT1 and CMT2, thus showing the great genetic and clinical heterogeneity of these pathologies. Among axonal forms, CMT2A was described as the most common subtype, being responsible for the 16-33% of all axonal cases. CMT2A is associated to mutations in mitofusin 2 gene (MFN2), which codes for a dynamin-like GTPase found in the outer mitochondria and on the membranes of endoplasmic reticulum (ER). Together with its orthologue MFN1, it mediates the events leading to fusion of outer mitochondria membranes. Both MFN1 and MFN2 are orthologues of the fzo proteins found in invertebrates and yeast and share with them a conserved domain structure. Mammals' mitofusin 1 and 2 have a GTPase domain at the N-terminal, a coiled coil region (HR1) a transmembrane domain and a second coiled coil region (HR2) at the C-terminus. Mitofusins on opposite mitochondria are able to interact via their HR2 regions to form homo or hetero-oligomers which tether mitochondria outer membranes prior to fusion. A functional GTPase domain is necessary to permit this function and most likely provides the energy for the subsequent fusion event. More than 80 CMT2 disease causing mutations have been described in *MFN2*. They are most frequently missense mutations with dominant inheritance and are located preferentially in the GTPase domain or in the region between this and the HR1 region. However, recently some rare cases of recessively inherited MFN2 mutations were reported. Mitofusin 2 mutations can frequently lead to a CMT phenotype complicated by other symptoms. Patients with optic atrophy, sensoryneural hearing loss or alterations in the central nervous system have been reported. The

severity of the phenotype is usually related to the age of onset, and patients with earlier manifestations of the pathology are frequently more severely affected. This clinical subdivision between early-onset severe and late-onset mild patients does not transpose to a clear genotype relation. Indeed the way mutations in *MFN2* lead to CMT2A is almost unexplained. The comprehension of the molecular mechanisms underlying this neuropathy is complicated by the fact that recently the involvement of MFN2 in cellular processes other than mitochondria fusion has been described. *MFN2* and *MFN1* have not completely redundant function, and even if they are both ubiquitous proteins, they have some differences in tissue specific expression. Contrary to MFN2, MFN1 is involved also in the fusion of inner mitochondria membranes, being its presence required for the action of OPA1, the inner mitochondria membrane pro-fusion protein. On the other hand MFN2 seems also involved in the transport of mitochondria along microtubules. Being the highly active synaptic terminals far from the soma as much as one meter, motorneurons are greatly dependant on axonal transport of organelles and vesicles. The role of MFN2 in axonal transport of mitochondria was not well elucidated, but it was demonstrated that MFN2 directly interacts with the Miro/Milton protein complex, which allows the movement of mitochondria along microtubules in a Ca^{++} dependant manner. The presence of alterations in mitochondria distribution along axons of patients seems to favour this as the main pathological mechanism of CMT2A disease. MFN2 is found in a little extent also on the membrane of endoplasmic reticulum (ER). There, by forming homo-dimers with other MFN2 molecules or hetero-dimers with MFN1, it mediates the tethering of ER to mitochondria. This is a core event allowing the efficient transport of Ca^{++} between these two organelles. In the absence of MFN2 or when mutated forms are expressed, mitochondria detach from ER causing an overload of Ca^{++} in the cytosol upon stimulation. This may have important implications on Ca^{++} signalling and induction of apoptosis, but also on the Ca^{++} mediated mitochondria movement. MFN2 has also a role in cell signalling, which is triggered by its Ras binding domain in the N-terminal. Besides all these new evidences, the relation of these multiple functions of MFN2 and their role in neurodegeneration are still unexplained and particularly the mechanism of action of *MFN2* mutations leading to CMT2A is not well established. In vitro analysis demonstrated that mutations can both disrupt or retain the capacity of the protein to induce mitochondria fusion, thus meaning that both gain and loss of function of MFN2 could cause the disease. Interestingly the fusion-incompetent mutations, as R94Q and T105M, are able in the presence of wild-type MFN1 but not MFN2, to induce the recovering of mitochondria tubules. This led to the hypothesis that cells with lower MFN1 expression, as neurons, are more susceptible to alterations in MFN2 function. Some mutations

were reported to alter ER-mitochondria tethering and mitochondria transport, but those studies were performed mainly on the R94Q mutation and other mutant forms of the protein have not been intensely studied. With the aim to identify the genotype-phenotype correlation and clarify the mechanism of action of *MFN2* gene mutations, in this thesis I proceeded in two different research lines. On one hand I performed a screening for *MFN2* mutations in a cohort of 25 patients with diagnosis of CMT2 to identify new causative mutations and to get further insight into the genotype-phenotype correlation. On the other hand, considering the lack of a useful animal model for CMT2A, I tried to model this disease in zebrafish (*Danio rerio*) by knock-down experiments and gain of function analysis of *mfn2*.

Patients enrolled in this study were diagnosed with axonal CMT on the basis of clinical symptoms and electroneurography, which was performed on all adult subjects. Fourteen (56%) displayed autosomal dominant and two (8%) autosomal recessive inheritance, while the others were sporadic cases. They all presented with the usual CMT clinical symptoms while upper limb involvement was reported in nine (36%) subjects. Additional complicating symptoms, commonly found in CMT2A patients, were present in 6 (24%) subjects. Age at onset was variable and comprised between 1 and 50 years of age.

Sequencing of all *MFN2* exons allowed the identification of 6 causative mutations in 5 probands, since a patients was found to be a compound heterozygote. Of these mutations, 4 were never reported and were not found in control subjects. The *MFN2* mutation frequency found in our CMT2 patients (20%) is in perfect agreement with that reported in literature (16-33%). All mutations located preferentially in the N-terminal region of the protein, involved conserved aminoacidic residues. Four were missense, but two novel single aminoacid deletions were also identified.

Three mutations involved residues that were previously known to be affected, and indeed two of these were just described in the literature. The novel mutation R94P, identified in patient 10, involves the arginine 94, which is the most frequently mutated aminoacid found in MFN2. Substitutions of this residue with the aminoacids glutamine and tryptophan were reported a total of 22 times independently, in both familial and sporadic cases of CMT2A. It was already known that this site represents a mutational hot spot, and the finding of a different substitution with proline at this position confirms this hypothesis. Although CMT2A is a phenotypically heterogeneous disease, which can present also with different severity in patients of the same kindred, mutations in arginine 94 usually cause severe disease. CMT2A linked to R94Q, for example, generally has an onset between 2 and 7 years of age and is frequently complicated by

additional symptoms, particularly optic atrophy. Patient 10 displays a later onset of the disease, with the first walking difficulties appearing at 16 years. However his clinical symptoms appear uncommonly severe for an axonal CMT, being affected by flaccid tetraparesis. From the pedigree, is possible to speculate that the mutation was dominantly inherited through his mother (Fig. 2.7). Being so, the mutation R94P in this kindred shows phenotypic heterogeneity, since the affected mother has a much milder phenotype.

The mutation H165R was found in patient 21. This substitution was already reported five times in literature and several other mutations affecting histidine 165 were described (see Fig. 2.1). Patients with H165R mutation display a mild phenotype, generally involving only lower limbs, and a relatively late onset (6-50 years, mean 20 years). These data are in accordance with the clinical features of patient 21, who shows an extremely mild disease with late onset.

A third mutation, affecting a previously described residue, is the substitution of a threonine with a methionine at position 362 identified in patient 24. Interestingly, this patient was found to be a compound heterozygote, bearing also the previously undescribed mutation K38del. T362M was reported only in another patient affected by CMT2A with two *in trans MFN2* mutations (76). Also in that case, the parent bearing the T362M mutation was unaffected, thus implying a recessive inheritance. Patient 24 is not the first compound heterozygote described, and recently other subjects with mutations in both *MFN2* alleles have been reported. In all cases the parents of the proband, bearing only one mutation, result unaffected, although some subclinical manifestations, as *pes cavus*, has been described (76, 77). People with compound heterozygous or homozygous mutations have always early onset and severe phenotype, and this is in accordance with the clinical manifestations found in patient 24. Indeed this subject shows a disease of uncommon severity for a CMT2A.. He suffers of all the complicating symptoms described independently in other patients (optic atrophy, deafness, upper limb involvement, respiratory failure) with the addition of facial muscle weakness, never reported in CMT2A. Interestingly, T362M was described also in a CMT2 family where this mutation shows dominant inheritance and a very mild phenotype. This implies that T362M is a semi-dominant MFN2 allele. Only another mutation (R707W) was described to cause both dominant and recessive pattern of inheritance, while the other recessive *MFN2* mutations were found in affected patients exclusively in homozygosis or compound heterozygosis. This is fascinating, since indicate that possibly these two groups of mutations act via different molecular mechanisms. Specifically, the fact that mutations found in homozygosis or compound-heterozygosis cannot induce a phenotype when alone, may indicate they act through a loss of function mechanism. Interestingly in mouse the complete knock-out of *mfn2* is lethal. The fact

that these putative loss of function mutations, when present in both alleles, do not cause a lethal phenotype, probably means they retain a certain level of functionality. It was observed that in yeast, fzo alleles with loss of function mutations in different domains of the protein are able to complement each other (64). In this view, it is interesting to note that, of all patients with recessive MFN2 mutations, compound heterozygotes, in 5 cases on a total of 6, bear mutations located in two different domains of the protein.

Patient 5 was found to carry an in frame deletion of 3 nucleotides leading to the deletion of glutamic acid residue at position 329 (E329del). This mutation, located in a conserved position between the GTPasic domain and HR1, was never reported before and was not found in control subjects. This mutation is associated to an early onset severe CMT2A phenotype complicated by optic atrophy. Besides the single aminoacid deletion K38del found in patient 10, only another in frame deletion (L379_M381del) was described in literature (40). Unfortunately in the paper by Verhoeven and colleagues, a detailed phenotypic report associated to L379_M381del is not given, so it is impossible to make a confrontation with the findings of patient 5.

In one kindred with a dominant axonal CMT I found the missense mutation A738V. This mutation is located in the C-terminal of the protein, after the HR2 domain. Mutations outside the GTPase region or the GTPase-HR1 linking region are rare and only 6 of such mutations have been reported so far (16, 40, 75, 125).

Among the 25 patients I investigated, 20 resulted not to be mutated. To evaluate the possibility that *MFN2* rearrangements were responsible for the pathology in these subjects, I performed a MLPA (Multiplex Ligation-dependent Probe Amplification) analysis. This was considered necessary since in recent years there is growing evidence that large gene rearrangements, involving entire exons, may be causative of several human genetic diseases previously associated only to point mutations. Some examples are the duplication of PMP22 gene that cause CMT1A (126) and its deletion, which is associated to hereditary neuropathy with liability to pressure palsies (HNPP) (127). Among hereditary spastic paraparesis, the subtype SPG4 is caused in the 40% of cases by exons deletions in spastin gene (128). Moreover, in a recent paper (77) a deletion comprising exons 7 and 8 of MFN2 was found associated to CMT2A disease, thus proving that, even though probably rare, deletions of whole exons can be also a cause of the pathology. MLPA analysis revealed that none of the non-mutated patients bear a gene rearrangement in MFN2, thus meaning that probably *MFN2* rearrangements are a rare cause of CMT2A.

The *MFN2* screening in CMT2 patients allowed the identification of new disease causing mutations. Although the phenotype of the disease was confirmed to be variable, some suggestions of a genotype-phenotype correlation and some possible molecular explanations were given. A whole comprehension of molecular mechanisms of *MFN2* mutations can however only be reached through *in vitro* and *in vivo* studies. While *in vitro* studies have proved to be useful to understand some aspects of wild-type and mutant *MFN2*, *in vivo* studies have been slowed down for a long time by the lack of a good model of the disease. Knock-out mice for either *Mfn1* or *Mfn2* are full viable and fertile in heterozygous state, but in homozygosity they die due to placenta defects. *Mfn2* conditional knock-out mice display perinatal lethality as well, but are also motor impaired (62). However, this is due to the degeneration Purkinje cells in the cerebellum, rather than alterations in motorneurons. To date three mouse lines expressing only two of the *MFN2* disease related mutations (R94Q and T105M) were developed and just one has a phenotype resembling CMT2A disease (82).

Since the study of numerous different *MFN2* mutations, both in man and animal models, is crucial to understand in detail the pathomechanisms of CMT2A, and considering that that the strategies used so far appear to be not exhaustive, in the second part of my project I decided to move on a different animal model. Zebrafish (*Danio rerio*) offers several advantages that make it a useful complement to the mouse models of disease. With its short reproductive cycle and the large number of progeny, contrary to mammal models, it is amenable to several forward genetic analysis. However, as in mouse, experiments of reverse genetics, particularly knock-down and over-expression of genes, are also possible and in some cases even more easily performed. Furthermore, being a vertebrate, anatomy and physiology are more similar to that of mammals rather than other widely used invertebrate models as *Drosophila* and *Caenorhabditis*. Due to its transparency, zebrafish neuromuscular system has been characterized in detail and it was shown that its development and functioning is exceedingly similar to that of higher vertebrates. For this reasons zebrafish appears especially suitable for the study of neurodegenerative and neuromuscular disorders, and indeed some important successes in this field have just been obtained. To analyse mitofusin 2 in zebrafish, I first performed a bioinformatical analysis to retrieve zebrafish mfn2 and evaluate its conservation degree with the mitofusins of other organisms. *mfn2* was found in zebrafish as a single copy and maps on chromosome 8. This is an important finding, since several genes are duplicated in zebrafish and the analysis of a gene present in two copies can be more difficult due to the fact that the two paralogues may both retain the same redundant functions or diverge completely.

As expected, zebrafish genome codes also for *mfn1*, and this is a significant feature as well, since is known that mitofusin 1 is able to interact and modify the phenotypic expression of mitofusin 2 mutations. In this view studying mitofusin 2 functions and mutations in a model with both mitofusins is of great importance, since the results obtained will be more easily and directly translated to human beings. The conservation analysis made by comparing the protein sequence of zebrafish mfn2 with that of other organisms, demonstrates the high conservation of this protein, a feature that is compatible with a very important function of this gene. Mitofusins 2 appears more highly conserved than mitofusins 1, as displayed by the lengths of branches in the phylogenetic tree reported in figure 3.6. Not only the aminoacidic sequence, but also the intron-exon gene organisation and the genomic location are retained. A comparison between human, mouse and zebrafish mitofusin 2 proteins reveals that zebrafish share a high percentage of similarity (92%) with both mammals and that this similarity is particularly high in the active domains of the protein. The transmembrane region show a 99% of identity, thus indicating it has a fundamental role, probably for the correct localisation of the protein. Intriguingly mutations in this domain were never found in patients with CMT2A. To find out if the pattern of expression of *mfn2* in zebrafish resembles that of man and other mammals, I performed semiquantitative RT-PCR on embryos at different developmental stages and on several adult tissues. This analysis revealed that, as in other animals, mfn2 is ubiquitously expressed and it has also maternal expression. This is common for genes that are important to sustain the rapid and energy demanding early cell divisions (129), a property that is also expected for *mfn2*. While *mfn2* expression shows minimal differences on embryos up to 5 days post fertilisation (dpf), the analysis of adult tissues revealed that in zebrafish *mfn2* is highly expressed in heart, muscles, brain and eyes. This pattern of expression resembles that described in humans, in which MFN2 is ubiquitous but enriched particularly in heart and skeletal muscles. To analyse more deeply the expression pattern of *mfn2* mRNA also in larval stages, I performed whole mount in situ hybridisation on embryos and larvae from 1 cell to 2 dpf. This analysis confirmed the maternal expression of the gene. Moreover it was found that its expression remains ubiquitous in the very first stages of development, while from the stage of 18 somites it starts to localise specifically in some regions. Interestingly by 48 hpf the mfn2 mRNA has gained almost the same tissue specificity found in adults, being expressed mainly in somitic muscles, heart, brain and eyes. To have an indication of the role of *mfn2* during zebrafish development, this gene has been knocked-down by injecting a specific antisense morpholino in one-four cell stage embryos. Morpholinos (MOs) are the most widely used anti-sense knock-down tools available in zebrafish. They have the same bases of DNA, but their neutrally charged

phosphorodiamidate backbone results in molecules with a higher binding affinity for RNA than siRNA. MOs, typically long 25 bases, act by steric hindrance and can be both constructed on the translational start site or on the splice-site of a RNA species. In the first case, MOs will be able to inhibit both maternal and zygotic transcripts, while in the second case they will only act on zygotic mRNAs. To perform the knock-down of *mfn2*, a splice-morpholino (MO-mfn2) was used essentially for 2 reasons. First the silencing effect of a splice-morpholino is more easily monitored than translation-MO and requires the execution of a simple RT-PCR analysis, rather than a western-blot. Second, since in mouse the complete knock-out is lethal and considering that in zebrafish mfn2 is probably important during the first cell divisions, by using a splice-morpholino total embryonic lethality observed in knock-out mice was avoided. MO-mfn2 was designed over the acceptor splice site of intron 2. Being exon 1 and exon 2 5'UTR coding, this was the most upstream protein coding region targetable. In this way it should be avoided the possibility of the production of shorter peptides with potential gain of function effect. By titrating different doses of MO, I found that the injection of 7,5 ng of MO-mfn2 per embryo gave the best result in term of vitality and penetrance of the phenotype. Indeed it was immediately clear that *mfn2* morphants have a dramatically reduced vitality that resulted dose-dependent. Moreover a semiquantitative RT-PCR analysis, performed on RNA extracted from embryos treated with different doses of MO, showed that doses greater than 7,5 ng do not cause a higher silencing effect. MO-mfn2 acts by inducing the skipping of exon 3, an event which introduces a premature stop codon in exon 4. This altered transcript is supposed to code for a protein lacking GTPase and for this reason results probably inactive. In addition, the triggering of nonsense mediated decay (NMD) of this miss-spliced transcript can be hypothesized on the basis of the semiquantitative RT-PCR analysis. Using this morpholino-injection protocol, that allowed to reduce *mfn2* expression of about the 70%. evident phenotypic and behavioural abnormalities in the majority of *mfn2* zebrafish morphants were induced. These alterations were mainly evident in 48 hpf embryos. A small group of larvae presented with heavy structural abnormalities, while a more frequent one show a distinctive phenotype, defined by the presence of facial prognathism, underdeveloped eyes, brain ventricles enlargement and curly-tail. Notably these alterations occurred in the tissue where *mfn2* mRNA is expressed at highest level in the 48 hpf larvae, as demonstrated by WISH. Moreover, the morphological phenotype I obtained was remarkably similar to that observed in two morphants developed to study hereditary spastic paraplegia, where MO knock-down experiments were performed silencing *SPG8* and *SLC33A1* genes (130, 131). Morphants are also severely impaired in motor capability. At 48 hpf one third is unable to respond by

swimming to a soft touch stimulus at the tail, a reaction that is commonly observed in larvae at this stage of development. Since at 2 dpf the neuromuscular system of zebrafish is quite completely formed, the absence of reaction or the diminished response, evident in quite a half of larvae, could indicate the presence of severe alterations in the neuromuscular system of morphants. An analysis of neurons structure, performed by immunohistochemistry against the pan-neural marker acetylated-tubulin, revealed that MO-mfn2 injected larvae have evident alterations in the morphology of primary motor neurons innervating ventral somites. Larvae showed differently altered nerves, and both miss-branched, truncated and absent motorneurons were noticed. Moreover the acetylated-tubulin staining performed in morphants revealed a less strong signal than controls, with motorneurons frequently hardly visible due to their thinness. This could imply that motorneurons are abnormally depleted of stable microtubules, a feature that was noticed in other zebrafish morphants for genes associated to neuromuscular diseases, as atlastin (132) and spastin (112). To further characterize the neuronal alterations in morphants, I performed an analysis of neuromuscular junctions (NMJs) formation by staining pre-synaptic terminals with sv2 antibody and post-synaptic acetylcholine receptors (AChR) clusters with fluorescent α-bungarotoxin (BTX). It was demonstrated that during neuromuscular development, AChRs pre-pattern in muscle fibres before their innervation and this is independent from the expression of growth factors released by pre-synaptic axons. Later in development, only innervated AChR clusters stabilise. In zebrafish, AChRs pre-patterning is evident from 16 hpf, but by 20 hpf, with the completion of CaP motorneurons elongation, NMJs are formed and AChRs that are not innervated are rapidly reabsorbed (124). I analysed NMJ structure in morphant at 48 hpf, a stage in which evident morphological and movement abnormalities are just visible, but in which the innervation of muscles and the stabilisation of AChR clusters should be completed. This analysis revealed that *mfn2* morphants have a highly reduced axonal arborisation and an altered distribution of AChRs clusters, which are reduced in number and size and do not co localize properly with the axon terminals, especially in the distal part of nerves. This allows to hypothesize that the innervations of the lateral myotomes should be slightly reduced. Since CMT2A is characterised by muscle atrophy, that is secondary to the denervation, I decided to investigate if zebrafish *mfn2* morphants display also alterations in somitic muscles. By staining F-actin with a fluorescent phalloidin toxin, I was able to evaluate the morphology of somites and measure the thickness of muscle fibres with a confocal microscope. An evident disorganization of the muscle structure was observed in 48 hpf MO-mfn2 injected larvae. While controls have a V-shaped myoseptum and well-organized myofibres, mfn2 morphants exhibited U-shaped somites. Moreover, a significant reduction of

muscle fibres diameter was demonstrated. Since *mfn2* has a high expression in muscles, it is not clear if these alterations are a consequence of the depletion of mfn2 in muscles or a direct effect of their denervation. This last possibility is attractive, since it would mimic what happens in CMT2A patients. However future studies have to be performed to confirm this hypothesis.
Besides the morpholino technique is a simple and rapid method to obtain the knock-down of a gene in zebrafish, it is not exempted to problems. The main inconvenience is their knock-down effect on other genes, an event known as off-target. To control for such a possibility, the most robust method is to perform a phenotypic rescue by coinjecting the MO with a mRNA coding for the targeted gene. I performed rescue experiment using the mRNA coding for human MFN2. This was done not only to control for off-target, but also to have a functional indication of the conservation of mitofusin 2 in humans and zebrafish. Human *MFN2* mRNA significantly increased the survival rate of rescued embryos, which reached almost the same level observed in controls, suggesting that human MFN2 can efficiently compensate the depletion of endogenous zebrafish mRNA in early stages of development. Phenotypically, the number of embryos with a normal morphology was significantly increased and morphants with mild and severe phenotype reduced. Human MFN2 could also ameliorate the motor impairment found in morphants, although with a slightly less efficiency. Anyway, the most important result was obtained at the level of motorneurons, where MFN2 succeeded in completely restore the distinctive alterations of *mfn2* morphants. The fact that the mRNA rescue could not completely restore the phenotype of mfn2 morphants for some aspects can be easily explained. Indeed complete rescue can be difficult to obtain for genes with a strict time-dependant regulation of their expression pattern or for non-ubiquitous genes. In fact in these cases the mRNA injected to rescue the MO will be expressed also in times and/or tissues where they are normally absent, thus potentially leading to other gain of function phenotypes different from that obtained with the MO. Moreover, mRNA distribute not as equally as MO among cells, and this can lead to a some degree of mosaic expression of the protein. I have demonstrated that in zebrafish, mfn2 has a some degree of tissue-specificity. Moreover the mRNA I injected was almost 3 Kb long, so I can expect it has some difficulty in equally distributing between cells. For all these reasons, the amelioration of the phenotype I obtained is to be considered a success. Altogether these results demonstrate that human MFN2 is able to complement for the absence of zebrafish endogenous protein, and provide the evidence not only that the alterations found in morphant are specific, but also that man and zebrafish mitofusin 2 genes share the same functions and that mitofusin 2 plays an important role in the development of the neuromuscular system. This

may also indicate that zebrafish could be a useful tool to study in living embryos the effects of mutations identified in CMT2A patients.

For this reason, in the last part of my project, I exploited this possibility, performing *mfn2* morphant rescue experiment and gain of function analysis of the CMT2A causing mutation R94Q. The choice to study this mutation was not accidental. This residue is the most frequently mutated in CMT2A patients and R94Q is usually associated to early onset and severe disease. Moreover, this mutation has been extensively studied in both *in vitro* and in *vivo* models, and it was suggested that it disrupts the capacity of mfn2 to induce the fusion of mitochondria and their tethering to ER (63, 70). Furthermore it was also shown that mitofusin R94Q the capability to promote mitochondria transport along axons (65, 68). However, as for the other *MFN2* mutations, the mechanism of action of R94Q, and particularly its gain or loss of function activity, is not clear. In mouse the R94Q knock-in line is completely healthy in the heterozygous state. Homozygous mutants are lethal but in later developmental stages than the complete knock-out, thus implying that probably R94Q retains some degree of functionality. A transgenic line overexpressing R94Q in the nervous system was recently developed by Cartoni and colleagues (82). The homozygous transgenics are motor impaired and show some features, as muscular atrophy and alterations in mitochondria distribution along axons, which phenocopies at some degree the human disease. Contrarily to the transgenic for T105M mutation, that of Cartoni display these alterations late, from 5 months of age.

To study R94Q mutation in zebrafish, I first performed some rescue experiments of the *mfn2* morphant using the mutated human MFN2 mRNA. This was performed to evaluate if R94Q act via a loss of function mechanism. This mode of action seems to be favoured by in vitro studies performed so far, which are in contrast with the findings on the mouse transgenic model. Altogether the rescue analysis performed in zebrafish indicates that the R94Q allele has a diminished ability than the wild-type in inducing the amelioration of morphant phenotype. This diminished capacity is not equally distributed between the several phenotypic alterations I analysed. R94Q in fact is completely unable to recover the lethality and the motorneuron alterations of morphants, but is able to recover, the phenotypic alterations, although with less efficacy than the wild-type allele. Surprisingly I found that the ability of R94Q in the amelioration of movement alterations is of the same extent of that obtained with the non mutated mRNA. It is to note that movement alterations are not as efficiently recovered as other features by the wild-type mRNA. Thus slight differences in the effect of wild-type and R94Q mRNA in rescue the morphant phenotype could be hardly noticeable. To evaluate the

possibility that R94Q act via a gain of function mechanism, which seems favoured by the results obtained in mouse, I induced the over-expression of the mutated R94Q allele by injecting high doses of mRNA in 1-4 cell stage embryos. These experiments were performed using a dose 25 times higher than that used for rescue experiments. In this way I expected to obtain an over-expression of the protein sufficient to disclose a gain of function effect of R94Q. Titration experiments, performed using the wild-type transcript, demonstrated that this dose is tolerated by zebrafish embryos, thus any phenotypic alteration I would found in zebrafish injected with R94Q mRNA will be specifically caused by the mutated protein. Over-expression experiments did not reveal any gain of function effect of R94Q in the first stages of zebrafish development. Larvae at 48 hpf have the same vitality and morphology of wild-type MFN2 transcript or water control injected embryos. Moreover, they did not display any alteration neither in the neuromuscular system, as demonstrated by immunohistochemistry and not in NMJ and muscular fibres. These results demonstrate that, as in mouse, in the first stages of development the over-expression of R94Q do not induce phenotypic alterations. Unfortunately it is not possible to evaluate the effects of the over-expression of R94Q in zebrafish using mRNA injection only, since transcripts are rapidly degraded. This analysis is however possible using a transgenic line overexpressing R94Q along all the zebrafish life, and several technologies that would permit to generate this line are just available.

By finding new MFN2 mutations, with this thesis work I contributed to clarify the possible genotype-phenotype relations involved in CMT2A disease. Moreover, I demonstrated that in zebrafish, *mfn2* if required for the correct development of the neuromuscular system. Last, since in zebrafish loss of *mfn2* can be complemented by the expression of the human orthologue, I gave also evidences that this animal model can be a useful tool to dissect the molecular and cellular pathways leading to the disease, though probably it would be necessary to develop transgenic lines to model *MFN2* disease mutations in this animal. The validation of a zebrafish model for CMT2A could have in future some important applicative outcomes, since zebrafish is easily amenable to high throughput drug screens experiments, which could lead to the identification of active molecules to be used for the treatment of CMT2A (Wheeler & Brändli, 2009).

Bibliography

1. Merkwirth C & Langer T (2008) Mitofusin 2 builds a bridge between ER and mitochondria. (Translated from eng) *Cell* 135(7):1165-1167 (in eng).
2. Eura Y, Ishihara N, Yokota S, & Mihara K (2003) Two mitofusin proteins, mammalian homologues of FZO, with distinct functions are both required for mitochondrial fusion. (Translated from eng) *J Biochem* 134(3):333-344 (in eng).
3. Charcot JM & Marie P (1886) Sur une forme particuliére d'atrophie musculaire progressive souvent familial debutant par les pieds et les jambes et atteignant plus tard les mains. *Revue médicale* 6:97-138.
4. Tooth HH (1886) The peroneal type of progressive muscular atrophy. (H.K. Lewis & Co, Ltd, London).
5. Braathen GJ, Sand JC, Lobato A, Hoyer H, & Russell MB (2011) Genetic epidemiology of Charcot-Marie-Tooth in the general population. (Translated from eng) *Eur J Neurol* 18(1):39-48 (in eng).
6. Barisic N, *et al.* (2008) Charcot-Marie-Tooth disease: a clinico-genetic confrontation. (Translated from eng) *Ann Hum Genet* 72(Pt 3):416-441 (in eng).
7. Harding AE & Thomas PK (1980) The clinical features of hereditary motor and sensory neuropathy types I and II. (Translated from eng) *Brain* 103(2):259-280 (in eng).
8. Patzko A & Shy ME (2011) Update on charcot-marie-tooth disease. (Translated from eng) *Curr Neurol Neurosci Rep* 11(1):78-88 (in eng).
9. P.J. Dyck, P. K. Thomas, J. W. Griffin, Low PA, & Poduslo JF (1993) *Hereditary motor and sensory neuropathies. In: Peripheral Neuropathy* (W.B. Saunders, Philadelphia, PA) 3rd Ed.
10. Garcia CA, *et al.* (1995) Clinical variability in two pairs of identical twins with the Charcot-Marie-Tooth disease type 1A duplication. (Translated from eng) *Neurology* 45(11):2090-2093 (in eng).
11. Lawson VH, Graham BV, & Flanigan KM (2005) Clinical and electrophysiologic features of CMT2A with mutations in the mitofusin 2 gene. (Translated from eng) *Neurology* 65(2):197-204 (in eng).
12. Berciano J & Combarros O (2003) Hereditary neuropathies. (Translated from eng) *Curr Opin Neurol* 16(5):613-622 (in eng).
13. Zuchner S & Vance JM (2006) Mechanisms of disease: a molecular genetic update on hereditary axonal neuropathies. (Translated from eng) *Nat Clin Pract Neurol* 2(1):45-53 (in eng).
14. Mersiyanova IV, *et al.* (2000) A new variant of Charcot-Marie-Tooth disease type 2 is probably the result of a mutation in the neurofilament-light gene. (Translated from eng) *Am J Hum Genet* 67(1):37-46 (in eng).
15. Perez-Olle R, *et al.* (2005) Mutations in the neurofilament light gene linked to Charcot-Marie-Tooth disease cause defects in transport. (Translated from eng) *J Neurochem* 93(4):861-874 (in eng).
16. Zuchner S, *et al.* (2004) Mutations in the mitochondrial GTPase mitofusin 2 cause Charcot-Marie-Tooth neuropathy type 2A. (Translated from eng) *Nat Genet* 36(5):449-451 (in eng).
17. Puls I, *et al.* (2003) Mutant dynactin in motor neuron disease. (Translated from eng) *Nat Genet* 33(4):455-456 (in eng).

18. Zuchner S, *et al.* (2005) Mutations in the pleckstrin homology domain of dynamin 2 cause dominant intermediate Charcot-Marie-Tooth disease. (Translated from eng) *Nat Genet* 37(3):289-294 (in eng).
19. Hinshaw JE (2000) Dynamin and its role in membrane fission. (Translated from eng) *Annu Rev Cell Dev Biol* 16:483-519 (in eng).
20. Schafer DA, *et al.* (2002) Dynamin2 and cortactin regulate actin assembly and filament organization. (Translated from eng) *Curr Biol* 12(21):1852-1857 (in eng).
21. Verhoeven K, *et al.* (2003) Mutations in the small GTP-ase late endosomal protein RAB7 cause Charcot-Marie-Tooth type 2B neuropathy. (Translated from eng) *Am J Hum Genet* 72(3):722-727 (in eng).
22. Kappe G, *et al.* (2003) The human genome encodes 10 alpha-crystallin-related small heat shock proteins: HspB1-10. (Translated from eng) *Cell Stress Chaperones* 8(1):53-61 (in eng).
23. Vos MJ, Hageman J, Carra S, & Kampinga HH (2008) Structural and functional diversities between members of the human HSPB, HSPH, HSPA, and DNAJ chaperone families. (Translated from eng) *Biochemistry* 47(27):7001-7011 (in eng).
24. Kostenko S & Moens U (2009) Heat shock protein 27 phosphorylation: kinases, phosphatases, functions and pathology. (Translated from eng) *Cell Mol Life Sci* 66(20):3289-3307 (in eng).
25. Carra S, Seguin SJ, & Landry J (2008) HspB8 and Bag3: a new chaperone complex targeting misfolded proteins to macroautophagy. (Translated from eng) *Autophagy* 4(2):237-239 (in eng).
26. Fontaine JM, Sun X, Benndorf R, & Welsh MJ (2005) Interactions of HSP22 (HSPB8) with HSP20, alphaB-crystallin, and HSPB3. (Translated from eng) *Biochem Biophys Res Commun* 337(3):1006-1011 (in eng).
27. Antonellis A, *et al.* (2003) Glycyl tRNA synthetase mutations in Charcot-Marie-Tooth disease type 2D and distal spinal muscular atrophy type V. (Translated from eng) *Am J Hum Genet* 72(5):1293-1299 (in eng).
28. McLaughlin HM, *et al.* (2010) Compound heterozygosity for loss-of-function lysyl-tRNA synthetase mutations in a patient with peripheral neuropathy. (Translated from eng) *Am J Hum Genet* 87(4):560-566 (in eng).
29. Jordanova A, *et al.* (2006) Disrupted function and axonal distribution of mutant tyrosyl-tRNA synthetase in dominant intermediate Charcot-Marie-Tooth neuropathy. (Translated from eng) *Nat Genet* 38(2):197-202 (in eng).
30. Latour P, *et al.* (2010) A major determinant for binding and aminoacylation of tRNA(Ala) in cytoplasmic Alanyl-tRNA synthetase is mutated in dominant axonal Charcot-Marie-Tooth disease. (Translated from eng) *Am J Hum Genet* 86(1):77-82 (in eng).
31. Brittis PA, Lu Q, & Flanagan JG (2002) Axonal protein synthesis provides a mechanism for localized regulation at an intermediate target. (Translated from eng) *Cell* 110(2):223-235 (in eng).
32. Benard G, *et al.* (2007) Mitochondrial bioenergetics and structural network organization. (Translated from eng) *J Cell Sci* 120(Pt 5):838-848 (in eng).
33. Chen H & Chan DC (2009) Mitochondrial dynamics--fusion, fission, movement, and mitophagy--in neurodegenerative diseases. (Translated from eng) *Hum Mol Genet* 18(R2):R169-176 (in eng).
34. Cuesta A, *et al.* (2002) The gene encoding ganglioside-induced differentiation-associated protein 1 is mutated in axonal Charcot-Marie-Tooth type 4A disease. (Translated from eng) *Nat Genet* 30(1):22-25 (in eng).

35. Pedrola L, *et al.* (2005) GDAP1, the protein causing Charcot-Marie-Tooth disease type 4A, is expressed in neurons and is associated with mitochondria. (Translated from eng) *Hum Mol Genet* 14(8):1087-1094 (in eng).
36. Niemann A, Ruegg M, La Padula V, Schenone A, & Suter U (2005) Ganglioside-induced differentiation associated protein 1 is a regulator of the mitochondrial network: new implications for Charcot-Marie-Tooth disease. (Translated from eng) *J Cell Biol* 170(7):1067-1078 (in eng).
37. Cassereau J, *et al.* (2011) Mitochondrial dysfunction and pathophysiology of Charcot-Marie-Tooth disease involving GDAP1 mutations. (Translated from eng) *Exp Neurol* 227(1):31-41 (in eng).
38. Ben Othmane K, *et al.* (1993) Localization of a gene (CMT2A) for autosomal dominant Charcot-Marie-Tooth disease type 2 to chromosome 1p and evidence of genetic heterogeneity. (Translated from eng) *Genomics* 17(2):370-375 (in eng).
39. Zhao C, *et al.* (2001) Charcot-Marie-Tooth disease type 2A caused by mutation in a microtubule motor KIF1Bbeta. (Translated from eng) *Cell* 105(5):587-597 (in eng).
40. Verhoeven K, *et al.* (2006) MFN2 mutation distribution and genotype/phenotype correlation in Charcot-Marie-Tooth type 2. (Translated from eng) *Brain* 129(Pt 8):2093-2102 (in eng).
41. Chung KW, *et al.* (2006) Early onset severe and late-onset mild Charcot-Marie-Tooth disease with mitofusin 2 (MFN2) mutations. (Translated from eng) *Brain* 129(Pt 8):2103-2118 (in eng).
42. Zuchner S, *et al.* (2006) Axonal neuropathy with optic atrophy is caused by mutations in mitofusin 2. (Translated from eng) *Ann Neurol* 59(2):276-281 (in eng).
43. Chung KW, *et al.* (2010) Early-onset Charcot-Marie-Tooth patients with mitofusin 2 mutations and brain involvement. (Translated from eng) *J Neurol Neurosurg Psychiatry* 81(11):1203-1206 (in eng).
44. Brockmann K, *et al.* (2008) Cerebral involvement in axonal Charcot-Marie-Tooth neuropathy caused by mitofusin2 mutations. (Translated from eng) *J Neurol* 255(7):1049-1058 (in eng).
45. Zhu D, *et al.* (2005) Charcot-Marie-Tooth with pyramidal signs is genetically heterogeneous: families with and without MFN2 mutations. (Translated from eng) *Neurology* 65(3):496-497 (in eng).
46. Hales KG & Fuller MT (1997) Developmentally regulated mitochondrial fusion mediated by a conserved, novel, predicted GTPase. (Translated from eng) *Cell* 90(1):121-129 (in eng).
47. Santel A, *et al.* (2003) Mitofusin-1 protein is a generally expressed mediator of mitochondrial fusion in mammalian cells. (Translated from eng) *J Cell Sci* 116(Pt 13):2763-2774 (in eng).
48. Mozdy AD & Shaw JM (2003) A fuzzy mitochondrial fusion apparatus comes into focus. (Translated from eng) *Nat Rev Mol Cell Biol* 4(6):468-478 (in eng).
49. Koshiba T, *et al.* (2004) Structural basis of mitochondrial tethering by mitofusin complexes. (Translated from eng) *Science* 305(5685):858-862 (in eng).
50. Song Z, Ghochani M, McCaffery JM, Frey TG, & Chan DC (2009) Mitofusins and OPA1 mediate sequential steps in mitochondrial membrane fusion. (Translated from eng) *Mol Biol Cell* 20(15):3525-3532 (in eng).
51. Cipolat S, Martins de Brito O, Dal Zilio B, & Scorrano L (2004) OPA1 requires mitofusin 1 to promote mitochondrial fusion. (Translated from eng) *Proc Natl Acad Sci U S A* 101(45):15927-15932 (in eng).
52. Yoon Y, Krueger EW, Oswald BJ, & McNiven MA (2003) The mitochondrial protein hFis1 regulates mitochondrial fission in mammalian cells through an interaction with

the dynamin-like protein DLP1. (Translated from eng) *Mol Cell Biol* 23(15):5409-5420 (in eng).
53. James DI, Parone PA, Mattenberger Y, & Martinou JC (2003) hFis1, a novel component of the mammalian mitochondrial fission machinery. (Translated from eng) *J Biol Chem* 278(38):36373-36379 (in eng).
54. Westermann B (2010) Mitochondrial dynamics in model organisms: what yeasts, worms and flies have taught us about fusion and fission of mitochondria. (Translated from eng) *Semin Cell Dev Biol* 21(6):542-549 (in eng).
55. Alexander C, *et al.* (2000) OPA1, encoding a dynamin-related GTPase, is mutated in autosomal dominant optic atrophy linked to chromosome 3q28. (Translated from eng) *Nat Genet* 26(2):211-215 (in eng).
56. Ishihara N, Fujita Y, Oka T, & Mihara K (2006) Regulation of mitochondrial morphology through proteolytic cleavage of OPA1. (Translated from eng) *EMBO J* 25(13):2966-2977 (in eng).
57. Casari G, *et al.* (1998) Spastic paraplegia and OXPHOS impairment caused by mutations in paraplegin, a nuclear-encoded mitochondrial metalloprotease. (Translated from eng) *Cell* 93(6):973-983 (in eng).
58. Waterham HR, *et al.* (2007) A lethal defect of mitochondrial and peroxisomal fission. (Translated from eng) *N Engl J Med* 356(17):1736-1741 (in eng).
59. Hwa JJ, Hiller MA, Fuller MT, & Santel A (2002) Differential expression of the Drosophila mitofusin genes fuzzy onions (fzo) and dmfn. (Translated from eng) *Mech Dev* 116(1-2):213-216 (in eng).
60. Ishihara N, Eura Y, & Mihara K (2004) Mitofusin 1 and 2 play distinct roles in mitochondrial fusion reactions via GTPase activity. (Translated from eng) *J Cell Sci* 117(Pt 26):6535-6546 (in eng).
61. Chen H, *et al.* (2003) Mitofusins Mfn1 and Mfn2 coordinately regulate mitochondrial fusion and are essential for embryonic development. (Translated from eng) *J Cell Biol* 160(2):189-200 (in eng).
62. Chen H, McCaffery JM, & Chan DC (2007) Mitochondrial fusion protects against neurodegeneration in the cerebellum. (Translated from eng) *Cell* 130(3):548-562 (in eng).
63. Detmer SA & Chan DC (2007) Complementation between mouse Mfn1 and Mfn2 protects mitochondrial fusion defects caused by CMT2A disease mutations. (Translated from eng) *J Cell Biol* 176(4):405-414 (in eng).
64. Griffin EE & Chan DC (2006) Domain interactions within Fzo1 oligomers are essential for mitochondrial fusion. (Translated from eng) *J Biol Chem* 281(24):16599-16606 (in eng).
65. Baloh RH, Schmidt RE, Pestronk A, & Milbrandt J (2007) Altered axonal mitochondrial transport in the pathogenesis of Charcot-Marie-Tooth disease from mitofusin 2 mutations. (Translated from eng) *J Neurosci* 27(2):422-430 (in eng).
66. Vallat JM, *et al.* (2008) Histopathological findings in hereditary motor and sensory neuropathy of axonal type with onset in early childhood associated with mitofusin 2 mutations. (Translated from eng) *J Neuropathol Exp Neurol* 67(11):1097-1102 (in eng).
67. Funalot B, Magdelaine C, Sturtz F, Ouvrier R, & Vallat JM (2009) [Ultrastructural lesions of axonal mitochondria in patients with childhood-onset Charcot-Marie-Tooth disease due to MFN2 mutations]. (Translated from fre) *Bull Acad Natl Med* 193(1):151-160; discussion 160-151 (in fre).
68. Misko A, Jiang S, Wegorzewska I, Milbrandt J, & Baloh RH (2010) Mitofusin 2 is necessary for transport of axonal mitochondria and interacts with the Miro/Milton complex. (Translated from eng) *J Neurosci* 30(12):4232-4240 (in eng).

69. Glater EE, Megeath LJ, Stowers RS, & Schwarz TL (2006) Axonal transport of mitochondria requires milton to recruit kinesin heavy chain and is light chain independent. (Translated from eng) *J Cell Biol* 173(4):545-557 (in eng).
70. De Brito OM & Scorrano L (2008) Mitofusin 2 tethers endoplasmic reticulum to mitochondria. (Translated from eng) *Nature* 456(7222):605-610 (in eng).
71. Wang X & Schwarz TL (2009) The mechanism of Ca2+ -dependent regulation of kinesin-mediated mitochondrial motility. (Translated from eng) *Cell* 136(1):163-174 (in eng).
72. Chen KH, *et al.* (2004) Dysregulation of HSG triggers vascular proliferative disorders. (Translated from eng) *Nat Cell Biol* 6(9):872-883 (in eng).
73. de Brito OM & Scorrano L (2009) Mitofusin-2 regulates mitochondrial and endoplasmic reticulum morphology and tethering: the role of Ras. (Translated from eng) *Mitochondrion* 9(3):222-226 (in eng).
74. Chung KW, *et al.* (2008) Early-onset stroke associated with a mutation in mitofusin 2. (Translated from eng) *Neurology* 70(21):2010-2011 (in eng).
75. Calvo J, *et al.* (2009) Genotype-phenotype correlations in Charcot-Marie-Tooth disease type 2 caused by mitofusin 2 mutations. (Translated from eng) *Arch Neurol* 66(12):1511-1516 (in eng).
76. Nicholson GA, *et al.* (2008) Severe early-onset axonal neuropathy with homozygous and compound heterozygous MFN2 mutations. (Translated from eng) *Neurology* 70(19):1678-1681 (in eng).
77. Polke JM, *et al.* (In press) Early onset recessive axonal Charcot Marie Tooth Disease due to compound heterozygous mitofusin 2 mutations. *Neurology* In publication.
78. Neusch C, *et al.* (2007) Mitofusin 2 gene mutation (R94Q) causing severe early-onset axonal polyneuropathy (CMT2A). (Translated from eng) *Eur J Neurol* 14(5):575-577 (in eng).
79. Honda S, Aihara T, Hontani M, Okubo K, & Hirose S (2005) Mutational analysis of action of mitochondrial fusion factor mitofusin-2. (Translated from eng) *J Cell Sci* 118(Pt 14):3153-3161 (in eng).
80. Detmer SA, Vande Velde C, Cleveland DW, & Chan DC (2008) Hindlimb gait defects due to motor axon loss and reduced distal muscles in a transgenic mouse model of Charcot-Marie-Tooth type 2A. (Translated from eng) *Hum Mol Genet* 17(3):367-375 (in eng).
81. Huang P, Yu T, & Yoon Y (2007) Mitochondrial clustering induced by overexpression of the mitochondrial fusion protein Mfn2 causes mitochondrial dysfunction and cell death. (Translated from eng) *Eur J Cell Biol* 86(6):289-302 (in eng).
82. Cartoni R, *et al.* (2010) Expression of mitofusin 2(R94Q) in a transgenic mouse leads to Charcot-Marie-Tooth neuropathy type 2A. (Translated from eng) *Brain* 133(Pt 5):1460-1469 (in eng).
83. Miller SA, Dykes DD, & Polesky HF (1988) A simple salting out procedure for extracting DNA from human nucleated cells. (Translated from eng) *Nucleic Acids Res* 16(3):1215 (in eng).
84. Don RH, Cox PT, Wainwright BJ, Baker K, & Mattick JS (1991) "Touchdown" PCR to circumvent spurious priming during gene amplification. (Translated from eng) *Nucleic Acids Res* 19(14):4008 (in eng).
85. Schouten JP, *et al.* (2002) Relative quantification of 40 nucleic acid sequences by multiplex ligation-dependent probe amplification. (Translated from eng) *Nucleic Acids Res* 30(12):e57 (in eng).

86. Cho HJ, Sung DH, Kim BJ, & Ki CS (2007) Mitochondrial GTPase mitofusin 2 mutations in Korean patients with Charcot-Marie-Tooth neuropathy type 2. (Translated from eng) *Clin Genet* 71(3):267-272 (in eng).
87. Kimmel CB, Ballard WW, Kimmel SR, Ullmann B, & Schilling TF (1995) Stages of embryonic development of the zebrafish. (Translated from eng) *Dev Dyn* 203(3):253-310 (in eng).
88. Barbazuk WB, *et al.* (2000) The syntenic relationship of the zebrafish and human genomes. (Translated from eng) *Genome Res* 10(9):1351-1358 (in eng).
89. Postlethwait J, Amores A, Force A, & Yan YL (1999) The zebrafish genome. (Translated from eng) *Methods Cell Biol* 60:149-163 (in eng).
90. Postlethwait JH, *et al.* (1998) Vertebrate genome evolution and the zebrafish gene map. (Translated from eng) *Nat Genet* 18(4):345-349 (in eng).
91. Taylor AM & Zon LI (2009) Zebrafish tumor assays: the state of transplantation. (Translated from eng) *Zebrafish* 6(4):339-346 (in eng).
92. Xia W (2010) Exploring Alzheimer's disease in zebrafish. (Translated from eng) *J Alzheimers Dis* 20(4):981-990 (in eng).
93. Taylor KL, Grant NJ, Temperley ND, & Patton EE (2010) Small molecule screening in zebrafish: an in vivo approach to identifying new chemical tools and drug leads. (Translated from eng) *Cell Commun Signal* 8:11 (in eng).
94. Grunwald DJ (1996) A fin-de siecle achievement: charting new waters in vertebrate biology. (Translated from eng) *Science* 274(5293):1634-1635 (in eng).
95. Haffter P, *et al.* (1996) The identification of genes with unique and essential functions in the development of the zebrafish, Danio rerio. (Translated from eng) *Development* 123:1-36 (in eng).
96. Amsterdam A, *et al.* (1999) A large-scale insertional mutagenesis screen in zebrafish. (Translated from eng) *Genes Dev* 13(20):2713-2724 (in eng).
97. Amsterdam A, *et al.* (2004) Identification of 315 genes essential for early zebrafish development. (Translated from eng) *Proc Natl Acad Sci U S A* 101(35):12792-12797 (in eng).
98. Bassett DI, *et al.* (2003) Dystrophin is required for the formation of stable muscle attachments in the zebrafish embryo. (Translated from eng) *Development* 130(23):5851-5860 (in eng).
99. Newport J & Kirschner M (1982) A major developmental transition in early Xenopus embryos: II. Control of the onset of transcription. (Translated from eng) *Cell* 30(3):687-696 (in eng).
100. Newport J & Kirschner M (1982) A major developmental transition in early Xenopus embryos: I. characterization and timing of cellular changes at the midblastula stage. (Translated from eng) *Cell* 30(3):675-686 (in eng).
101. Kane DA & Kimmel CB (1993) The zebrafish midblastula transition. (Translated from eng) *Development* 119(2):447-456 (in eng).
102. Robu ME, *et al.* (2007) p53 activation by knockdown technologies. (Translated from eng) *PLoS Genet* 3(5):e78 (in eng).
103. Eisen JS & Smith JC (2008) Controlling morpholino experiments: don't stop making antisense. (Translated from eng) *Development* 135(10):1735-1743 (in eng).
104. Moens CB, Donn TM, Wolf-Saxon ER, & Ma TP (2008) Reverse genetics in zebrafish by TILLING. (Translated from eng) *Brief Funct Genomic Proteomic* 7(6):454-459 (in eng).
105. Carroll D, Beumer KJ, Morton JJ, Bozas A, & Trautman JK (2008) Gene targeting in Drosophila and Caenorhabditis elegans with zinc-finger nucleases. (Translated from eng) *Methods Mol Biol* 435:63-77 (in eng).

106. Kawakami K (2007) Tol2: a versatile gene transfer vector in vertebrates. (Translated from eng) *Genome Biol* 8 Suppl 1:S7 (in eng).
107. Udvadia AJ & Linney E (2003) Windows into development: historic, current, and future perspectives on transgenic zebrafish. (Translated from eng) *Dev Biol* 256(1):1-17 (in eng).
108. Myers PZ, Eisen JS, & Westerfield M (1986) Development and axonal outgrowth of identified motoneurons in the zebrafish. (Translated from eng) *J Neurosci* 6(8):2278-2289 (in eng).
109. Westerfield M, McMurray JV, & Eisen JS (1986) Identified motoneurons and their innervation of axial muscles in the zebrafish. (Translated from eng) *J Neurosci* 6(8):2267-2277 (in eng).
110. Panzer JA, *et al.* (2005) Neuromuscular synaptogenesis in wild-type and mutant zebrafish. (Translated from eng) *Dev Biol* 285(2):340-357 (in eng).
111. Boon KL, *et al.* (2009) Zebrafish survival motor neuron mutants exhibit presynaptic neuromuscular junction defects. (Translated from eng) *Hum Mol Genet* 18(19):3615-3625 (in eng).
112. Wood JD, *et al.* (2006) The microtubule-severing protein Spastin is essential for axon outgrowth in the zebrafish embryo. (Translated from eng) *Hum Mol Genet* 15(18):2763-2771 (in eng).
113. Butler R, Wood JD, Landers JA, & Cunliffe VT (2010) Genetic and chemical modulation of spastin-dependent axon outgrowth in zebrafish embryos indicates a role for impaired microtubule dynamics in hereditary spastic paraplegia. (Translated from eng) *Dis Model Mech* 3(11-12):743-751 (in eng).
114. Facchin L, Argenton F, & Bisazza A (2009) Lines of Danio rerio selected for opposite behavioural lateralization show differences in anatomical left-right asymmetries. (Translated from eng) *Behav Brain Res* 197(1):157-165 (in eng).
115. Westerfield M ed (2007) *The Zebrafish Book-A guide for the laboratory use of zebrafish (Danio rerio)* (University of Oregon Press, Eugene), 5th Edition Ed.
116. Altschul SF, *et al.* (1997) Gapped BLAST and PSI-BLAST: a new generation of protein database search programs. (Translated from eng) *Nucleic Acids Res* 25(17):3389-3402 (in eng).
117. Thompson JD, Higgins DG, & Gibson TJ (1994) CLUSTAL W: improving the sensitivity of progressive multiple sequence alignment through sequence weighting, position-specific gap penalties and weight matrix choice. (Translated from eng) *Nucleic Acids Res* 22(22):4673-4680 (in eng).
118. Dereeper A, *et al.* (2008) Phylogeny.fr: robust phylogenetic analysis for the non-specialist. (Translated from eng) *Nucleic Acids Res* 36(Web Server issue):W465-469 (in eng).
119. Fujita PA, *et al.* (2010) The UCSC Genome Browser database: update 2011. (Translated from Eng) *Nucleic Acids Res* (in Eng).
120. Thisse C & Thisse B (2008) High-resolution in situ hybridization to whole-mount zebrafish embryos. (Translated from eng) *Nat Protoc* 3(1):59-69 (in eng).
121. Shenoy AR & Visweswariah SS (2003) Site-directed mutagenesis using a single mutagenic oligonucleotide and DpnI digestion of template DNA. (Translated from eng) *Anal Biochem* 319(2):335-336 (in eng).
122. Paquet D, *et al.* (2009) A zebrafish model of tauopathy allows in vivo imaging of neuronal cell death and drug evaluation. (Translated from eng) *J Clin Invest* 119(5):1382-1395 (in eng).

123. Sun QY, *et al.* (2001) Translocation of active mitochondria during pig oocyte maturation, fertilization and early embryo development in vitro. (Translated from eng) *Reproduction* 122(1):155-163 (in eng).
124. Flanagan-Steet H, Fox MA, Meyer D, & Sanes JR (2005) Neuromuscular synapses can form in vivo by incorporation of initially aneural postsynaptic specializations. (Translated from eng) *Development* 132(20):4471-4481 (in eng).
125. Engelfried K, *et al.* (2006) Charcot-Marie-Tooth neuropathy type 2A: novel mutations in the mitofusin 2 gene (MFN2). (Translated from eng) *BMC Med Genet* 7:53 (in eng).
126. Raeymaekers P, *et al.* (1991) Duplication in chromosome 17p11.2 in Charcot-Marie-Tooth neuropathy type 1a (CMT 1a). The HMSN Collaborative Research Group. (Translated from eng) *Neuromuscul Disord* 1(2):93-97 (in eng).
127. Chance PF, *et al.* (1993) DNA deletion associated with hereditary neuropathy with liability to pressure palsies. (Translated from eng) *Cell* 72(1):143-151 (in eng).
128. Depienne C, *et al.* (2007) Exon deletions of SPG4 are a frequent cause of hereditary spastic paraplegia. (Translated from eng) *J Med Genet* 44(4):281-284 (in eng).
129. Dumollard R, Duchen M, & Carroll J (2007) The role of mitochondrial function in the oocyte and embryo. (Translated from eng) *Curr Top Dev Biol* 77:21-49 (in eng).
130. Valdmanis PN, *et al.* (2007) Mutations in the KIAA0196 gene at the SPG8 locus cause hereditary spastic paraplegia. (Translated from eng) *Am J Hum Genet* 80(1):152-161 (in eng).
131. Lin P, *et al.* (2008) A missense mutation in SLC33A1, which encodes the acetyl-CoA transporter, causes autosomal-dominant spastic paraplegia (SPG42). (Translated from eng) *Am J Hum Genet* 83(6):752-759 (in eng).
132. Fassier C, *et al.* (2010) Zebrafish atlastin controls motility and spinal motor axon architecture via inhibition of the BMP pathway. (Translated from eng) *Nat Neurosci* 13(11):1380-1387 (in eng).